



HAL
open science

Residential Solid Oxide Fuel Cell Generator Fuelled by Ethanol: Cell, Stack, and System Modelling with a Preliminary Experiment

Andrea Lanzini, Massimo Santarelli, Gianmichele Orsello

► **To cite this version:**

Andrea Lanzini, Massimo Santarelli, Gianmichele Orsello. Residential Solid Oxide Fuel Cell Generator Fuelled by Ethanol: Cell, Stack, and System Modelling with a Preliminary Experiment. *Fuel Cells*, 2010, 10 (4), pp.654. 10.1002/fuce.201000004 . hal-00552373

HAL Id: hal-00552373

<https://hal.science/hal-00552373>

Submitted on 6 Jan 2011

HAL is a multi-disciplinary open access archive for the deposit and dissemination of scientific research documents, whether they are published or not. The documents may come from teaching and research institutions in France or abroad, or from public or private research centers.

L'archive ouverte pluridisciplinaire **HAL**, est destinée au dépôt et à la diffusion de documents scientifiques de niveau recherche, publiés ou non, émanant des établissements d'enseignement et de recherche français ou étrangers, des laboratoires publics ou privés.



Residential Solid Oxide Fuel Cell Generator Fuelled by Ethanol: Cell, Stack, and System Modelling with a Preliminary Experiment

Journal:	<i>Fuel Cells</i>
Manuscript ID:	face.201000004.R1
Wiley - Manuscript type:	Original Research Paper
Date Submitted by the Author:	30-Mar-2010
Complete List of Authors:	Lanzini, Andrea; Politecnico di Torino, Energetics Santarelli, Massimo; Politecnico di Torino, Energetics Orsello, Gianmichele; Turbocare Spa
Keywords:	Ejector, Ethanol, Recirculation, Tubular, System Modelling



Formatted: Italian (Italy)

Residential Solid Oxide Fuel Cell Generator Fuelled by Ethanol: Cell, Stack, and System Modelling with a Preliminary Experiment

Andrea Lanzini^a, Massimo Santarelli^a, Gianmichele Orsello^b

^a Department of Energy, Politecnico di Torino, Turin, Italy

^b TurboCare spa, Turin, Italy

Andrea Lanzini Department of Energy, Politecnico di Torino, Corso
Duca degli Abruzzi 24 -10129, Torino, Italy, phone: +38 011
0904523, fax: + 39 0110904499, andrea.lanzini@polito.it

Massimo Santarelli Department of Energy, Politecnico di Torino, Corso
Duca degli Abruzzi 24 – 10129, Torino, Italy, phone: +38 011
090 44 87, fax: + 39 0110904499, massimo.santarelli@polito.it

Gianmichele Orsello Turbocare Spa, Corso Romania 661 – 10156, Torino,
Italy, phone: +39 011 005 9931,
gianmichele.orsello@siemens.com

Abstract

The flexibility and feasibility of a 5 kW SOFC generator designed for natural gas and fuelled by a non-conventional liquid fuel such ethanol is analysed. A complete generator model is implemented to predict and determine the main criticalities when ethanol fuel is adoperated. The main Balance-of-Plant (BoP) units considered are the reformer, the recirculation system based on an ejector, the tubular cells bundles constituting the stack unit, the after-burner zone and the air blower. The electrical and global efficiencies achieved at nominal operating conditions show how ethanol

Deleted: as

Deleted: model of the

Deleted: used

Deleted: as a fuel

Deleted: components

Deleted: the stack with

Deleted: a

Deleted: point are calculated,

Deleted: showing

maintains generator performance good, while only slightly reducing the system AC efficiency from 48% (achieved by natural gas) to 45%. The effectiveness and flexibility of the recirculation system when changing the fuel is also verified since a safe steam-to-carbon ratio (STCR) is established after the fuel is switched from natural gas ethanol. The stack thermal management is analysed in detail and related to the system performances, showing how a high endothermic fuel reforming reaction is required to maintain the overall system efficiency. A preliminary experiment with ethanol feeding the Siemens generator is finally presented. The system response to the new fuel is monitored by several measured parameters and the system regulation is explained.

- Deleted:
- Deleted: demonstrated
- Deleted: ,
- Deleted: because
- Deleted: STCR (
- Deleted:)
- Deleted: when ethanol fuel is used
- Deleted: Finally, details on t
- Deleted: are
- Deleted: presented
- Deleted: in order
- Deleted: on
- Deleted: in
- Deleted: als
- Deleted: o

1. Introduction

Natural gas (NG) is considered the major fuel for SOFCs due to its widespread availability, well-known catalytic reforming techniques to produce hydrogen and carbon monoxide, and reduced costs. Several SOFC systems running on natural gas are already installed, and some of them have already achieved several operating hours with high conversion efficiency rates for electricity production [1,2]. Still, natural gas is a fossil fuel, and its consumption to produce energy implies having a net balance of CO₂ emissions. One attractive feature of SOFC technology is the possibility to operate on different fuels. The relatively high operating temperature permits to have an integrated plant for converting hydrocarbons or alcohols into H₂ and CO, which are subsequently electro-oxidised in a SOFC to produce electricity).

- Deleted: means
- Deleted: because
- Deleted: t
- Deleted: makes favourable
- Deleted: (species can be readily
- Deleted: an
- Deleted: device

Among the others, fuels that can be derived from a biological path (e.g. biogases or bio-fuels) are of great interest to assure a sustainable energy production since the net carbon dioxide balance emissions is in principle zero. Of course, depending on the particular fuel composition, a proper device for the catalytic reforming (preferably internally integrated into the stack) has to be selected in order to assure both an adequate conversion of the hydrocarbons or alcohols, as well as to prevent carbon deposition on the anode side of the cells.

- Deleted: because
- Deleted: would be
- Deleted: in

1 The physical status of a fuel at environmental pressure and temperature is also a feature to consider
 2
 3 when selecting a fuel. The general advantage of liquid fuels is the high specific energy density,
 4
 5 which translates directly into easier and more convenient storage and transportation. Especially for
 6
 7 maritime transportation and aircrafts (where the fuel volume storage is a significant parameter),
 8
 9 liquid fuels are of a great interest. One available option is the use of alcohols (e.g. methanol,
 10
 11 ethanol, DME) in an SOFC generator with internal or in-stack fuel reforming to provide power to
 12
 13 high energy-demanding auxiliary units [3]. Methanol is a good candidate, since it is readily
 14
 15 available, but usually a fossil fuel such as natural gas or coal is used as the initial feedstock.
 16
 17 Moreover, methanol is toxic and special handling and safety issues must be considered. Ethanol is a
 18
 19 very promising candidate as well, since it can be produced from renewable resources and has no
 20
 21 toxicity issues.

Deleted: convenience

Deleted: in

Deleted: some particular but wide fields such as

Deleted: or on-board

Deleted: Therefore, one possibility

Deleted: provided

Deleted: an

Deleted: zone

Deleted: favourabl

Deleted: e

Deleted: because

Deleted: because

Deleted: of course

22
 23 In general, an important issue arising when considering bio-fuels, either gaseous or liquid, is how
 24
 25 much energy is actually spent to produce a certain available amount fuel starting from the biomass;
 26
 27 the debate was and still is very intense, particularly regarding the ethanol production. In fact, the
 28
 29 Well-to-Tank (*WTT*) value of the first-generation bio-ethanol, is around 1.51 MJ/MJ (mean value
 30
 31 obtained from different production pathways), which is still far from the values reached by the
 32
 33 traditional fossil fuels (e.g. 0.19 for natural gas) [4]. It has recently been reported [5] that corn
 34
 35 ethanol is energy-efficient, as indicated by an energy output/input ratio of 1.34, while other studies
 36
 37 state that producing ethanol requires more energy than that stored in the final fuel [6]. Of course,
 38
 39 this clearly depends strongly on the specific production pathway selected and the type of starting
 40
 41 biomass.

Deleted: An

Deleted: question

Deleted: in

Deleted: both

Deleted: gas

Deleted: and

Deleted: th

Deleted: e

Deleted: starting from the available

Deleted: biomass

Deleted: is

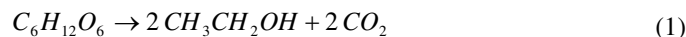
Deleted: especially for

Deleted: n fact

42
 43 There is still of course a great opportunity to improve the production and distribution paths of bio-
 44
 45 fuels, and the second generation is developing fast. In addition, bio-ethanol could reach a good
 46
 47 performance level in terms of the «generalised» Tank-to-Wheel (*TTW*) ratio. As shown in the
 48
 49 results of this paper, a good electric and CHP efficiency can be reached when a SOFC is used as the
 50
 51 device converting the bio-fuel into electricity and heat.

The consolidated bio-ethanol production technology essentially uses biomass waste as the raw material. Most of the worldwide production relies on the microbial fermentation of sugars (prior eventually the hydrolysis of the starch-containing compounds to the corresponding sugar).

The standard path from sugar (glucose) follows the basic overall reaction:



Sugarcane (wide production and use in Brazil) or corn (especially in the US) can be used as feedstock biomass and the two have different ethanol yields per kg of biomass.

Through hydrolysis, a cellulosic biomass is feasible as well, since enzymes capable of hydrolysing cellulose and preparing it for fermentation have been widely discovered and selected. This technology could turn a number of cellulose-containing agricultural by-products such as corncobs, straw, and sawdust into renewable energy resources. Some enzymes are able to hydrolyse agricultural residues such as corn stover, wheat straw, and sugar cane bagasse as well as energy crops such as switchgrass into fermentable sugars [7].

Ethanol is also relatively easy to convert in hydrogen and carbon monoxide through catalytic steam reforming (which is already generally performed in large SOFC systems to convert natural gas).

When bio-ethanol is coupled with a high-energy conversion system, such as an SOFC, a complete sustainable and efficient electricity production is available. For these reasons, an SOFC system fuelled by ethanol is an option worthy of consideration.

2. Scope of this study

The main purpose of this study is to establish a detailed and complete modelling framework of an SOFC generator that is able to consider both hydrocarbons and alcohols as fuel inlet. The model is validated against the real generator operating with tubular cells and running on natural gas.

System simulations are performed to show how ethanol could be used to efficiently produce energy (electricity and heat) using an SOFC device as power generator. An experiment with ethanol fuel feeding the real generator is finally performed to check the validity of the simulation results and

Deleted: There is great opportunity for improvement in the production and distribution paths of the bio-fuels, especially considering the use of *second generation* typologies. Also, bio-ethanol could reach a good performance level in terms of the «generalised» Tank-to-Wheel (TTW) ratio, because, as described below, a good electric and CHP efficiency can be reached if ethanol would be used in an SOFC plant. ¶ It has recently been reported [5] that corn ethanol is energy-efficient, as indicated by an energy output/input ratio of 1.34, while other studies state that producing ethanol requires more energy than that stored in the final fuel [6]. Of course, this clearly depends strongly on the specific production pathway selected and the type of starting biomass. ¶ Nevertheless,

Formatted: Font: Italic

Deleted: manufacturing

Deleted: and the production techniques have been consolidated through the years.

Deleted: or

Formatted: English (U.K.), Lowered by 6 pt

Deleted: $C_6H_{12}O_6 \rightarrow 2 CH_3CH_2OH + 2 CO_2$.

Deleted: ¶

Deleted: In general, ethanol production from biomass with biochemical processes makes it quite an attractive fuel, provided that a sustainable pathway is carefully selected. For non-biological production, e

Deleted: ¶ If

Deleted: pathway can arise

Deleted: n

Deleted: ¶ ¶

Deleted: model

Deleted: s

Deleted: , along with its

Deleted: validation

Deleted: a

Deleted: that

Deleted: s

Deleted: In this study, we

Deleted: aim also to show how

Deleted: device as

support the main findings. In particular, the generator fuel-flexibility is checked with particular concern to the ejector-based recirculation system and the stack thermal management.

Deleted: §
Moreover, the high

Deleted: of an SOFC generator

Deleted: shown

Deleted: , even

Deleted: when running on a recirculator-based ejector system with the new fuel.

Deleted: solution

3. Balance-of-Plant of the SOFC system

In this section, the reference case (a generator fuelled by natural gas) and the proposed alternative (a generator running on ethanol fuel) are compared together. A wide range of topics related to the operation with a non-conventional fuel are discussed. For both feeding cases, the BoP is maintained the same; in this way, the fuel flexibility of the generator is assessed while the system design and configuration are kept unchanged.

Deleted: In

Deleted: essentially

Deleted: evaluated

Deleted: considering

Deleted: fixed the

A complete system model of a 5 kW SOFC generator was developed in the present work. The main modules considered are the fuel processing zone (with a thermally integrated in-stack reformer), the stack unit, the after-burner zone, the ejector-based recirculation system and the cathode air blower.

Deleted: module

Deleted: the

Deleted: ventilator

Deleted: , and the recirculation system based on an ejector.

The SOFC system described is representative of the SFCα6 Siemens Fuel Cell design, of which a prototype unit was installed and has been running at Turbocare Spa (Torino) since April 2006.

Deleted: has been

Deleted: SOFC

The stack consists of 88 tubular cells with a 75 cm active length. The cell design and materials are well known and are reported in [8]. The cells are packed together in a 4 bundles arrangement, each one consisting of 22 tubular cells. Within every bundle, two strings of 11 series-connected cells are connected together in parallel. According to this electrical connection, the voltages produced by the 4 bundles are summed together to provide the overall stack voltage.

Deleted: stacked

Deleted: a

Figure 1 - Installation of the 5 kW Siemens Generator in Turbocare Spa

The generator has a nominal AC electric power around 3-3.5 kW_{el}, with a respective DC stack current of 120-150 A and a voltage of 29-26.5 V. The peak power is 5 kW DC. The nominal thermal recovered power is in the range of 2.5-3.1 kW_{th}. The nominal operating temperature of the stack is 970 °C. A scheme of the BoP main modules is presented in Figure 2.

Natural gas is the designed fuel and can be provided directly from the industrial grid, where it is available at pressure of approximately 5 bars. A valve reduces the pressure to a value of 3 bars just

Deleted: (NG)

Deleted: pipelines

Deleted: with

Deleted: an

before the generator inlet. As the first step, the fuel enters the desulphuriser, a two reactor beds connected in series, the first one filled with zeolites and the second one with activated carbon. After the cleaning stage, the NG enters the ejector at a pressure that is dependent on the nominal flow. A maximum NG flow of 30 SLPM with an inlet pressure of 2.75 bars is achievable at the ejector inlet. The fuel flow is heated as it is piped inside the hot-box of the system: measurements provide an inlet ejector temperature of around 700°C. Inside the ejector, the primary fuel (NG) entrains part of the anodic exhaust due to fluid-dynamics effects. By mixing with the latter flow, NG is additionally heated. The recirculation factor of the ejector, and especially the exhaust composition, are strictly dependent on the main operative parameters of the system, which are essentially the Fuel Utilisation (FU) and the current load requested to the stack.

Figure 2 - Basic BoP design of the SOFC generator analysed

In the system BoP is included an auxiliary steam line used mainly for the start-up and partial load operation of the generator. Under these circumstances, the NG flow entering the generator is much reduced from the nominal value, and is unable to entrain water (steam) enough from the anode exhaust to accomplish the reforming reactions. Additional steam is therefore externally added to the stack to guarantee a safe operation in terms of carbon-deposition (that could affect both the reformer and the cells catalytic activity and long-term integrity).

With regards to the ethanol feeding case study, the steam line is actually used to pump the ethanol into the ejector. This option was selected since it represented the most convenient and easy way to feed the stack with a liquid fuel. A benefit of dealing with a liquid fuel is that the energy required to pump the fuel into the ejector at an adequate pressure is a negligible fraction of the overall stack power output. Thus, the ethanol was pumped at room temperature as a liquid towards the ejector and the stack. Before reaching the ejector, the steamer available was used to vaporise it. A more detailed description is reported in the experimental section of this paper.

4. Cell, stack and system modelling of the 5 kW Generator

- Deleted: inlet into the
- Deleted: First
- Deleted: natural gas
- Deleted: (
- Deleted:)
- Deleted: a
- Deleted: at the ejector inlet
- Deleted: In the reference case, the NG flow is provided from the industrial grid. A
- Deleted: is present
- Deleted: and shut-down procedure
- Deleted: s
- Deleted: , and in case the
- Deleted: .
- Deleted: In fact, in this case it
- Deleted: enough
- Deleted: in
- Deleted: recirculated
- Deleted: for
- Deleted: the
- Deleted: ,
- Deleted: and a
- Deleted: from
- Deleted: has to be added in order
- Deleted: to operate
- Deleted: ly
- Deleted: in terms of carbon deposition
- Deleted: Referring now
- Deleted: to
- Deleted: This is quite
- Deleted: an
- Deleted: procedure
- Deleted: , because ethanol is a liquid at room temperature. Another
- Deleted: pumping
- Deleted: energy to reach the pressure required by the ejector
- Deleted: Of course t
- Deleted: has to be vaporised, and this step is accomplished in the steamer heat exchanger
- Deleted: (a
- Deleted:)
- Deleted: ¶
- Deleted: S
- Deleted: S

4.1 Tubular cell model

Deleted: C

Deleted: M

Deleted: a

The Siemens Generator employs cathode-supported tubular cells. The cathode support consists of a 2.2 mm thick doped LaMnO₃ layer fabricated by extrusion-sintering. The inner diameter is ~22 cm.

Deleted: By atmospheric plasma-spraying the

Deleted: a

The YSZ electrolyte (40 μm), the Ni-YSZ anode (100 μm) and the doped LaCrO₃ interconnector (100 μm) layer are successively deposited onto the cathode surface by atmospheric plasma-spraying technique. A thin protective interlayer of CeO₂ is deposited between the cathode and the electrolyte using an impregnation technique.

Deleted: \

Deleted: in

The cathode tube is continuous, generating a seal-less design, where air is always contained on the inside of the cells. Each cell has an uncovered portion of cathode (where no electrolyte or anode are deposited) where the interconnector layer is placed. A nickel felt is attached onto this layer to provide electrical connection with the other stack cells.

Deleted: where

Once the cell geometry and materials are defined, the cell voltage characteristics have been modelled as a function of the current load with a detailed polarisation model. Many models of SOFC single cells exist in the literature; those used here as references are reported in [9-11].

The Nernst potential has been calculated as:

$$V_{Nernst} = \frac{R \cdot T}{4 \cdot F} \log \left(\frac{p_{O_2,cat}^{channel}}{p_{O_2,an}^{channel}} \right), \quad (2)$$

where the oxygen partial pressures are evaluated respectively in the fuel and air channels, before the gas mixture enters the diffusion zone inside the porous electrodes. The losses arising from the diffusion of reacting and produced species inside the anode and cathode layers are evaluated as concentration losses, as later described.

Deleted: also

Ohmic losses occur due to the flow of electrons or ionic species inside the cells. The electron paths inside the cells' active layers due to the particular cylinder shape of the cells have been calculated, along with ohmic losses arising in the Ni-felts and the interconnector contact layers between one

cell and another. The path is circumferential inside the anode and cathode, and radial into the electrolyte, interconnector and felt. The formulas used are those proposed in [12]:

$$\eta_{ohm}^{tot} = \eta_{ohm,an} + \eta_{ohm,cat} + \eta_{ohm,ely} + \eta_{ohm,int\ er} + \eta_{ohm,felt} \quad (3)$$

$$\eta_{ohm,an} + \eta_{ohm,cat} = j \cdot \frac{\pi D}{2} \cdot \left(\frac{\rho_{an}}{l_{an}} + \frac{\rho_{cat}}{l_{cat}} \right) \frac{1}{2} \frac{\pi D}{2} \quad (4)$$

$$\eta_{ely} = j \cdot \rho_{ely} \cdot l_{ely} \quad (5)$$

$$\eta_{ohm,int\ er} + \eta_{ohm,felt} = j \cdot \pi D \cdot \left(\rho_{int\ er} \frac{l_{int\ er}}{w_{int\ er}} + \rho_{felt} \frac{l_{felt}}{w_{felt}} \right) \quad (6)$$

Deleted: the

Deleted: following as

Deleted: $\eta_{ely} = j \cdot \rho_{ely} \cdot l_{ely}$ (5)

$\eta_{ohm,int\ er} + \eta_{ohm,felt} = j \cdot \pi D \cdot \left(\dots \right)$ (6)

Formatted: Left, Indent: Left: 177.6 pt, First line: 34.8 pt

Figure 3 shows a schematic view of the electrons migrating from the Ni-felt of a cell to that of the subsequent cell, passing through the anode, cathode and electrolyte layer. The current collector zones (interconnector + felt) are located at each semicircle. A uniform current distribution inside the tube is assumed.

Figure 3 – Ohmic losses in the tubular cell

Deleted: cell tube

The anodic concentration losses are evaluated with the flowing expression:

$$\eta_{diff,an} = -\frac{RT}{2F} \log \left(\frac{P_{H_2,an}^{int} \cdot P_{H_2O,an}^{channel}}{P_{H_2,an}^{channel} \cdot P_{H_2O,an}^{int}} \right) \quad (7)$$

Deleted: polarisations

Formatted: English (U.K.), Lowered by 17 pt

Formatted: Bullets and Numbering

An analogous expression was derived for the CO diffusion, being this species considered electrochemical active as well as H₂ in the proposed electrochemical model.

Formatted: Subscript

The Fick's law is solved at the anode to account for the partial pressure change of the gas species diffusing through the electrode along the anode thickness direction [13]:

Deleted: using

$$N_i = -D_i^{eff} \frac{P}{RT} \nabla y_i \quad (8)$$

Formatted: Bullets and Numbering

Deleted: ¶

$N_i = -D_i^{eff} \frac{P}{RT} \nabla y_i$ (7) ¶

Since a multi-species gas diffusion is present, the diffusion coefficient of each species inside the mixture is calculated as reported in [14]:

Deleted: In the anode,

Deleted: . T

Deleted: defined

$$D_i^{eff} = \frac{\varepsilon}{\tau} \left[\frac{1 - \alpha_{i,m} \cdot y_i}{D_{i,m}} + \frac{1}{D_i^K} \right]^{-1} \quad (9)$$

Formatted: Bullets and Numbering

Deleted: $D_i^{eff} = \frac{\varepsilon}{\tau} \left[\frac{1 - \alpha_{i,m} \cdot y_i}{D_{i,m}} \right]$
 Deleted: (8)

Deleted: where

Deleted: given by

$\alpha_{i,m}$ is a dimensionless parameter defined as:

$$\alpha_{i,m} = 1 - \left(\frac{M_i}{\sum_k^{n_{species}} M_k / n_{species}} \right) \quad (10)$$

Formatted: Bullets and Numbering

where

$$D_{i,m} = \frac{1 - y_i}{\sum_{j \neq i} \frac{y_j}{D_{ij}}} \quad (11)$$

Deleted: $\alpha_{i,m} = 1 - \left(\frac{M_i}{\sum_k^{n_{species}} M_k / n} \right)$
 Deleted: (9) and

Formatted: Justified

Formatted: Bullets and Numbering

The dusty-gas model is used at the cathode side [15]. The most significant concentration loss occurs here due to the higher thickness of the cathode compared to the anode layer. An higher accuracy is

sought when in evaluating this overpotential. The superiority of dusty-gas model with respect to the

Fick's law has been reported in literature [16]. The equation for oxygen partial pressure at the cathode/electrolyte interface, considering O_2 self-diffusion into the cathode layer, takes the

following form once solved:

$$p_{O_2,cat}^{int} = \frac{p_{cat}^{tot}}{\delta_{O_2}} - \left(\frac{p_{cat}^{tot}}{\delta_{O_2}} - p_{O_2}^{channel} \right) \cdot \exp \left(\frac{\delta_{O_2} \cdot R \cdot T \cdot j \cdot I_{cat}}{4F \cdot D_{O_2}^{eff} \cdot p_{cat}^{tot}} \right) \quad (12)$$

Deleted: $D_{i,m} = \frac{1 - y_i}{\sum_{j \neq i} \frac{y_j}{D_{ij}}}$ (10)

Deleted: ,

Deleted: so

Deleted: a

Deleted: required

Deleted: kind of

Deleted: when

Formatted: Bullets and Numbering

where

$$\frac{1}{D_{O_2}^{eff}} = \frac{\tau_{cat}}{\varepsilon_{cat}} \cdot \left(\frac{1}{D_{O_2,K}} + \frac{1}{D_{O_2-N_2}} \right) \quad N_i = -D_i^{eff} \frac{p}{RT} \nabla y_i \quad (13)$$

Deleted: ,

Deleted: $p_{O_2,cat}^{int} = \frac{p_{cat}^{tot}}{\delta_{O_2}} - \left(\frac{p_{cat}^{tot}}{\delta_{O_2}} - p_{O_2}^{channel} \right)$
 Deleted: (11)

Formatted: Justified, Tabs: 240.95 pt, Centered + 423.75 pt, Left

Formatted: Bullets and Numbering

Formatted: Bullets and Numbering

$$\delta_{O_2} = \frac{D_{O_2,K}^{eff}}{D_{O_2,K}^{eff} + D_{O_2-N_2}^{eff}} \quad (14)$$

The binary diffusion and Knudsen diffusion coefficients have been calculated according to the Chapman-Enskog kinetic theory [17]. For a low-density gas, the binary coefficients are calculated

as:

Deleted: $\frac{1}{D_{O_2}^{eff}} = \frac{\tau_{cat}}{\varepsilon_{cat}} \cdot \left(\frac{1}{D_{O_2,K}} \right)$
 Deleted: (12)

Deleted: $\delta_{O_2} = \frac{D_{O_2,K}^{eff}}{D_{O_2,K}^{eff} + D_{O_2-N_2}^{eff}}$ (13)

$$V(j) = V_{Nernst} - \eta_{ohm}^{tot} - \eta_{act,an} - \eta_{act,cat} - \eta_{diff,an} - \eta_{diff,cat} \quad (21)$$

The set of equations (Eqs. 2-21) provided permits to evaluate the cell polarisation behaviour as a function of the current load requested. The present model was solved for a 1D discretised domain of the tubular cell (see Figure 4). The domain has been divided into equidistant sectors along the tube length, and the polarisation model is solved for each discretised tube element. Because the gases in each solved tube section diffuse in a direction orthogonal to the fuel flow in the channel, a quasi-2-D model is derived. A uniform current distribution along the tube length is assumed. Since both the H₂ and CO coming from the reforming of CH₄ are considered as being electrochemical active species, a value of 3 was assumed as the one expressing that ratio between H₂ and CO reacted to provide the overall current requested. This empirical assumption agrees with the literature [11], and in our case it is supported also by the chromatographic analysis of the stack outlet gas, which were performed routinely during the generator operation.

Along the tube, the anodic and cathodic gas mixtures change composition according to Faraday's law. At the generic tube element along the domain, the following equations hold:

$$I_{H_2,i} + I_{CO,i} = \frac{I_{CELL}}{N} \quad (22)$$

$$n_{H_2,i+1} = n_{H_2,i} - I_{H_2,i} = n_{H_2,i} - \frac{3/4 \cdot (I_{CELL}/N)}{2 \cdot F} \quad (23)$$

$$n_{H_2O,i+1} = n_{H_2O,i} + \frac{3/4 \cdot (I_{CELL}/N)}{2 \cdot F} \quad (24)$$

$$n_{CO,i+1} = n_{CO,i} - (I_{CELL}/N - I_{H_2,i}) = n_{CO,i} - \frac{1/4 \cdot (I_{CELL}/N)}{2F} \quad (25)$$

$$n_{CO_2,i+1} = n_{CO_2,i} + \frac{1/4 \cdot (I_{CELL}/N)}{2 \cdot F} \quad (26)$$

$$n_{O_2,i+1} = n_{O_2,i} - \frac{(I_{CELL}/N)}{4 \cdot F} \quad (27)$$

Figure 4 - Fuel and air flows along the tubular cell

Formatted: English (U.K.), Lowered by 7 pt

Formatted: Bullets and Numbering

Deleted: $V(j) = V_{Nernst} - \eta_{ohm}^{tot} + \dots$ (20)

Deleted: giving

Deleted: under

Deleted: is

Deleted: Because

Deleted: (

Deleted:)

Deleted: available

Deleted: to provide current through electrochemical oxidation at the anod

Deleted: e

Deleted: ratio

Deleted: of

Deleted: has been

Deleted: assumed

Deleted: to

Deleted: reacting

Deleted: in the stack

Deleted: fully

Deleted: several times

Formatted: English (U.K.), Lowered by 12 pt

Formatted: Bullets and Numbering

Formatted: English (U.K.), Lowered by 12 pt

Formatted: Bullets and Numbering

Formatted: English (U.K.), Lowered by 12 pt

Formatted: Bullets and Numbering

Formatted: English (U.K.), Lowered by 12 pt

Formatted: Bullets and Numbering

Formatted: English (U.K.), Lowered by 12 pt

Formatted: Bullets and Numbering

Formatted: English (U.K.), Lowered by 12 pt

Formatted: Bullets and Numbering

Deleted: $I_{H_2,i} + I_{CO,i} = \frac{I_{TOT}}{N}$

Formatted: Left

Deleted: (21)

Formatted: ... [1]

Formatted: ... [2]

Deleted: ¶ ... [3]

The value representative of the cell voltage is the mean of the voltage values calculated at each discretised sector (or element) along the tube length.

Formatted: Indent: Left: 18 pt

In Table 1 the main geometrical, microstructural and electrochemical parameters used as an input to solve the tubular cell model are reported.

Formatted: Font: Not Italic

4.2 Stack model

Deleted: M

Each tubular cell is assumed to work under the same identical conditions to the other cells inside the stack and with the same performances. Thus, the polarisation model presented in Section 4.1 is solved just for one cell and the results obtained are extended to every cell in the stack. As mentioned in Section 3, the total number of cells is 88, and they are stacked together in bundles of 22 cells each. A schematic view of the electrical connection among the cells inside a bundle is reported in Figure 5. The terminal cells at both sides of the bundle are welded to current-collecting metallic sheets. Referring to the electrical arrangement described before, the same current is flowing in each bundle being all connected together in series. Therefore the overall stack current output is the double of that flowing in each cell. When measuring the generator stack voltage (the only voltage measurement available for the real generator), the cells average voltage can be obtained by dividing the former voltage by 44 (which is half of the total number of cells within the stack).

Deleted: inside the stack

Deleted: in

Deleted: §

Deleted: is just

Deleted: ,

Deleted: and the results

Deleted: extended

Deleted: §

Deleted: of

Deleted: the

Deleted: a

Deleted: bundle is the same, because

Deleted: the latter

Deleted: are

Deleted: The

Deleted: therefore

Deleted: passin

Deleted: g

Deleted: A

Deleted: can

Deleted: stack

Deleted: output

Figure 5 - Cells arrangement inside a bundle

The stack is air-cooled, which means that air in excess to the stoichiometric quantity needed for the electrochemical reactions is used to cool the stack. The stack thermal balance is solved to evaluate the stoichiometric air excess.

Formatted: Left

Deleted: ¶

Formatted: English (U.K.), Lowered by 7 pt

Formatted: Left

Formatted: Bullets and Numbering

The heat internally produced by the stack is calculated as:

$$Q_{stack} = Q_{react} + Q_{loss} = |T_{stack} \cdot \Delta S_{stack}| + Q_{loss} \quad (28)$$

Deleted: ¶

$$Q_{stack} = Q_{react} + Q_{loss} = T_{stack} \cdot \Delta S_{stack} + Q_{loss} \quad (27)$$

Deleted: ¶

The two heat source terms in Eq. 28 are respectively defined as:

$$\begin{cases} T_{stack} \cdot \Delta S_{stack} = \Delta H_{stack} - \Delta G_{stack} \\ Q_{loss} = I_{stack} \cdot \left(\frac{\Delta G_{fuel(H_2,CO)}^{ox}(T_{stack}, y_{fuel})}{2 \cdot F} - V(I) \right) \end{cases} \quad (29)$$

Deleted: ¶

Formatted: Justified

Deleted: 6

Formatted: Bullets and Numbering

The first equation refers to the entropic heat of reaction, arising from the electrochemical oxidation of H₂ and CO in H₂O and CO₂ respectively, while the second term is related to the irreversibilities originated by the cells' overvoltages.

The air excess ratio is the parameter used to control the stack temperature; it can be calculated solving the energy balance equations around a control volume representative of the stack itself; the following expression is obtained for the air excess ratio:

$$\lambda_{air} = \frac{Q_{stack} + Q_{ref} + Q_{fuel}}{n_{air,stech} \cdot c_{p,air} (T_{stack} - T_{air,inlet})} \quad (30)$$

The stack air inlet temperature has been set to 750 °C, as measured during the real generator operation. A particular feature of the Siemens BoP is the air pre-heating zone, which is integrated into the stack 'hot-box'. The cathode inlet air enters the generator at the upper side. As the air heads down towards the stack, it encounters the after-burner unit, just located at the top of generator. In this way, the inlet air, before entering the stack, is preheated to the temperature mentioned before.

4.3 System model

Several works on the modelling of a complete SOFC system are available in literature. Notably are those reported in [19-25]; among these, only Riensche et al. [19,20], Marsano et al. [21], Milewski et al. [22] and Campanari [23] have included an ejector model in their simulations. Of these, just Marsano included a detailed fluid-dynamic description of the ejector-based recirculation system, and accounted in his model for a detailed ejector geometry.

The other equations required to describe the generator behaviour consist of mass and energy balances throughout each component of the BoP, coupled to the electrochemical balances and reactions previously described for the stack (which are basically the Faraday's law and an electrochemical polarisation model of the tubular cell). A simple combustion model for the after-burner is used for the stack exhaust burning.

- Deleted: ¶ ... [41]
- Deleted: expression
- Deleted: .
- Deleted: is linked to the thermal ... [5]
- Deleted: simply
- Deleted: by applying
- Deleted: an
- Deleted: to
- Formatted: Bullets and Numbering
- Deleted: ¶ ... [6]
- Formatted: Left, Indent: Left: 0 pt
- Deleted: (29)
- Formatted ... [7]
- Deleted: in the stack
- Deleted: real operation of the generator
- Deleted: comes from
- Deleted: stack
- Deleted: upper side
- Deleted: .
- Deleted: As
- Deleted: the air
- Deleted: flows
- Deleted: through the top area of ... [8]
- Deleted: where
- Deleted: zone
- Deleted: is located, it
- Deleted: mentioned above
- Deleted: before reaching the cell ... [9]
- Deleted: System model
- Formatted: Font: Italic
- Formatted ... [10]
- Formatted: Font: Italic
- Deleted: Examples
- Deleted: of
- Deleted: s
- Deleted: can be found
- Deleted: in
- Deleted: 3
- Deleted: only
- Deleted: and Milewski et al. [21]
- Deleted: n
- Deleted: . In this manner, a
- Deleted: model
- Deleted: is solved
- Deleted: used for describing

1
2 Since gas mixtures are generally present throughout the system (namely CH₄, C₂H₅OH, H₂, CO,
3
4 H₂O, CO₂, O₂, N₂), detailed polynomial fitting functions for the specific heats, enthalpies, entropies
5
6 and Gibbs function values are considered according to the thermochemical data available from the
7
8 literature [26, 27].

Deleted: Because

Deleted: available

Deleted: from

Deleted: 4

Deleted: 5

Deleted: ¶

Deleted: ¶

Deleted: model

10 4.3.1 Ejector

11 The ejector is one of the most important components of the BoP since a proper management of
12
13 anode recirculation mechanism is crucial to safely operate the generator. The ejector is required to
14
15 provide the reformer with a sufficient amount of steam, which has to be enough to fully reformat
16
17 the NG hydrocarbons (of which CH₄ is the most abundant) as well as to avoid carbon deposition on
18
19 the catalyst present in the reformer or in the piping within the generator. The ejector behaviour for
20
21 SOFC applications is well described in [21,28,30]. The fluid-dynamic equations used in this work
22
23 are those proposed by Zhu et al. [28,29]. The ejector has a nozzle where the fuel (natural gas or
24
25 NGEtOH/H₂O as in our case) is injected at a relatively high pressure and accelerated at sonic
26
27 velocities (Ma > 1). The fuel flow ('primary flow') is thus able to entrain a secondary flow, which
28
29 is a fraction of the total anodic exhaust produced into the stack. The entrainment is mainly due to
30
31 the combined effects of viscous forces and a local pressure differential occurring at the nozzle outlet
32
33 between the primary and the secondary flows. The model considered solves the conservation
34
35 equations (of mass, momentum and energy) at the main sections of the ejector. The assumption of
36
37 the fuel reaching a Ma > 1 at the nozzle outlet is used to determine the velocity profile of the
38
39 secondary flow between the primary/secondary streams boundary and the wall. This assumption
40
41 was verified observing that the inlet fuel pressure measured at the nozzle inlet was always such to
42
43 enable a critical flow through the nozzle, which indeed means having a Ma = 1 at the nozzle throat.
44
45 Further detail on this aspects are nicely reported in the extensive work on ejectors developed by De
46
47 Chant [31]. The mass flow of the entrained secondary stream is finally determined integrating the
48
49 radial velocity profile over the available flow area and multiplying it over the density [28].
50

Deleted: on

Deleted: inside

Deleted: for SOFCs applications

Deleted: 6

Deleted: -

Deleted: 29

Deleted: 6

Deleted: 7

Deleted: fuel

Deleted: flow

Deleted: In this way t

Besides the fuel nozzle area, the ejector includes a mixing zone, where the two flows have time and space enough to get homogeneous before entering the reformer/stack zone, and a diffuser which converts part of the dynamic pressure of the flow into static pressure in order to overcome the reformer and stack fuel compartment pressure drops. A schematic design of the ejector is reported in Figure 6.

Figure 6 - Ejector scheme

The primary flow is accelerated in the nozzle (just convergent in our design) to obtain high entrainment ratios of the secondary flow: the anodic exhaust. The molar entrainment ratio of the ejector is hence defined as the ratio between the recirculated flow (a fraction of the total anodic exhaust) and the incoming fresh fuel:

$$\omega = \frac{n_s}{n_p} = \frac{f_{recirc} \cdot n_{exhaust}}{n_{fuel}} \quad (31)$$

Since an ejector is generally designed to operate at supersonic speeds, the inlet primary fuel flow passing through the nozzle can be expressed by the following relation:

$$G_{fuel} = \sqrt{f_{loss} \cdot k \cdot R} \cdot \left(\frac{2}{k+1} \right)^{\frac{k+1}{2(k-1)}} \cdot \rho_{fuel} \cdot A_t \cdot \sqrt{T_{fuel}} \quad (32)$$

The previous equation expresses the critical mass flowing into a nozzle of a defined geometry (where A_t represents the throat area of the nozzle), once provided the thermodynamic properties of the fluid. By substituting the ideal gas law into the density term, the pressure term becomes explicit.

As stated before, the ejector has the task of providing enough steam for reforming the NG. Rather than using an external water source, the steam produced by the electrochemical oxidation of H_2 is internally "recycled", and part of it is transferred from the stack zone to the reformer zone. At the top of the anodic chamber containing the tubular cells, a duct is placed in such a way to permit part of the anodic exhaust to reach the ejector. The exhaust anodic gas consists of a mixture of unspent fuel (H_2 , CO), whose quantity depends on the FU of the generator, and by-products of the

Deleted: T

Deleted: 3

Formatted: Bullets and Numbering

Deleted: ¶

$$\omega = \frac{n_s}{n_p} = \frac{f_{recirc} \cdot n_{exhaust}}{n_{fuel}} \dots ($$

30)¶
Because

Formatted: Bullets and Numbering

Deleted: ¶

$$G_{fuel} = \sqrt{f_{loss} \cdot k \cdot R} \cdot \left(\frac{2}{k+1} \right)^{\frac{k+1}{2(k-1)}} \cdot \rho_{fuel} \cdot A_t \cdot \sqrt{T_{fuel}} \quad (31)¶$$

Formatted: Indent: Left: 0 pt

Deleted: Substituting

Deleted: the

Deleted: of

Deleted: as

1 electrochemical reactions (H_2O , CO_2). Since the driving force to entrain the exhaust gas is provided
 2 by the accelerated primary fuel (NG) through the ejector nozzle, once the ejector geometry is fixed,
 3
 4 the fraction of the anodic exhaust recirculated depends on its molar composition and on the
 5
 6 thermodynamic state and mass flow of the primary stream.

Deleted: Because

Deleted: when

Deleted: of

Deleted: fluid along with its mass flow

Deleted: ¶

10 4.3.2 Reformer and after-burner

Deleted: hydrocarbons

11 The component where the reforming of NG takes place to produce hydrogen and carbon monoxide
 12 is the so-called 'in-stack reformer'. The reformer is placed just between the two central bundles of
 13 the generator. The BoP has been designed in such a way that the high endothermic reforming
 14 reactions receive heat directly from the bundles where heat sources are actually located. The heat
 15 exchanged between the reformer and the stack bundles is predominately ruled by radiative
 16 phenomena. Since the reformer is receiving heat from the stack, its average temperature is always
 17 lower than that of the stack. In our calculations, the reforming equilibrium reactions have been
 18 carried out at a temperature of 800 °C. This temperature can be regarded as an average between the
 19 reformer inlet and outlet temperatures.

Deleted: is basically the

Deleted: mean of

Deleted: find

Deleted: our

Deleted: was used

Deleted: this

Deleted: study

Deleted: , as reported by gas analysis measurements

Deleted: .

Deleted: of the CH_4

Deleted: ont

Deleted: o

Deleted: all of

Deleted: available

Deleted: almost

Deleted: in reacting with

Deleted: basically

Deleted: A

Deleted: therefore

Deleted: (

Deleted: it does not for

Deleted: ,

Deleted: is

Deleted: in a significant amount

Deleted:)

29 A chemical equilibrium software provided by NASA [24], based on the minimisation of the Gibbs
 30 free energy, has been used to determine the equilibrium composition of the flow entering the
 31 reformer (fresh fuel + anodic recirculated flow). The NASA code, written in FORTRAN, has been
 32 built into a Matlab© code, which we developed to solve all of the equations reported in the present
 33 work.

34 The reformer is catalysed by Ni-Al-Mg pellets through which the fuel mixture flows. In the real
 35 plant operation, up to 95% of the methane fuel is known to be converted inside the reformer. The
 36 rest is converted directly over the cells' anode surface. In our calculations, the methane is allowed
 37 to react entirely in the reformer. The reformer is treated as being completely selective towards H_2O
 38 in the methane conversion reactions, while the CO_2 remains unreacted. In this way, a full steam
 39 reforming reaction takes place, while dry-reforming is completely inhibited even if the CO_2 is
 40 available, as significant fraction in the recirculated flow, CH_4 is by itself thermodynamically more

favoured to choose steam rather than CO₂, if both available, for its conversion in H₂ and CO, but of course is the catalyst chosen inside the reformer that determines the reactions taking place inside it. Our assumption is therefore supported by the particular catalyst known to be available in the reformer. The reformer selectivity has been intrinsically taken into account in our model as a non-reacting CO₂ was constrained within the equilibrium routine solved for calculating the reformer outlet composition.

The fraction of the anodic exhaust that is not recirculated join the exhaust air in the upper part of the stack module; the after-burner-zone.

The after-burner section is the region where the hot exhaust cathodic air and the non-recirculated fraction of the anodic exhaust mix together in a combustion chamber. What actually burns are the H₂ and CO not consumed by the electrochemical reactions within the stack. The combustion is therefore strictly related to the generator FU. The combustion has been modelled again by a tool available within the NASA program, CEA [24], assuming a constant volume and pressure combustion, which is highly representative of what actually takes place in the after-burner region of the generator.

A final consideration has to be made for some internal combustion of H₂ and CO inside the stack, which introduces the concept of fuel consumption (FC). Inside a stack, some air leaks into the anode chamber due to imperfect sealing between the anode and cathode compartments. This phenomenon is due to the alumina structure holding the tubes in place, which is not completely gas-tight. The FC is defined as the overall fraction of H₂ and CO consumed inside the stack, either by electrochemical or combustion processes, while the FU just takes into account the electrochemical consumption. For the 5 kW Generator, the FC is estimated to be around 3% higher than the FU.

Once the leak is fixed, the fuel flow and the operating FU automatically determine the overall amount of H₂ and CO burning inside the stack. This kind of direct internal combustion inside the stack has a detrimental effect not just in terms of wasted fuel, but also in terms of thermal management of the stack itself. The combusted H₂ and CO generate more heat that if they were

Deleted: likely

Deleted:

Deleted: reforming

Formatted: Subscript

Deleted: but

Deleted: is

Deleted: especially sensitive to the catalysts chosen inside the reformer

Deleted: that play an important role in selecting one reaction over another

Deleted: of the reformer

Deleted: "

Deleted: "

Deleted: the

Deleted: equilibrium calculation

Deleted: performed in the model,

Deleted: imposed as a constraint

Deleted: solving

Deleted: mixes

Deleted: with

Deleted: :

Deleted: is

Deleted: fraction of CO and

Deleted: ; therefore, t

Deleted: operating FU of the

Deleted: present in

Deleted: ,

Deleted: ,

Deleted: fixed

Deleted: is

Deleted: when they are

converted electrochemically. We accounted for this phenomenon in our model, and its effect on the air excess is not negligible. Actually taking into account this aspect, the calculated air excess ratio was in a better agreement with the value experienced by the generator during its real operation.

- Deleted: at all.
- Deleted: , considering
- Deleted: that
- Deleted: real

4.4 Model validation

The complete system model has been validated against experimental data available from the 5 kW Siemens generator. The output stack voltage provided by the model matches that of the real system at an operation point within the nominal range of the generator (120 A of stack current and an FU of 85%), as well as in a wide interval of off-design points, with a stack current ranging from 100 to 170 A. The voltages predicted by the model reproduce the experimental ones with a maximum relative error of 2%.

- Formatted: Bullets and Numbering
- Deleted: whole
- Deleted: for the

The model has been validated for the reference case (NG feeding) also verifying a close match between the modelled and the real generator in terms of other significant operating, such as λ_{air} , W_{th} , f_{recirc} and $STCR$, which were either available from the BoP design or directly measured during the generator operational life.

- Deleted: with respect to
- Deleted:) and
- Deleted: considering
- Deleted: values measured on the generator SFC5a6, specifically $W_{el,DC}$.

In particular, the excess air ratio requested by the stack to keep its temperature constant at 970 °C was calculated by the model with value very close to the real measured one (3.47 against an experimental value of 3.34, at 120 A).

- Deleted: .
- Deleted: needed
- Deleted: generator
- Deleted: obtained by the model
- Deleted: was very close to that o
- Deleted: f the real generator
- Deleted: ¶
¶

5 System simulation results

The model described in the previous section was solved iteratively as to compute the ejector module, an initial guess over the anode recirculated molar fraction was necessary. At each iteration step, the exhaust molar composition is corrected and updated until convergence is reached. A schematic diagram of the iteration step within the system model is shown in Figure 7.

- Deleted: ;
- Deleted: 4

Figure 7 - Schematic sheet describing the iteration step for determining the molar composition of the anodic exhaust

The results of the system model numerical simulations that illustrate the main energy fluxes exchanged within the SOFC generator with two different fuels feeding, methane and ethanol, are respectively reported in Figures 8-9. The simulations are evaluated both at a stack current of 120 A.

Deleted: system simulation results

Deleted: , respectively

Deleted: both

Deleted: with a

Deleted: ¶

Deleted: a

Deleted: stack

5.1 System modelling of the 5kW generator fuelled by natural gas (reference case)

The system simulation results of the generator running on natural gas are reported in Figure 8. It can be observed how the generator is working with a safe STCR, over 2.5, and an air excess ratio that is relatively low due the highly endothermic reaction of the methane reforming. The power ratio of the plant (defined as net AC electrical power output over thermal one) is ~ 1.15.

Figure 8 - Detailed flow-sheet with natural gas reference case

The net electrical AC efficiency is over 48%, which is close to the value observed in the real plant.

Actually, a value around 44-45% is measured in the real configuration, essentially because of bad inverter efficiency, while in the model a value as high as 95% was used.

Deleted: of

Deleted: the

Deleted: in the real system is

Deleted: not as high as the value used in the model, which

Deleted: is

The temperature of the anodic exhaust reaching the ejector has was taken at 925 °C rather than the 970 °C of the stack. This correction has been used to match the real operation of the generator, where the anodic exhaust cools down slightly before reaching the ejector. The temperature of the mixed flow at the outside of the ejector is calculated using this corrected temperature. An identical assumption has been made for the ethanol case, where again the secondary ejector flow was set at 925 °C.

Deleted: been fixed at a temperature of 925

Deleted: instead of

Deleted: (

Deleted: the operating temperature of the stack)

Deleted: on

Deleted: is

Regarding the fuel temperature at the ejector inlet, again a temperature of 700 °C was experimentally derived. The fuel pipe reaching the ejector passes before through the combustion zone of the stack (the after-burner), where is heated near the temperature indicated above.

Deleted: Consideration on t

Deleted: inlet temperature at the ejector is also necessary. The temperature of

Deleted: is

Deleted: again

Deleted:

Deleted: wher

Deleted: e the exhaust gases burn

Deleted: and is

Deleted: important while

Deleted: .

A correct determination of the ejector inlet flows' temperatures is fundamental when solving the ejector model to correctly evaluate the thermodynamic state of the inlet flows.

As a concluding remark on this section, each flow cooling or heating inside the generator 'hot-box' has always been accounted for in such a way as to preserve the consistency of the energy conservation principle.

5.2 System modelling of the 5kW generator fuelled by ethanol

The simulation results for the ethanol feeding are reported in Figure 9. Ethanol is provided to the stack through a pump that extracts the liquid fuel from a reservoir tank and conveys it to a vaporiser (steamer of the actual BoP). The power absorbed by this component is a negligible fraction of the electric output of the plant. A favourable feature of dealing with liquid fuels is the possibility of having a pump instead of a compressor to flow the fuel into the ejector, with an associated enthalpy change much lower than that required when compressing a gas.

Figure 9 - Detailed flow-sheet with ethanol feeding

By comparing the two flow sheets in Figures 8 and 9, it can be concluded that the ethanol feeding produces overall system performances comparable with those achieved with the reference natural gas fuel. The net AC efficiency drops of about 3 points when the fuel is switched from natural gas to pure ethanol. An higher LHV to produce the same overall quantity of stack current is required by the ethanol fuel. This accounts for ~1.5% of efficiency loss. The remaining loss arises from the higher power consumption of the blower due to the increased air excess of the ethanol-fuelled stack.

The local Nernst voltage curves for NG and EtOH under a stack current of 120 A are reported in Figure 10. The curves have of course a similar trend, where the voltage drop observed is related to the gradual consumption along the tube of the reactive moles due to the electrochemical reactions occurring in the cell. Apart from the terminal region of the tube, the Nernst cell voltage is always higher for ethanol than for methane. The lower STCR achieved with ethanol means a less-diluted anode fuel which consequently brings a slower descent of the open circuit voltage as the fuel reactive moles (H₂ and CO) are depleted along the tubular cell channel. Nevertheless, at the tube

- Deleted: a general
- Deleted: energy conservation inside the model
- Deleted: a
- Deleted: stack
- Deleted: 10
- Deleted: Actually, a
- Deleted: potential positive
- Deleted: a
- Deleted: generator
- Deleted: since the
- Deleted:
- Deleted: associated with compressing a liquid is
- Deleted: an that
- Deleted: by
- Deleted: ¶
- Deleted: 9
- Deleted: 10
- Deleted: is just
- Deleted: percentage
- Deleted: lower
- Deleted: is used instead of natural gas
- Deleted: is required for producing
- Deleted: with
- Deleted: as compared to NG
- Deleted: a
- Deleted: comes
- Deleted: Nevertheless, the polarisation of the stack when ethanol fuel is feeding the generator is actually slightly higher than for NG. Under the hypothesis of a proper reforming of ethanol, the fuel quantity in both feeding cases is such as to preserve the overall H₂-equivalents entering the system. Thus, the Nernst voltage of the stack should not be affected significantly. This aspect has been analysed in more detail by (... [11])
- Deleted: polarisation
- Deleted: with
- Deleted: the
- Deleted: same
- Deleted: for
- Deleted: taking place over
- Deleted: Except for
- Deleted: in
- Deleted: The reason for this is that a
- Deleted: is
- Deleted: and a
- Deleted: causes

end the lower local FU obtained with the ethanol feeding is responsible for the more pronounced local Nernst voltage drop (see section 5.3 for a detailed explanation of the local FU).

Figure 10 - Comparison of the calculated Nernst voltage along the fuel channel (cell tube length) for both natural gas and ethanol feeding

Deleted: Figure 9 - Detailed flow-sheet with ethanol feeding

With reference to the ethanol feeding case, the ejector recirculation system is able in principle to provide enough water for the reforming reaction, thus avoiding the need for an external water source; as explained with further detail later in this section, the lower STCR achieved by the ethanol fuel is essentially due to a different exhaust molar composition (richer in CO) established in the anodic exhaust.

Formatted: English (U.K.)

Deleted: The

Deleted: in the ethanol case is in principle able

Formatted: Normal

The lowered STCR achieved is enough to avoid carbon deposition from equilibrium thermodynamic considerations, but its value is just located on the lower bound of a safety range, which generally lies between 2 and 2.5. A possible way to compensate for a too low STCR, without changing the ejector design, could be directly mixing some water with the ethanol feeding stream. Since water and ethanol have very similar vaporisation points, they could be easily mixed together when in the liquid phase, and subsequently vaporised and conveyed together to the ejector nozzle (this will be actually the solution adopted by the Authors in the experimental part of this work).

Deleted: the STCR

Deleted: is just

Deleted: at

Deleted: the

Deleted: generally

From the simulations results obtained, a mass entrainment ratio of ~8 is obtained with NG, while a much lower value of ~3 is obtained with EtOH. The main reason is that when EtOH is used as a fuel, the primary flow in the ejector nozzle is almost doubled on a mass basis, consequently the available flow area for the secondary stream is significantly decreased, and eventually a reduced entrained secondary flow is obtained (values of $11.0 \times 10^{-4} \text{ kg s}^{-1}$ and $7.7 \times 10^{-4} \text{ kg s}^{-1}$ are respectively obtained for NG and EtOH).

Deleted: The reason for the lower STCR is related to the lowered recirculation factor achieved in the ejector (0.52 versus 0.65 with NG); in addition to this, a different exhaust molar composition (richer in CO) can lower the STCR (this aspect is discussed further on this paper with more details). The lowered STCR is enough to avoid carbon deposition, from a thermodynamic point of view.¶

Formatted: Superscript

The following considerations explain with some more detail why the primary flow increases while changing the inlet fuel. Ethanol and natural gas have a molecular weight ratio of 46:16, while 2:3 is the ratio established to produce the same amount of electricity regardless of the fuel used (for a

better clarification on this peculiar feature see Section 6.1 as well). These two ratios should be multiplied together to get the NG:EtOH mass flow inlet ratio. A value close to 2 is obtained, exactly meaning that an almost doubled mass flow passing through the ejector nozzle is established when the fuel is changed from NG to EtOH.

We have now clarified the reasons behind a different mass entrainment ratio between the NG and the EtOH fuels. Nevertheless, the ejector entrainment ratio would be more meaningful if expressed on a molar basis, being the STCR defined on the very same basis. Under the assumption (quite realistic according to our calculations) that the average molecular weight of the anodic exhaust is identical between NG and EtOH, the mass entrainment ratio achieved for each fuel can be related to the molar one by simply multiplying the former ratio for the molar ratio of the two fuels (which is 2:3, according to the strategy of keeping constant the electricity produced by the generator and thus the H₂-equivalents number entering the stack). If the value obtained is multiplied over the ratio of secondary mass flows established by each fuel (which is 7.65:11, as reported before), a value close to 1 is now found, meaning that eventually almost the same molar entrainment ratio is obtained for both the fuel feeding cases, consistently also to what reported in Figure 8 and 9.

In Table 2 the molar entrainment ratios and the molar compositions of the recirculated flow for both NG and EtOH are reported. The water entrained by the ejector normalised to the molar flow of fuel entering into the stack is reported as well: from now on this parameter will be defined as the H₂O stoichiometry of the ejector. Otherwise, the STCR is defined according to the following formula:

$$STCR = \frac{y_{H_2O} \cdot n_{an,recirc}}{n_{fuel} + y_{CO} \cdot n_{an,recirc}} \quad (33)$$

The difference between the two parameters lies in that the STCR accounts also for the CO in its definition, being this species potentially able to produce carbon deposition as well as CH₄.

As shown in Table 2, and provided that methane and ethanol require the same stoichiometric amount of water in the reforming process, the H₂O stoichiometry achieved for both fuels is

Formatted: Font: (Default) Times New Roman

Formatted: Subscript

Deleted: Referring to the lower entrainment achieved in the ejector with ethanol fuel, a simple explanation is that a lower mass flow (compared to the reference NG) is entering into the fuel nozzle and thus less driving force is available to entrain the secondary flow. A possible way to compensate for this, without changing the ejector design, could be to provide some kind of 'support flow' into the nozzle. Since water and ethanol have very similar vaporisation points, they could be mixed and vaporised together, and then conveyed to the nozzle. In this case the STCR would raise for two reasons: i) a direct one, which of course is due to the extra water present into the ethanol feeding, ii) an indirect one, which is the increase of the entrainment ratio due to the augmented flow entering the nozzle.

Formatted: Line spacing: Double

Deleted: 1

Deleted: in

Deleted: feeding cases

Deleted: also calculated and

Deleted: stoichs

Deleted: Instead

Deleted: , t

Deleted: as the

Deleted:

Deleted: ¶

Deleted: ¶ ... [12]

Formatted: Left

Formatted: Bullets and Numbering

Deleted: (36)¶

Formatted: Tabs: 460.7 pt, Left

Deleted: ¶

Deleted: For the fuels consider ... [13]

Deleted: is

Deleted: is also accounted for ... [14]

Deleted: recognising it as

Deleted: a

Formatted: Subscript

Deleted: 1

Deleted: considering

Deleted: procoess

Deleted: stoichs

Deleted: in

Deleted: feeding cases

Deleted: are

essentially the same. The fact of having a lower STCR for the ethanol is only due to the higher amount of CO present in its anode exhaust gas, as already mentioned before.

Table 2 - Molar compositions of the recirculated flow entrained by the ejector and total steam fraction recirculated normalised to the primary flow entering the ejector itself

The power ratio is ~ 1 for the ethanol fuel, meaning that almost the same amounts of electrical and thermal powers are generated. The air excess λ is almost 40% higher than the NG reference fuel, due to an overall less endothermic reaction in the reformer zone. This aspect is further analysed and explained in more detail in the next section, where some experimental evidence is brought to show how the reformer increases its mean temperature due to the presence of a less endothermic reaction when ethanol replaces NG flow.

5.3 Local FU of the generator

An useful and meaningful parameter to monitor within the stack is the local FU achieved. The values caclualted for the NG and EtOH are respectively 78.0% and 82.4%.

In what following, we briefly derive an expression of local FU in terms of the other significant parameters of the generator.

The local FU is defined as:

$$FU_{local} = \frac{I_{TOT}/2F}{n_{H_2,CO}^+} = \frac{FU \cdot (1 - f_{recirc})}{1 - FU \cdot f_{recirc}} \quad (34)$$

The expression in Eq. 34 is derived considering that the molar flow reaching the cell ($n_{H_2+CO}^+$) in terms of H₂ and CO is the sum of two contributions: i) the inlet methane converted in the reformer, and ii) the H₂ and CO present in the recirculated anodic flow. This term is then written as:

$$n_{H_2,CO}^+ = n_{H_2,CO}^{CH_4} + f_{recirc} \cdot n_{H_2,CO}^+ \cdot (1 - FU_{local}) \quad (35)$$

The global FU is defined as:

Deleted: feeding

Deleted: produced

Deleted: .

Deleted: .

Deleted: which is ascribed

Deleted: shown

Deleted: . In this experiment,

Deleted: ¶

Deleted: It is interesting to evaluate

Deleted:

Deleted:

Deleted: by each of the two feeding cases

Deleted: .

Deleted: with the ethanol fuel and 78% with natural gas. The local FU can be also directly related to the polarisation difference observed between the NG and EtOH feeding cases. ¶

Deleted: the

Formatted: Bullets and Numbering

Deleted: ¶

$$FU_{local} = \frac{I_{TOT}/2F}{n_{H_2,CO}^+} = \frac{FU \cdot (1 - f_{recirc})}{1 - FU \cdot f_{recirc}} \quad (32)¶$$

Deleted: 2

Deleted: (in terms of H₂ and CO) r

Deleted:

Deleted: The

Deleted: overall reactive species can be written as

Formatted: Bullets and Numbering

$$n_{H_2,CO}^+ = n_{H_2,CO}^{CH_4} + f_{recirc} \cdot n_{H_2,CO}^+ \cdot (1 - FU_{local}) \quad (34)¶$$

$$FU = \frac{I_{TOT}}{2F \cdot n_{H_2,CO}^{CH_4}} \quad (36)$$

Combining Eqs. 35 and 36, yields the expression reported in Eq. 34.

The local FU is useful to define the fuel utilisation which is effectively experienced by a stack where an anodic exhaust ‘recycling’ (or recirculation) is carried out. Since the ethanol-fuelled generator brings a lower recirculation fraction of the anodic exhaust, a less diluted fuel enters the stack. This has a positive effect on the Nernst voltage (as pointed out before). At the same time, the Nernst voltage is sensitive to the FU (the latter increasing, the former decreasing). The local Nernst voltage behaviour for the ethanol fuel (as observed in Figure 10) brings with it exactly these two contrasting effects (higher local FU, but with a less diluted fuel).

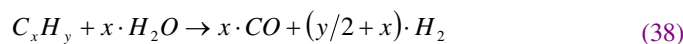
6 The preliminary experiment with ethanol fuel

6.1 Experimental

The SFC 5 kW system has been tested for few hours with a mixture of ethanol and water. During the experiment, the ethanol mixture has been progressively replacing the NG nominal flow. The latter can be calculated once the stack DC current, operating FU and fuel composition are known. The overall fuel flow required by the stack at a specified current load and FU is given by the following formula:

$$n_{FUEL} = \frac{(I_{stack} / 2) \cdot n_{cells}}{2 \cdot F} \cdot \frac{1}{H_{2,eq}^{reform\ min\ g} \cdot FU} \quad (37)$$

In the above expression, the stack current is related to the molar flow of inlet fuel. The H₂-equivalents is a value characteristic of each fuel or fuel mixture. By definition, the number of H₂-equivalents expresses how many reactive moles are obtained by an un-reformed fuel mol undertaking a complete steam reforming reaction:



Formatted: Bullets and Numbering

Deleted: ¶

$$FU = \frac{I_{TOT}}{2F \cdot n_{H_2,CO}^{CH_4}}$$

(35)¶

¶ 3-...4...5

[15]

Deleted: defines ...that is...in which...achieves ..., and ...an ...e of FU causes it to ...e...In this sense, t...generates ...two ..., but... which sum together and finally produce an overall positive effect on the Nernst voltage (as observed in Figure 10)...¶
Figure 10 - Comparison of the calculated Nernst voltage along the fuel channel (cell tube length) for both natural gas and ethanol feeding... [16]

Deleted: Experiments: 5 kW SOFC with

Deleted: description

Deleted: several ...In the experimental time period...substituted ...to ...NG flow...According to the standard procedure employed while operating the generator, ...t...is...determined ...upon DC ... load... FU of the generator, and type of fuel entering it. ¶
For simplicity, we refer here just to methane as a fuel (even if the real fuel is natural gas); the methane...is th... [17]

Formatted: English (U.K.), Lowered by 17 pt

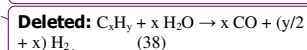
Formatted: Bullets and Numbering

$$Deleted: n_{CH_4} = \frac{(I_{stack} / 2) \cdot n_{cell}}{2 \cdot F} \quad (37)¶$$

¶ a ...reactive species...Two factors can modify Eq. 37: i) the effective fuel consumption (FC), which is greater than the FU, since some air leakage occurs inside the stack (the denominator of Eq. 37 should in fact be FC instead of FU); ii) the stack NG flow is not pure methane, thus the effective inlet molar composition of the fuel gas should be taken into account to calculate the exact number of H₂-equivalents. The modifications due to these two effects are relatively low, because the air leaks inside the generator are rather low and the relative error committed in considering just methane as the fuel flow is lower than 1% when evaluating H_{2,eq}. ¶
number ... of fuels; it has to be taken into account to determine the primary inlet fuel necessary to satisfy a certain... [18]

Formatted: English (U.K.), Lowered by 7 pt

Formatted: Bullets and Numbering

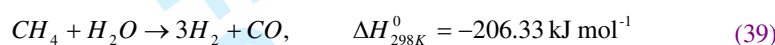


Formatted ... [19]

NG is a mixture of various hydrocarbons plus some N_2 and CO_2 in small amounts. The composition varies from site to site, and significant differences in the methane content subsist over the different countries. From the data records on the NG composition available in Turbocare Spa (IT – Torino), the gas from the grid contained on average a methane fraction of ~ 91-92%.

For simplicity, we always considered the NG as composed of just methane in all our simulations. This of course leads to some inaccuracy in the results obtained. Nevertheless the error was estimated to be less than 1% in the evaluation of the system efficiencies.

The basic idea under which part of the nominal NG flow has been replaced with EtOH was to provide the generator always with the same amount of H_2 -equivalents. The reforming reactions of methane and ethanol are respectively the following:



It is trivial to see how 1 mole of fully steam-reformed ethanol gives 6 H_2 -equivalent reactive moles (H_2+CO) compared to the 4 provided by the methane undertaking the same kind of reforming reaction. The 6:4 ratio obtained is also the one driving the switch from NG to ethanol fuel.

Looking at the reactions listed above, the enthalpy reaction for EtOH reforming is higher than for CH_4 ; but, since for each CH_4 mole just 4/6 EtOH moles are needed, the heat absorbed by the fuel reforming changes with this ratio as well. Considering that the H_2 -equivalent moles are kept the same in both feeding cases, the heat of the reforming reactions for NG is 1.2 higher than that required to reformat EtOH. Therefore, fuelling the stack with ethanol reduces the heat sink of the reforming reaction. As a direct consequence, a higher air mass flow is necessary to keep the temperature constant inside the various cell bundles (this aspect is also clear from the system simulation results reported in Figures 8 and 9, where the EtOH feeding case requires a λ_{air} of 5 against a 3.5 value attained by NG).

The ethanol was not flowed pure to the stack, rather an EtOH/ H_2O mixture was used. The water/ethanol ratio has been set in order to operate the system in safe conditions towards the carbon

Deleted: , upon...stack fuel ...removed and ...an ... mixture,...always ...an overall fuel mixture that was able to provide the stack with the same amount of equivalent reactive moles of H_2 of the nominal NG flow, while undertaking a full steam-reforming ... [20]

Deleted: Taking ...a closer observation at the..., we hav...e ... [21]

Formatted: Subscript ... [21]

Formatted: English (U.K.), Lowered by 6 pt

Formatted: Bullets and Numbering

Formatted: ... [22]

Formatted: Bullets and Numbering

Deleted: ¶

Deleted: $CH_4 + H_2O \rightarrow 3H_2 + CO$, ($\Delta H_{react}(298 K) = 206.33 \text{ kJ mol}^{-1}$) (39)]
 $C_2H_5OH + H_2O \rightarrow 4H_2 + 2CO$, ($\Delta H_{react}(298 K) = 256.79 \text{ kJ mol}^{-1}$). (40)]
 that a ..., when fully steam-refor... [23]

Formatted: Subscript

Deleted: moles ...per mole of steam-reformed...is ...ratio ...es..., thus maintaining the number of H_2 -equivalents constant. ... [24]

Formatted: Subscript

Deleted: /...in-stack ... [25]

Deleted: imposed ...to be ...reforming required ...for a NG...feeding than for an... feeding...aspect ...fully evident in... ...4.7 instead ...of ...with N... [26]

Formatted: Subscript

Deleted: In terms of the ethanol fuel mixture..., t...chosen ...with respect to...carbo ... [27]

deposition. In Figure 11, using the CEA chemical equilibrium software [24], the mixture equilibrium composition, as a function of temperature are plotted for a liquid volumetric EtOH/H₂O ratio of 60/40 (the ratio shifts to 33.3/66.7 with the species in the gas phase). The graph shows how the water content in the mixture is already enough to suppress carbon deposition at temperatures above 600 °C.

Deleted: 8

Deleted: by means of

Deleted: a

Deleted: s

Deleted: against

Deleted: , referring to the species in the liquid state (

Deleted: in the

Deleted: It can be seen

Deleted:

Figure 11 - Equilibrium compositions of an ethanol/water mixture in a volumetric ratio 60/40 at different temperatures

At the stack's nominal operating condition (120 Amps), the ethanol supplied was ~ 3.5 SLPM, while the total EtOH/H₂O mixture was almost 11 SLPM; the NG flow was correspondingly decreased to less than 6 SLPM.

Deleted: simultaneously

The EtOH/H₂O mixture has been supplied through the steam line of the generator; this line was already installed from the beginning in the BoP to provide external steam during start-up and shut-down procedures and at off-load operation. Under these circumstances, either the anodic recirculation flow rich in H₂O or CO₂ is not available or low, to guarantee a safe steam reforming of the NG. The external water reservoir was, with and the liquid EtOH/H₂O mixture. The latter was vaporised in the steamer, and pumped to the stack ejector inlet with a volumetric pump. A schematic view of the experiment set-up is shown in Figure 12.

Deleted: of the system

Deleted: when

Deleted: , or generally when the load is too low to electrochemically provide an internal steam production

Deleted:

Deleted: steamer

Deleted: has been filled

Deleted: both water and

Deleted:

Formatted: Subscript

Deleted: either in a liquid state or

Deleted: by electric heating

Deleted: then

Figure 12 - Schematic view of the 5 kW Generator to respect of the fuel and air feeding flows

The choice of passing the EtOH/H₂O mixture into the ejector is worthy of discussion because the steam already present in the EtOH mixture is enough to suppress carbon deposition at the reformer temperature, as mentioned before. Figure 13 reports the carbon boundary of the ethanol steam reforming reaction calculated using again thermodynamic equilibrium considerations. At 700 °C, 2 mol of H₂O are sufficient to suppress carbon deposition, while even less are required as the temperature grows. Since this was a preliminary experiment, our choice was motivated by safety, meaning that a high amount of H₂O to suppress carbon deposition was voluntarily injected along with the EtOH fuel. The extra steam provided with the exhaust flow recirculated by the ejector

Deleted: It can be seen that a

Deleted: Because

satisfied our safe operation requirement. In addition, it has been reported that ethanol steam-reforming in H₂ and CO is more difficult than methane reforming [32].

Obviously this extra-safe operating condition reduced stack performances, since an excessively high water dilution of reformed fuel negatively affects the Nernst voltage of the fuel mixture entering the stack anode compartment as well as increases the cell overvoltages. This point is discussed with more detail in the next section, where the experimental results are reported.

Figure 13 - Carbon boundary for the ethanol steam reforming

6.2 Results

In Figure 14, the NG and EtOH flow are plotted along with the measured ejector primary pressure. As already described before, the fuel feeding strategy was to gradually substitute the NG flow with EtOH while keeping constant the H₂-equivalents produced respectively by the two fuels, and assuming a complete steam reforming reaction occurring. Thus the mixture entering the ejector (primary flow) consisted partly of NG from the grid and partly vaporised EtOH/H₂O. A complete substitution of NG with ethanol maintaining the nominal stack current load was not possible due to a limitation on the maximum capacity of the pump extracting the liquid fuel from the tank. A maximum EtOH volumetric flow of 15 cc min⁻¹ was achieved. In terms of H₂-equivalents, at the maximum EtOH feeding, half of the generator current load was provided by ethanol, while the remaining half was covered by NG.

Figure 14 - Ejector pressure increase during EtOH/H₂O mixture feeding

In Figure 14, the volumetric flows of NG and EtOH (60% vol. of EtOH tank mixture) are plotted against the volumetric EtOH/H₂O mixture pumped from the liquid reservoir tank. The graph reports the approximate behaviour of the water finally present in the EtOH/H₂O/NG conveyed into the stack during the experiment. The initial water content in the primary fuel is due to the water already present inside the EtOH/H₂O feeding tank. After the ejector, due to the mixing with the recirculated fraction of the anodic exhaust, the overall water content further increases. The hypothesis that the

Deleted: Also

Deleted: production of

Deleted: when using ethanol than when using methane

Deleted: 0

Deleted: , as also

Deleted: later

Deleted: along with

Deleted: Experimental result

Deleted: against time, and

Deleted: is reported

Deleted: in feeding the stack

Deleted: ethanol

Deleted: number of equivalent hydrogen

Formatted: Subscript

Deleted: reactive moles producible

Deleted: Due to the maximum capacity of the pump extracting the liquid from the tank, a maximum volumetric flow of 15 cc min⁻¹ of EtOH mixture was achieved

Deleted: while also maintaining the nominal stack current load

Deleted: With respect to

Deleted: by

Deleted: and the remaining half by ethanol.

Deleted: the

Deleted: versus

Formatted: Subscript

Deleted: ing of the latter tank mixtur

Deleted: e

Deleted: aims to give

Deleted:

Deleted: The ini

Deleted: tial

Deleted:

Deleted: total

Deleted: increased

normalised molar steam flow entrained by the primary flow is constant ~~was assumed~~. In Figure 15, the H₂O stoichiometry behaviour is plotted against an increasing EtOH/H₂O feeding. As stated before, the H₂O stoichiometry represents the actual steam available in the final mixture flowing into the ejector over the stoichiometric water needed for the steam reforming reaction of the NG or EtOH (it should be noted that both fuels need only 1 mol of H₂O for accomplishing the conversion reactions).

The hypothesis ~~made can be~~ only partially justified from what is reported in Table 2, where very similar values for the entrainment ratios and steam-to-fuel ratios are achieved regardless of the fuel. In the experiment, the ethanol is already pre-mixed with some water from the liquid reservoir tank. With respect to the pure ethanol feeding modelled before, now we have an even further increased mass flow entering the fuel nozzle. Such an increased mass flow could actually prevent a proper entrainment of the secondary flow. This is the reason why the assumption of a constant molar entrainment ratio of the ejector during the ethanol experiment, can not certainly considered a conservative one. The H₂O stoichiometry value reported in Figure 15 is probably somewhat higher than the value actually experienced by the reformer.

Figure 15 - Water stoichiometry in the NG/EtOH mixture reaching the stack

According to Figure 15, and to our recommendations about the not-conservative feature of our assumption on the ejector entrainment during the experiment, the steam excess in the fuel flow entering the stack could be regarded as only slightly increased to respect of the nominal NG feeding. This aspect should produce a negative effect on the stack voltage, as already outlined, which is indeed confirmed by the experimental data in terms of a decrease of the stack voltage. In Figure 16, it is evident how the stack voltage reaches a minimum when the EtOH/H₂O mixture is at the maximum level. The voltage loss is quite limited, though: less than 1 V is lost when partly switching the fuel from NG to EtOH as in our experiment. During the experiment, the stack current was kept constant managing the generator control system to force the stack to provide a set amount of current. The system demonstrated the ability to convert the new fuel into H₂ and CO and to

Deleted: was made

Deleted: This assumption means that the ejector is working in a rather flat area of its characteristic curve, where the recirculation factor is almost constant (flat) when varying the inlet primary flow

Deleted: . Such a

Deleted: could

Deleted: also

Deleted: presented

Deleted: !

Deleted: quite

Deleted: similar

Formatted: English (U.K.)

Formatted: English (U.K.),

Formatted: English (U.K.)

Formatted: English (U.K.)

Deleted: In Figure 15, the H₂O stoichs' behaviour is plotted against an increasing EtOH/H₂O feeding. As stated before, the H₂O stoichs represent the excess steam present in the final mixture flow that exits the ejector with respect to the stoichiometric water needed for the steam reforming reaction of the NG or ethanol fuel (it should be noted that both need 1 mol of H₂O to reform one mol of CH₄ or EtOH, respectively). ¶

Deleted: stoichs

Deleted: T

Deleted: total

Deleted: s

Deleted: due to water present in the EtOH flow

Deleted: , which increases during the ethanol experiment as well

Deleted: s

Deleted: gives

Deleted: value

Deleted: by

Deleted: of the generator so as

Deleted: the

1 provide the requested current. This represents only a preliminary result and longer experiments
 2 should be carried out to fully demonstrate the fuel flexibility of the generator. The durability of the
 3 reformer against a new fuel and the possible formation of carbon deposits in a long-term period are
 4 aspects that should addressed with more detail in the future.

Deleted: especially be assessed

Deleted: The reformer is a component to be carefully selected and maybe re-considered in the current system design in order to guarantee stability against fuels different from NG.

5 The 1 V loss could be also partially ascribed to a not proper or full conversion of the EtOH stream
 6 inside the reformer and the stack. Nevertheless, the increased water dilution of the fuel seems to be
 7 a much more plausible explanation. If a not proper catalytic conversion of ethanol was occurring, a
 8 more pronounced stack voltage loss and instable generator behaviour would have been observed.

17 **Figure 16 - Behaviour of stack voltage during the EtOH/H₂O feeding experiment**

Deleted: ¶

Formatted: Heading 1, Left

Deleted: 6

18 In Figure 17, the voltage behaviour for each stack string is reported (each bundle is divided into two
 19 strings electrically connected in parallel for a total number of 4 bundles inside the stack: the 4
 20 voltages for the generator that can be read in the system data logger are representative of each
 21 bundle voltage). The zoom is now on a wider time interval than in Figure 16. Two EtOH testing
 22 phases can be distinguished. The first one was just a short trail, while the second one is the
 23 experiment discussed and reported in Figure 16. Referring again to Figure 17, it is interesting to see
 24 to what extent the string voltages were perturbed each time the ethanol fuel began to flow into the
 25 stack.

Deleted: was used

Deleted: 3

Deleted: is

Deleted: experiment that is

Deleted:

Deleted: In

Deleted: also quite

Deleted: clear how

Deleted: was

Deleted: when

35 **Figure 17 - Comparison of string voltages during the EtOH/H₂O feeding experiment**

36 In Figure 18, on the same time interval as Figure 17, the stack current and voltage are reported
 37 during the experiment. As mentioned before, the current was kept constant during the experiment.
 38 The increase in the last part of it occurs when the EtOH flow has already reached its maximum and
 39 the NG nominal flow is restored. Regarding the behaviour of the generator control system, the
 40 current is generally defined as an external input that the stack is forced to match. However, when
 41 the voltage goes down below the set value, the control system automatically reduces the current
 42 requested to the stack. In Figure 18 is shown how the current was effectively kept constant during
 43

Formatted: Normal, Justified, Line spacing: Double

Deleted: in

Deleted: and current

Deleted: It can be seen that t

Deleted: the text

Deleted: tries

Deleted: In

Deleted: 6, it can be seen that

Deleted: the voltage

Deleted: constant

the ethanol feeding to value only slightly lower than that achieved by NG before the EtOH feeding perturbations.

Deleted: long ..., but ...the va [28]

Formatted: English (U.K.)

Figure 18 - Stack voltage and current behaviour

Figure 19 reports the temperature drop across the reformer as measured during the ethanol feeding.

Formatted: English (U.S.)

The temperature decreases across this component due to the endothermic reforming reactions occurring in it. Since the steam reforming of EtOH normalised to the H₂-equivalents is somewhat less endothermic than that of methane (as previously predicted by the system modelling results as well as by simple thermodynamic calculations on the enthalpies of reaction), a less pronounced temperature drop is indeed observed in the reformer, providing experimental evidence to our previous calculations. It is worth to note how the temperature drop is the lowest when the EtOH feeding is the highest, as we expected.

Formatted: English (U.K.)

Deleted: decrease...s [29]

Formatted: English (U.K.)

Deleted: that occurs

Formatted

Deleted: and also... [30]

Formatted: English (U.K.)

Deleted: y

Formatted: English (U.K.)

Deleted: diminished

Formatted: English (U.K.)

Deleted: ly...confirming [31]

Formatted: English (U.K.)

Deleted: the ...predictions [32]

Formatted: English (U.K.)

Deleted: also evident that

Formatted: English (U.K.)

Deleted: (basically more ethanol reforming is occurring than methane reforming).

Formatted: English (U.K.)

Deleted: s...various...during the ethanol experiment are...reformer ...is diminshe...d...About ...is shown to that happens...therefore [33]

Figure 19 - Reformer temperature drop during the ethanol experiment

In Figure 20, the temperature behaviour of different regions inside the generator is reported. For the reasons already discussed before, the temperature drop across the reformer decreases when ethanol replaces methane. Regarding the absolute temperature of the inlet reformer, it increases. This temperature is related to the mixing of the fresh fuel and the recirculated flow occurring in the ejector. Such an increase could be explained by a hotter recirculated exhaust coming from the stack.

Deleted: ...Temperature [34]

Figure 20 - Generator temperatures behaviour during the ethanol experiment

The air stoichiometry (air excess ratio) is reported in the same graph. The generator control system varies this parameter in such a way as to keep the stack temperature constant. Since a less endothermic reforming reaction is taking place, the stack temperature would increase if the air excess ratio would remain the same when switching the fuel from methane to ethanol. This effect is avoided by the control system increasing the air flow into the stack, leading to an augmented cooling of the generator. The air flow in the generator (and consequently the air stoichiometry

Deleted: also ...since this is the parameter managing the stack temperature. ...behaves ...and the reformer is thermally integrated into the stack, ...it makes sense that the ... should increase...increased...Actually, t...so stoichs [35]

number) is also regulated by the control system to avoid an excessively high temperature increase in the after-burner zone. As reported in Figure 20, when ethanol was provided to the stack, the burner temperature increased by ~ 30 °C. The increased air flow in the stack could therefore have occurred to compensate for this phenomenon. From Figure 20, and according to the temperatures and air flow behaviours measured, the second option looks like as the more plausible. In fact, there is some evidence on how the after burner temperature compensation brought an extra-cooling of the stack at the end of the experiment.

Figure 21 shows how the measured AC efficiency of the system varies during the ethanol experiment. The efficiency reaches its minimum when the ethanol flow is at its maximum, following the behaviour of the voltage. The decrease is only around 1%, underlining how ethanol could substitute methane without any appreciable system performance modifications.

Figure 21 - Generator electrical AC efficiency behaviour during the EtOH experiment

Conclusions

An SOFC tubular generator has been studied and modelled in detail. The main system components and the stack polarisation behaviour have been accounted for within the model. Among the system components, particular consideration was dedicated to the ejector and its role inside the generator as a whole.

The ejector flexibility to a fuel such as ethanol has been theoretically predicted. A safe generator operation could be guaranteed in terms of STCR with the new fuel. The thermal management of stack and its link to the reforming of the inlet fuel has been clearly established: it has been shown how a fuel alternative to NG could be used successfully, without significantly degrading the system performance, provided that a high endothermic conversion of the fuel within the reformer occurs.

According to our analysis, a multi-fuel generator running both on natural gas and ethanol could be feasible. Concerning the actual BoP, the only critical aspect identified is represented by the catalyst

Deleted: not only for keeping the stack temperature constant at a desired set-point, but also

Deleted: 18

Deleted: as

Deleted: , so t

Deleted: could be actually

Deleted: attributed to this

Deleted: as well

Deleted: . ¶

Deleted: From the

Deleted: s

Deleted: of temperatures and air flow

Deleted: and reported in Figure 18

Deleted: , it looks like

Deleted: is the

Deleted:

Deleted: one: the air flow has been growing more to compensate for the high temperature reached in the after-burner rather than to control the stack temperature

Deleted: .

Deleted: It can be seen in Figure 18

Deleted: that

Deleted: the stack is indeed extra-cooled

Deleted: In Figure 21, it is also interesting to observe how the inlet reformer temperature behaves similarly to that of the after-burner. The reformer temperature is governed by the fuel inlet temperature and the anodic exhaust temperature. If we consider the fuel inlet temperature to be constant, the anodic exhaust temperature is the one really affecting and governing that of the inlet reformer zone. We should also consider that the anodic exhaust has basically the same temperature of the stack at ... [37]

Deleted: 2

Deleted: 2

Deleted: the

Deleted: considered

Deleted: in

Deleted: attention

Deleted: has been paid

Deleted: The local FU has been ... [38]

Deleted: and it has been shown how a

Deleted: of the system

Deleted: Based on

Deleted: multi-fuel

Deleted: on

Deleted: One issue to note is th ... [39]

Nomenclature

1			
2			
3			
4	A_f	throat area of fuel nozzle inside the ejector / m^2	
5	BoP	balance-of-plant	
6	D	mean tubular cell mean diameter / m	
7	D_i	diffusion coefficient of species i / $cm^2 s^{-1}$	
8	D_i^K	Knudsen diffusion coefficient of species i / $cm^2 s^{-1}$	Formatted: English (U.K.), Lowered by 6 pt
9	E	activation energy / $J mol^{-1}$	Formatted: Superscript
10	EtOH	abbreviation for ethanol	
11	F	Faraday constant / $96485 C s^{-1}$	
12	f_{loss}	frictional loss coefficient	
13	F_{recirc}	recirculated fraction of the anodic exhaust	
14	FU	(global) fuel utilisation (referring to the inlet NG flow)	
15	FU_{local}	effective fuel utilisation experienced by the stack	
16	$G_{an,exhaust}$	exhaust anodic flow exiting the stack / $kg s^{-1}$	
17	G_{fuel}	fuel flow into the ejector / $kg s^{-1}$	
18	G_{ref}	mixed fuel flow entering the reformer / $kg s^{-1}$	
19	$G_{stack,inlet}$	reformed fuel flow entering the stack anode side / $kg s^{-1}$	
20	$H_{2,eq}$	H_2 -equivalents	
21	H_2O stoichiometry	moles of H_2O (steam) over stoichiometric moles of H_2O for reforming a selected fuel	Deleted: stoichs
22			
23	I	electric current / A	
24	I_{CELL}	electric current of a single cell / A	
25	I_{TOT}	total current requested/produced by all the stack cells ($= n_{cells} \cdot I_{cell}$) / A	
26	j	current density / $A cm^{-2}$	
27	$j_{0,an}$	anodic exchange current density / $A cm^{-2}$	
28	$j_{0,cat}$	cathodic exchange current density / $A cm^{-2}$	
29	k	isentropic coefficient of the ideal gas	
30	l	cell layer thickness / m	
31	LHV	low heating value / W	
32	M	molecular weight of species i / $g mol^{-1}$	
33	Ma	Mach number	Formatted: Font: Not Italic
34	n_{cells}	total number of tubular cells inside the stack ($= 88$)	
35	N	total number of discretised steps for solving the 1D cell domain	
36	NG	abbreviation for natural gas	
37	n_i	molar flow of species i / $mol s^{-1}$	
38	p	absolute pressure / Pa	
39	Q_{comb}	heat generated from the combustion of exhaust H_2 and CO in the after-burner / W	
40	Q_{evap}	heat required to evaporate the liquid fuel in the tank / W	Deleted: for evaporating
41	Q_{fuel}	heat required to heat the fuel at the stack temperature / W	
42	Q_{loss}	heat generated by irreversibilities of the stack polarisation / W	Deleted: ¶
43	Q_{react}	heat generated by the oxidation of H_2 and CO inside the stack / W	
44	Q_{ref}	heat required by the reformer / W	
45	Q_{stack}	overall internally heat produced by the stack / W	
46	r	mean pore radius / m	
47	SLPM	standard litre per minute	
48	STCR	steam-to-carbon ratio	
49	T_{stack}	operating temperature of the stack / $^{\circ}C$	
50	V	voltage / V	
51	w	interconnector width / m	

1		
2	W_{th}	available thermal power form the stack / W
3	y_i	molar fraction of species i
4	ε	electrode porosity
5	η	cell overvoltage / V
6	λ_{air}	air excess
7	ρ	gas density (kg m^{-3}) / electronic resistivity (ohm m) in Eqs. 3-6
8	τ	electrode tortuosity
9	ω	ejector molar entrainment ratio

10
11 *Subscripts and superscripts*

12	<i>act</i>	activation
13	<i>an</i>	anode
14	<i>cat</i>	cathode
15	<i>channel</i>	gas channel (outside the electrodes diffusion layer)
16	<i>diff</i>	diffusion
17	<i>ely</i>	electrolyte
18	<i>eq</i>	equivalent
19	<i>felt</i>	Ni-felt
20	<i>int</i>	interface (electrode/electrolyte)
21	<i>inter</i>	interconnector
22	<i>ohm</i>	ohmic
23	<i>ox</i>	oxidant
24	<i>pore</i>	electrode pore
25	<i>recirc</i>	recirculation
26		
27		
28		
29		
30		
31		
32		
33		
34		
35		
36		
37		
38		
39		
40		
41		
42		
43		
44		
45		
46		
47		
48		
49		
50		
51		
52		
53		
54		
55		
56		
57		
58		
59		
60		

Deleted: K . . Knusden

Formatted: Left

References

- [1] S.C. Singhal, *Solid State Ionics* **2005**, 135(1-4) 305-313.
- [2] M. Gariglio, M., F. De Benedictis, M. Santarelli, M. Cali, G. Orsello, *Int. J. Hydrogen Energy* **2009**, 34(10) 4661-4668.
- [3] S.L. Douvartzides, F.A. Coutelieris, A.K. Demin, P.E. Tsiakaras, *AIChE J.* **2003**, 49(1) 248-257.
- [4] H. Shapouri, J.A. Duffield, M. Wang, U.S. Department of Agriculture, Office of the Chief Economist, Office of Energy Policy and New Uses, Agricultural Economic Report No. 813 **2002**.
- [5] CONCAWE, EUCAR, JRC/IES, **2007**, "Well-To-Wheels analysis of future automotive fuels and powertrains in the European context: Well-To-Wheels Report", http://ies.jrc.ec.europa.eu/uploads/media/WTW_Report_010307.pdf.
- [6] D. Pimentel, T.W. Patzek, *Natural Resources Research* **2005**, 14(1) 65-76.
- [7] Y. Sun, J. Cheng, *Bioresour. Technol.* **2002**, 83(1) 1-11.
- [8] P.W. Li, M.K. Chyu, *J. Power Sources* **2003**, 124(2) 487-498.
- [9] P. Costamagna, P. Costa, V. Antonucci, *Electrochim. Acta* **1998**, 43(3-4) 375-394.
- [10] P. Aguiar, C.S. Adjiman, N.P. Brandon, 2004, *J. Power Sources* **2004**, 138(1-2) 120-136.
- [11] R. Suwanwarangkul, E. Croiset, E. Entchev, S. Charojrochkul, S., M.D. Pritzker, M.W. Fowler, P.L. Douglas, S. Chewathanakup, H. Mahaudom, *J. Power Sources* **2006**, 161(1), 308-322.
- [12] K. Tanaka, C. Wen, K. Yamada, *Fuel* **2000**, 79 1493-1507.
- [13] H. Yakabe, M. Hishinuma, M. Uratani, Y. Matsuzaki, I. Yasuda *J. Power Sources* **2000**, 86(1-2) 423-431.
- [14] F.N. Cayan, S.R. Pakalapati, S.R., F. Elizalde-Blancas, J. Celik, I., *J. Power Sources* **2009**, 192(2) 467-474.

Deleted: S.C., 2000, "Advance	[40]
Formatted: Bullets and Num	[41]
Deleted: ¶	
Formatted	[42]
Formatted	[43]
Formatted: Bullets and Num	[44]
Deleted: , F., ..., ...M.,	[45]
Formatted	[46]
Deleted: G.,	
Formatted	[47]
Deleted: , "Experimental activ	[48]
Formatted	[49]
Formatted	[50]
Deleted: S.L., ..., F.A.,	[51]
Deleted: A...K...,	[52]
Formatted	[53]
Deleted: , P.E.,	
Formatted	[54]
Deleted:	
Formatted	[55]
Deleted: "Fuel Options for sol	[56]
Formatted	[57]
Formatted	[58]
Deleted: H., ..., J.A., ...M., 200	[59]
Formatted	[60]
Deleted: "The Energy Balance	[61]
Deleted: ,	
Formatted	[62]
Deleted: D., ...T.W., 2005, "E	[63]
Formatted	[64]
Deleted: Y., ... J., 2002, "Hyc	[65]
Formatted	[66]
Deleted: Technology	
Formatted	[67]
Deleted: P.W., ..., M.K., 2003	[68]
Formatted	[69]
Deleted: , pp.	
Deleted: P.,	
Formatted	[70]
Deleted: P., ..., 1998, "Micro-n	[71]
Formatted	[72]
Deleted: ica	
Formatted	[73]
Deleted: P., ..., C.S., ...N.P., ...	[74]
Formatted	[75]
Deleted: ournal of	
Formatted	[76]
Deleted: R., ...E., ...E., ...M.I	[77]
Formatted	[78]
Deleted: , ...	[79]
Deleted: Design and evaluatio	[80]
Formatted	[81]
Deleted: 79 (
Formatted	[82]
Deleted:)	
Formatted	[83]
	[84]
	[85]
Formatted	[86]

[15] [S.H. Chan, K.A. Khor, Z.T. Xia, *J. Power Sources* **2001**, 93\(1-2\) 130-140.](#)

[16] [R. Suwanwarangkul, E. Croiset, M.W. Fowler, P.L. Douglas, E. Entchev, M.A. Douglas, *J. Power Sources* **2003**, 122\(1\), 9-16.](#)

[17] R.B. Bird, W. E. Stewart; E.N. Lightfoot, Transport Phenomena, 2 ed. New York, Wiley, **2005**.

[18] [P. Costamagna, A. Selimovic, M. Del Borghi, G. Agnew, *Chemical Engineering Journal* **2004**, 102\(1\), 61-69.](#)

[19] [E. Riensche, U. Stimming, G. Unverzag, *J. Power Sources* **1998**, 73\(2\) 251-256.](#)

[20] [E. Riensche, J. Meusinger, U. Stimming, G. Unverzag, G., *J. Power Sources* **1998**, 71\(1-2\), 306-314.](#)

[21] [F. Marsano, L. Magistri, A.F. Massardo, *J. Power Sources* **2004**, 129 216-228.](#)

[22] [J. Milewski, A. Miller, J. Sałaciński, *Int. J. Hydrogen Energy* **2007**, 32\(6\) 687-698.](#)

[23] [Campanari S., *J. Power Sources* **2001**, 92\(1-2\) 26-34.](#)

[24] [J. Van herle, Y. Membrez, O. Bucheli, *J. Power Sources* **2004**, 127\(1-2\) 300-312.](#)

[25] [Y. Yi, A.D. Rao, J. Brouwer, G.S. Samuelsen, *J. Power Sources* **2005**, 144\(1\) 67-76.](#)

[26] [S. Gordon, B.J. McBride, Computer program for calculation of complex chemical equilibrium compositions and applications I. Analysis **1994**, NASA Lewis Research Center, Cleveland.](#)

[27] [R.C. Reid, J.M. Prausnitz, T.K. Sherwood, *The properties of gas and liquids* **1977**, McGraw-Hill, New York.](#)

[28] [Y. Zhu Y., W. Cai, C. Wen, Y. Li, *J. Power Sources* **2007**, 173 437-449.](#)

[29] [Y. Zhu Y., W. Cai, Y. Li, C. Wen, *J. Power Sources* **2008**, 185\(2\) 1122-1130.](#)

[30] [M.L. Ferrari, A. Traverso, L. Magistri, A.F. Massardo, *J. Power Sources* **2005**, 149 22-32.](#)

[31] [L.J. De Chant, Combined numerical/analytical perturbation solutions of the Navier-Stokes equations for aerodynamic ejector/mixer nozzle flows **1998**, NASA Contractor Report 1998-207406.](#)

Deleted: S. H., ...K.A.,... Z.T. [87]

Formatted [88]

Deleted: R., ...E., ...M.W., ... [89]

Formatted [90]

Deleted:

Formatted [91]

Formatted [92]

Deleted: P., ...A.,... M., ... [93]

Formatted [94]

Deleted: pp.

Deleted: E., ...U., ...G., 1998, [95]

Formatted [96]

Deleted: E.,...J., ...U.,...1998, [97]

Formatted [98]

Deleted: , pp.

Formatted [99]

Formatted [100]

Formatted [101]

Formatted [102]

Formatted [103]

Formatted: Bullets and Nu [104]

Formatted [105]

Deleted: Milewski, J., Miller [106]

Formatted [107]

Deleted: 2004, "Biogas as a f [108]

Formatted [109]

Deleted: Y.,...A.D.,... J.,... [110]

Formatted [111]

Deleted: Journal of Power Sources

Formatted [112]

Deleted: S., ...B.J., 1994, " [113]

Formatted [114]

Deleted: "...National Aeron [115]

Deleted: R.C.,...J.M.,... T.K [116]

Formatted [117]

Deleted: "

Deleted: W.,...C., [118]

Formatted [119]

Deleted: Y., 2007, "Fuel ejec [120]

Formatted [121]

Deleted: Zhu, Y., Cai, W., Li [122]

Formatted [123]

Formatted [124]

Deleted: Marsano, F., Magist [125]

Formatted [126]

Deleted: M.L.,...A.,...L.,... [127]

Formatted [128]

Deleted: 2005, "Influence of [129]

Formatted [130]

Deleted: -

Formatted [131]

Formatted [132]

Formatted [133]

Formatted [134]

- 1
2
3
4
5
6
7
8
9
10
11
12
13
14
15
16
17
18
19
20
21
22
23
24
25
26
27
28
29
30
31
32
33
34
35
36
37
38
39
40
41
42
43
44
45
46
47
48
49
50
51
52
53
54
55
56
57
58
59
60
- [32] [N. Laosiripojana](#), [S. Assabumrungrat](#), [Y. Zhu](#), [Y. W. Cai](#), [C. Wen](#), [Y. Li](#), *J. Power Sources* **2007**, 163(2) 943-951.

Deleted: N.,

Formatted: English (U.K.)

Deleted: , S., 2007, "Catalytic steam reforming of methane, methanol, and ethanol over Ni/YSZ: The possible use of these fuels in internal reforming SOFC", *Journal of Power Sources*

Formatted: Font: 12 pt

Formatted: Font: Not Bold

For Peer Review

List of figures

Figure 1 - Installation of the 5 kW Siemens Generator in Turbocare Spa 5

Figure 2 - Basic BoP design of the SOFC generator analysed 6

Figure 3 – Ohmic losses in the tubular cell 8

Figure 4 - Fuel and air flows along the tubular cell 11

Figure 5 - Cells arrangement inside a bundle 12

Figure 6 - Ejector scheme 15

Figure 7 - Schematic sheet describing the iteration step for determining the molar composition of the anodic exhaust 18

Figure 8 - Detailed flow-sheet with natural gas reference case 19

Figure 9 - Detailed flow-sheet with ethanol feeding 20

Figure 10 - Comparison of the calculated Nernst voltage along the fuel channel (cell tube length) for both natural gas and ethanol feeding 21

Figure 11 - Equilibrium compositions of an ethanol/water mixture in a volumetric ratio 60/40 at different temperatures 26

Figure 12 - Schematic view of the 5 kW Generator to respect of the fuel and air feeding flows 26

Figure 13 - Carbon boundary for the ethanol steam reforming 27

Figure 14 - Ejector pressure increase during EtOH/H₂O mixture feeding 27

Figure 15 - Water stoichiometry in the NG/EtOH mixture reaching the stack 28

Figure 16 - Behaviour of stack voltage during the EtOH/H₂O feeding experiment 29

Figure 17 - Comparison of string voltages during the EtOH/H₂O feeding experiment 29

Figure 18 - Stack voltage and current behaviour 30

Figure 19 - Reformer temperature drop during the ethanol experiment 30

Figure 20 – Generator temperatures behaviour during the ethanol experiment 30

Figure 21 - Generator electrical AC efficiency behaviour during the EtOH experiment 31

List of tables

Table 1 - Parameters for the cell electrochemical model 10

Table 2 - Molar compositions of the recirculated flow entrained by the ejector and total steam fraction recirculated normalised to the primary flow entering the ejector itself 22

Deleted: 29

Deleted: [Figure 1 - Installation of the 5 kW Siemens Generator in Turbocare Spa](#) . 5¶

[Figure 2 - Basic BoP design of the SOFC generator analysed](#) . 6¶

[Figure 3 – Ohmic losses in the tubular cell](#) . 8¶

[Figure 4 - Fuel and air flows along the tubular cell](#) . 11¶

[Figure 5 - Cells arrangement inside a bundle](#) . 12¶

[Figure 6 - Ejector scheme](#) . 15¶

[Figure 7 - Schematic sheet describing the iteration step for determining the molar composition of the anodic exhaust](#) . 18¶

[Figure 8 - Detailed flow-sheet with natural gas reference case](#) . 19¶

[Figure 9 - Detailed flow-sheet with ethanol feeding](#) . 20¶

[Figure 10 - Comparison of the calculated Nernst voltage along the fuel channel \(cell tube length\) for both natural gas and ethanol feeding](#) . 21¶

[Figure 11 - Equilibrium compositions of an ethanol/water mixture in a volumetric ratio 60/40 at different temperatures](#) . 26¶

[Figure 12 - Schematic view of the 5 kW Generator to respect of the fuel and air feeding flows](#) . 26¶

[Figure 13 - Carbon boundary for the ethanol steam reforming](#) . 27¶

[Figure 14 - Ejector pressure increase during EtOH/H₂O mixture feeding](#) . 27¶

[Figure 15 - Water stoichiometry in the NG/EtOH mixture reaching the stack](#) . 28¶

[Figure 16 - Behaviour of stack voltage during the EtOH/H₂O feeding experiment](#) . 29¶

[Figure 17 - Comparison of string voltages during the EtOH/H₂O feeding experiment](#) . 29¶

[Figure 18 - Stack voltage and current behaviour](#) . 29¶

[Figure 19 - Reformer temperature drop during the ethanol experiment](#) . 30¶

[Figure 20 - Temperature behaviour during the ethanol experiment](#) . 30¶

[Figure 21 - Generator electrical AC efficiency behaviour during the EtOH experiment](#) . 31¶

[Figure 1 - Installation of the 5 kW Siemens Generator in Turbocare Spa](#) . 5¶

[Figure 2 - Basic BoP design of the SOFC generator analysed](#) . 6¶

[Figure 3 – Ohmic losses in the tubular cell](#) . 8¶

[Figure 4 - Fuel and air flows along the tubular cell](#) . 11¶

[Figure 5 - Cells arrangement inside a bundle](#) . 12¶

[Figure 6 - Ejector scheme](#) . 15¶

[Figure 7 - Schematic sheet describing the iteration step for determining the molar composition of the anodic exhaust](#) . 18¶

[Figure 8 - Detailed flow-sheet with natural gas reference case](#) . 19¶

[Figure 9 - Detailed flow-sheet with ethanol feeding](#) . 20¶

[Figure 10 - Comparison of the calculated Nernst voltage along the fuel channel \(cell tube length\) for both natural gas and ethanol feeding](#) . 24¶

[Figure 11 - Equilibrium compositions of an ethanol/water mixture in a volumetric ratio 60/40 at different tempera](#) (... [135])

Page 11: [1] Deleted andrea 3/6/2010 6:25:00 PM

(21)

$$n_{H_2,i+1} = n_{H_2,i} - I_{H_2,i} = n_{H_2,i} - \frac{3/4 \cdot (I_{CELL} / N)}{2 \cdot F} \quad (22)$$

$$n_{H_2O,i+1} = n_{H_2O,i} + \frac{3/4 I_{CELL}}{2 \cdot F} \quad (23)$$

$$n_{CO,i+1} = n_{CO,i} - (I_{CELL} / N - I_{H_2,i}) = n_{CO,i} - \frac{1/4 I_{CELL}}{2F} \quad (24)$$

$$n_{CO_2,i+1} = n_{CO_2,i} + \frac{1/4 I_{CELL}}{2 \cdot F} \quad (25)$$

$$n_{O_2,i+1} = n_{O_2,i} - \frac{I_{CELL}}{4 \cdot F} \quad (26)$$

Page 11: [2] Formatted andrea 3/6/2010 7:10:00 PM

Heading 1, Left, Indent: Left: 0 pt, Automatically adjust right indent when grid is defined, Line spacing: single, Adjust space between Latin and Asian text, Adjust space between Asian text and numbers

Page 11: [3] Deleted andrea 3/6/2010 7:10:00 PM

Page 13: [4] Deleted andrea 3/6/2010 7:16:00 PM

$$\begin{cases} T_{stack} \cdot \Delta S_{stack} = \Delta H_{stack} - \Delta G_{stack} \\ Q_{loss} = I_{stack} \cdot \left(\frac{\Delta G_{fuel(H_2,CO)}^{ox}(T_{stack}, y_{fuel})}{2 \cdot F} - V(I) \right) \end{cases} \quad (28)$$

Page 13: [5] Deleted andrea 3/20/2010 1:16:00 PM

is linked to the thermal balance of the stack

Page 13: [6] Deleted andrea 3/6/2010 7:58:00 PM

$$\lambda_{air} = \frac{Q_{stack} + Q_{ref} + Q_{fuel}}{n_{air,stech} \cdot C_{p,air} (T_{stack} - T_{air,inlet})}$$

Page 13: [7] Formatted andrea 3/20/2010 1:25:00 PM

Justified, Don't adjust right indent when grid is defined, Line spacing: Double, Don't adjust space between Latin and Asian text, Don't adjust space between Asian text and numbers

Page 13: [8] Deleted andrea 3/20/2010 1:23:00 PM

through the top area of the generator

Page 13: [9] Deleted andrea 3/20/2010 1:25:00 PM

before reaching the cells.

Page 13: [10] Formatted andrea 3/29/2010 4:11:00 PM

List Paragraph, Justified, Don't adjust right indent when grid is defined, Line spacing: Double, Outline numbered + Level: 2 + Numbering Style: 1, 2, 3, ... + Start at: 1 + Alignment: Left + Aligned at: 18 pt + Tab after: 0 pt + Indent at: 36 pt, Don't

Page 20: [11] Deleted andrea 3/27/2010 6:36:00 PM

Nevertheless, the polarisation of the stack when ethanol fuel is feeding the generator is actually slightly higher than for NG. Under the hypothesis of a proper reforming of ethanol, the fuel quantity in both feeding cases is such as to preserve the overall H₂-equivalents entering the system. Thus, the Nernst voltage of the stack should not be affected significantly. This aspect has been analysed in more detail by drawing the Nernst voltage along the fuel channel (which corresponds to the cell tube length) for both fuel cases.

Page 22: [12] Deleted andrea 3/6/2010 8:01:00 PM

$$STCR = \frac{y_{H_2O} \cdot n_{an,recirc}}{n_{fuel} + y_{CO} \cdot n_{an,recirc}}$$

Page 22: [13] Deleted andrea 3/27/2010 10:34:00 PM

For the fuels considered here, t

Page 22: [14] Deleted andrea 3/27/2010 10:35:00 PM

is also accounted for in the STCR number

1
2
3
4 Page 24: [15] Deleted andrea 3/6/2010 8:03:00 PM

5
6
7
8
9
10
$$FU = \frac{I_{TOT}}{2F n_{H_2,CO}^{CH_4}} \quad (35)$$

11
12
13

14 Page 24: [15] Deleted andrea 3/6/2010 8:02:00 PM

15 3-

16
17
18 Page 24: [15] Deleted andrea 3/6/2010 8:02:00 PM

19 4

20
21
22 Page 24: [15] Deleted andrea 3/6/2010 8:02:00 PM

23 5

24
25
26 Page 24: [16] Deleted andrea 3/27/2010 11:10:00 PM

27 defines

28
29
30 Page 24: [16] Deleted andrea 3/27/2010 11:10:00 PM

31 that is

32
33
34 Page 24: [16] Deleted andrea 3/27/2010 11:10:00 PM

35 in which

36
37
38 Page 24: [16] Deleted andrea 3/27/2010 11:14:00 PM

39 achieves

40
41
42 Page 24: [16] Deleted andrea 3/27/2010 11:15:00 PM

43 , and

44
45
46 Page 24: [16] Deleted andrea 3/27/2010 11:14:00 PM

47 an

48
49
50 Page 24: [16] Deleted andrea 3/27/2010 11:15:00 PM

51 e of FU causes it to

52
53
54 Page 24: [16] Deleted andrea 3/27/2010 11:15:00 PM

55 e

1
2
3
4 **Page 24: [16] Deleted** andrea 3/27/2010 11:12:00 PM

5 In this sense, t

6
7
8 **Page 24: [16] Deleted** andrea 3/27/2010 11:11:00 PM

9 generates

10
11
12 **Page 24: [16] Deleted** andrea 3/27/2010 11:12:00 PM

13 two

14
15
16 **Page 24: [16] Deleted** andrea 3/27/2010 11:12:00 PM

17 , but

18
19
20 **Page 24: [16] Deleted** andrea 3/27/2010 11:12:00 PM

21
22
23 **Page 24: [16] Deleted** andrea 3/27/2010 11:13:00 PM

24 which sum together and finally produce an overall positive effect on the Nernst voltage

25
26 (as observed in Figure 10)

27
28
29 **Page 24: [16] Deleted** andrea 3/27/2010 11:13:00 PM

30 .

31
32
33
34
35 **Figure 10 - Comparison of the calculated Nernst voltage along the fuel channel (cell**
36 **tube length) for both natural gas and ethanol feeding**

37
38
39 **Page 24: [17] Deleted** andrea 3/27/2010 11:17:00 PM

40 several

41
42
43 **Page 24: [17] Deleted** andrea 3/27/2010 11:17:00 PM

44 In the experimental time period

45
46
47 **Page 24: [17] Deleted** andrea 3/27/2010 11:18:00 PM

48 substituted

49
50
51 **Page 24: [17] Deleted** andrea 3/27/2010 11:18:00 PM

52 to

53
54
55 **Page 24: [17] Deleted** andrea 3/28/2010 12:30:00 AM

1
2
3 NG flow
4
5

6 **Page 24: [17] Deleted** andrea 3/28/2010 12:29:00 AM

7 According to the standard procedure employed while operating the generator,
8
9

10 **Page 24: [17] Deleted** andrea 3/28/2010 12:30:00 AM

11 t
12

13 **Page 24: [17] Deleted** andrea 3/28/2010 12:32:00 AM

14 is
15

16 **Page 24: [17] Deleted** andrea 3/28/2010 12:32:00 AM

17 determined
18

19 **Page 24: [17] Deleted** andrea 3/28/2010 12:30:00 AM

20 upon
21

22 **Page 24: [17] Deleted** andrea 3/28/2010 12:31:00 AM

23 DC
24

25 **Page 24: [17] Deleted** andrea 3/28/2010 12:33:00 AM

26 load
27

28 **Page 24: [17] Deleted** andrea 3/27/2010 11:19:00 PM

29 , FU of the generator, and type of fuel entering it.
30

31 For simplicity, we refer here just to methane as a fuel (even if the real fuel is natural gas);
32

33 the methane
34

35 **Page 24: [17] Deleted** andrea 3/27/2010 11:20:00 PM

36 is thus
37

38 **Page 24: [18] Deleted** andrea 3/6/2010 8:04:00 PM

$$n_{CH_4} = \frac{(I_{stack} / 2) \cdot n_{cells}}{2 \cdot F} \frac{1}{H_{2,eq}^{reforming} \cdot FU} \quad (37)$$

39 **Page 24: [18] Deleted** andrea 3/28/2010 12:34:00 AM

40 a
41
42
43
44
45
46
47
48
49
50
51
52
53
54
55
56
57
58
59
60

1
2
3 **Page 24: [18] Deleted** andrea 3/28/2010 12:35:00 AM
4 reactive species
5
6

7 **Page 24: [18] Deleted** andrea 3/28/2010 12:35:00 AM
8 Two factors can modify Eq. 37: i) the effective fuel consumption (FC), which is greater
9 than the FU, since some air leakage occurs inside the stack (the denominator of Eq. 37
10 should in fact be FC instead of FU); ii) the stack NG flow is not pure methane, thus the
11 effective inlet molar composition of the fuel gas should be taken into account to calculate
12 the exact number of H₂-equivalents. The modifications due to these two effects are
13 relatively low, because the air leaks inside the generator are rather low and the relative
14 error committed in considering just methane as the fuel flow is lower than 1% when
15 evaluating $H_{2,eq}$.
16
17
18
19
20
21
22
23
24
25
26
27

28 **Page 24: [18] Deleted** andrea 3/28/2010 12:36:00 AM
29 number
30
31

32 **Page 24: [18] Deleted** andrea 3/28/2010 12:36:00 AM
33 of fuels; it has to be taken into account to determine the primary inlet fuel necessary to
34 satisfy a certain stack current of the generator.
35
36
37

38 **Page 24: [18] Deleted** andrea 3/28/2010 12:36:00 AM
39
40
41
42

43 **Page 25: [19] Formatted** andrea 3/28/2010 7:13:00 PM
44 Subscript
45

46 **Page 25: [19] Formatted** andrea 3/28/2010 7:13:00 PM
47 Subscript
48

49 **Page 25: [20] Deleted** andrea 3/28/2010 12:38:00 AM
50 , upon
51

52 **Page 25: [20] Deleted** andrea 3/28/2010 12:38:00 AM
53 stack fuel
54
55

56 **Page 25: [20] Deleted** andrea 3/28/2010 12:38:00 AM
57 removed and
58
59
60

1
2
3
4 **Page 25: [20] Deleted** andrea 3/28/2010 12:38:00 AM

5 an

6
7
8 **Page 25: [20] Deleted** andrea 3/28/2010 12:38:00 AM

9 mixture,

10
11
12 **Page 25: [20] Deleted** andrea 3/28/2010 6:53:00 PM

13 always

14
15
16
17 **Page 25: [20] Deleted** andrea 3/28/2010 12:39:00 AM

18 an overall fuel mixture that was able to provide the stack with the same amount of

19 equivalent reactive moles of H₂ of the nominal NG flow, while undertaking a full steam-

20 reforming

21
22
23
24
25
26 **Page 25: [21] Deleted** andrea 3/6/2010 8:13:00 PM

27 Taking

28
29
30 **Page 25: [21] Deleted** andrea 3/8/2010 10:42:00 AM

31 a closer observation at the

32
33
34 **Page 25: [21] Deleted** andrea 3/28/2010 12:40:00 AM

35 , we hav

36
37
38 **Page 25: [21] Deleted** andrea 3/28/2010 12:40:00 AM

39 e

40
41
42 **Page 25: [22] Formatted** andrea 3/8/2010 10:41:00 AM

43 English (U.K.), Lowered by 6 pt

44
45 **Page 25: [22] Formatted** andrea 3/6/2010 8:12:00 PM

46 English (U.K.)

47
48 **Page 25: [22] Formatted** andrea 3/8/2010 10:41:00 AM

49 Formatted

50
51 **Page 25: [23] Deleted** andrea 3/6/2010 8:12:00 PM



53
54 (39)



(40)

Page 25: [23] Deleted andrea 3/8/2010 10:43:00 AM

that a

Page 25: [23] Deleted andrea 3/8/2010 10:43:00 AM

, when fully steam-reformed

Page 25: [24] Deleted andrea 3/8/2010 10:44:00 AM

moles

Page 25: [24] Deleted andrea 3/8/2010 10:44:00 AM

per mole of steam-reformed

Page 25: [24] Deleted andrea 3/8/2010 10:44:00 AM

Page 25: [24] Deleted andrea 3/28/2010 12:42:00 AM

is

Page 25: [24] Deleted andrea 3/28/2010 12:42:00 AM

ratio

Page 25: [24] Deleted andrea 3/8/2010 10:44:00 AM

es

Page 25: [24] Deleted andrea 3/28/2010 12:42:00 AM

, thus maintaining the number of H₂-equivalents constant.

Page 25: [25] Deleted andrea 3/8/2010 10:45:00 AM

/

Page 25: [25] Deleted andrea 3/28/2010 6:54:00 PM

in-stack

Page 25: [26] Deleted andrea 3/28/2010 6:54:00 PM

imposed

1
2
3 **Page 25: [26] Deleted** andrea 3/28/2010 6:54:00 PM

4 to be

5
6
7 **Page 25: [26] Deleted** andrea 3/28/2010 6:55:00 PM

8 reforming

9
10
11 **Page 25: [26] Deleted** andrea 3/28/2010 6:55:00 PM

12 required

13
14
15 **Page 25: [26] Deleted** andrea 3/28/2010 6:55:00 PM

16 for a NG

17
18
19 **Page 25: [26] Deleted** andrea 3/28/2010 6:55:00 PM

20 feeding than for an

21
22
23 **Page 25: [26] Deleted** andrea 3/28/2010 6:55:00 PM

24 feeding

25
26
27 **Page 25: [26] Deleted** andrea 3/28/2010 12:44:00 AM

28 aspect

29
30
31 **Page 25: [26] Deleted** andrea 3/28/2010 12:44:00 AM

32 fully evident in

33
34
35 **Page 25: [26] Deleted** andrea 3/28/2010 12:44:00 AM

36
37
38 **Page 25: [26] Deleted** andrea 3/28/2010 7:24:00 PM

39 4.7 instead

40
41
42 **Page 25: [26] Deleted** andrea 3/28/2010 7:24:00 PM

43 of

44
45
46 **Page 25: [26] Deleted** andrea 3/28/2010 12:44:00 AM

47 with NG

48
49
50 **Page 25: [27] Deleted** andrea 3/28/2010 12:45:00 AM

51 In terms of the ethanol fuel mixture

52
53
54 **Page 25: [27] Deleted** andrea 3/28/2010 12:47:00 AM

1
2
3 , t
4
5
6

7 **Page 25: [27] Deleted** andrea 3/28/2010 12:47:00 AM
8 chosen

9
10
11 **Page 25: [27] Deleted** andrea 3/28/2010 12:47:00 AM
12 with respect to

13
14
15 **Page 25: [27] Deleted** andrea 3/28/2010 7:25:00 PM
16 carbo

17
18
19 **Page 30: [28] Deleted** andrea 3/6/2010 8:54:00 PM
20 long

21
22
23 **Page 30: [28] Deleted** andrea 3/6/2010 8:54:00 PM
24 , but

25
26
27 **Page 30: [28] Deleted** andrea 3/6/2010 8:55:00 PM
28 the value

29
30
31 **Page 30: [28] Deleted** andrea 3/6/2010 8:53:00 PM

32
33
34
35 **Page 30: [29] Deleted** andrea 3/27/2010 11:26:00 PM
36 decrease

37
38
39 **Page 30: [29] Deleted** andrea 3/27/2010 11:26:00 PM
40 s

41
42
43
44 **Page 30: [30] Formatted** andrea 3/27/2010 11:26:00 PM
45 English (U.K.)

46 **Page 30: [30] Formatted** andrea 3/27/2010 11:26:00 PM
47 English (U.K.)

48
49 **Page 30: [30] Formatted** andrea 3/28/2010 7:38:00 PM
50 Subscript

51
52 **Page 30: [30] Formatted** andrea 3/27/2010 11:30:00 PM
53 English (U.K.)

54 **Page 30: [31] Deleted** andrea 3/28/2010 7:38:00 PM
55 and also

1			
2			
3	Page 30: [31] Deleted	andrea	3/28/2010 7:38:00 PM
4			
5			
6			
7	Page 30: [32] Deleted	andrea	3/27/2010 11:30:00 PM
8	ly		
9			
10			
11	Page 30: [32] Deleted	andrea	3/27/2010 11:30:00 PM
12	confirming		
13			
14			
15	Page 30: [33] Deleted	andrea	3/27/2010 11:30:00 PM
16	the		
17			
18			
19			
20	Page 30: [33] Deleted	andrea	3/27/2010 11:30:00 PM
21	predictions		
22			
23			
24	Page 30: [34] Deleted	andrea	3/27/2010 11:28:00 PM
25	s		
26			
27			
28	Page 30: [34] Deleted	andrea	3/27/2010 11:27:00 PM
29	various		
30			
31			
32	Page 30: [34] Deleted	andrea	3/27/2010 11:27:00 PM
33	during the ethanol experiment are		
34			
35			
36			
37	Page 30: [34] Deleted	andrea	3/28/2010 7:40:00 PM
38	reformer		
39			
40			
41	Page 30: [34] Deleted	andrea	3/27/2010 11:28:00 PM
42	is diminishe		
43			
44			
45	Page 30: [34] Deleted	andrea	3/27/2010 11:27:00 PM
46	d		
47			
48			
49	Page 30: [34] Deleted	andrea	3/28/2010 7:40:00 PM
50	About		
51			
52			
53	Page 30: [34] Deleted	andrea	3/28/2010 7:40:00 PM
54	is shown to		
55			
56			
57			
58	Page 30: [34] Deleted	andrea	3/27/2010 11:28:00 PM
59			
60			

1
2
3 that happens
4
5

6 **Page 30: [34] Deleted** andrea 3/27/2010 11:28:00 PM
7 therefore
8
9

10 **Page 30: [35] Deleted** andrea 3/29/2010 4:05:00 PM
11
12 -
13

14 **Page 30: [35] Deleted** andrea 3/29/2010 4:05:00 PM
15 **Temperature**
16
17

18 **Page 30: [36] Deleted** andrea 3/6/2010 8:55:00 PM
19 also
20
21

22 **Page 30: [36] Deleted** andrea 3/27/2010 11:33:00 PM
23 since this is the parameter managing the stack temperature.
24
25

26 **Page 30: [36] Deleted** andrea 3/27/2010 11:34:00 PM
27 behaves
28
29

30 **Page 30: [36] Deleted** andrea 3/27/2010 11:36:00 PM
31 and the reformer is thermally integrated into the stack,
32
33

34 **Page 30: [36] Deleted** andrea 3/27/2010 11:35:00 PM
35 it makes sense that the
36
37

38 **Page 30: [36] Deleted** andrea 3/27/2010 11:23:00 PM
39 should increase
40
41

42 **Page 30: [36] Deleted** andrea 3/27/2010 11:23:00 PM
43 increased
44
45

46 **Page 30: [36] Deleted** andrea 3/28/2010 7:41:00 PM
47 Actually, t
48
49

50 **Page 30: [36] Deleted** andrea 3/6/2010 8:58:00 PM
51 so
52
53

54 **Page 30: [36] Deleted** andrea 3/6/2010 8:16:00 PM
55
56
57
58
59
60

1			
2			
3			
4	Page 35: [42] Formatted	andrea	3/8/2010 1:04:00 PM
5	Font: Bold		
6	Page 35: [42] Formatted	andrea	3/8/2010 1:05:00 PM
7	Font: Not Bold		
8			
9	Page 35: [43] Formatted	andrea	3/8/2010 1:06:00 PM
10	Font: (Default) Times New Roman, (Asian) MS Mincho		
11			
12	Page 35: [44] Change	Unknown	
13	Formatted Bullets and Numbering		
14	Page 35: [45] Deleted	andrea	3/8/2010 1:05:00 PM
15	, F.,		
16			
17			
18	Page 35: [45] Deleted	andrea	3/8/2010 1:05:00 PM
19	,		
20			
21			
22			
23	Page 35: [45] Deleted	andrea	3/8/2010 1:05:00 PM
24	M.,		
25			
26			
27	Page 35: [46] Formatted	andrea	3/8/2010 1:07:00 PM
28	Font: 12 pt, Italic, English (U.K.), Do not check spelling or grammar		
29	Page 35: [47] Formatted	andrea	3/8/2010 1:06:00 PM
30	Font: Bold		
31			
32	Page 35: [48] Deleted	andrea	3/8/2010 1:06:00 PM
33	, “Experimental activity on two tubular solid oxide fuel cell cogeneration plants in a		
34			
35	real industrial environment”, International Journal of Hydrogen Energy,		
36			
37			
38			
39	Page 35: [49] Formatted	andrea	3/8/2010 1:06:00 PM
40	Font: Not Bold		
41	Page 35: [50] Formatted	andrea	3/8/2010 1:07:00 PM
42	French (France)		
43			
44	Page 35: [51] Deleted	andrea	3/8/2010 1:07:00 PM
45	S.L.		
46			
47			
48	Page 35: [51] Deleted	andrea	3/8/2010 1:07:00 PM
49	,		
50			
51			
52	Page 35: [51] Deleted	andrea	3/8/2010 1:07:00 PM
53	F.A.,		
54			
55			
56	Page 35: [52] Deleted	andrea	3/8/2010 1:07:00 PM
57	A		
58			
59			
60			

1			
2			
3			
4	Page 35: [52] Deleted	andrea	3/8/2010 1:07:00 PM
5	K		
6			
7			
8	Page 35: [52] Deleted	andrea	3/8/2010 1:07:00 PM
9	,		
10			
11			
12	Page 35: [53] Formatted	andrea	3/8/2010 1:07:00 PM
13	French (France)		
14			
15	Page 35: [54] Formatted	andrea	3/8/2010 1:08:00 PM
16	Font: Italic		
17			
18	Page 35: [55] Formatted	andrea	3/8/2010 1:18:00 PM
19	Font: Bold		
20			
21	Page 35: [56] Deleted	andrea	3/8/2010 1:08:00 PM
22	“Fuel Options for solid oxide fuel cells: a thermodynamic analysis”, AIChE Journal,		
23			
24			
25	Page 35: [57] Formatted	andrea	3/8/2010 1:07:00 PM
26	French (France)		
27			
28	Page 35: [58] Formatted	andrea	3/8/2010 1:08:00 PM
29	Font: Not Bold		
30			
31	Page 35: [59] Deleted	andrea	3/8/2010 1:08:00 PM
32	H.,		
33			
34	Page 35: [59] Deleted	andrea	3/8/2010 1:09:00 PM
35	J.A.,		
36			
37			
38	Page 35: [59] Deleted	andrea	3/8/2010 1:08:00 PM
39	M., 2002,		
40			
41			
42	Page 35: [60] Formatted	andrea	3/8/2010 1:10:00 PM
43	Font: Bold		
44			
45	Page 35: [61] Deleted	andrea	3/8/2010 1:09:00 PM
46	“The Energy Balance of Corn Ethanol: An Update”, U.S. Department of Agriculture,		
47			
48	Office of the Chief Economist, Office of Energy Policy and New Uses,		
49			
50	Agricultural Economic Report No. 813		
51			
52			
53			
54	Page 35: [62] Formatted	andrea	3/8/2010 1:12:00 PM
55	Font: Bold		
56			
57	Page 35: [63] Deleted	andrea	3/8/2010 1:13:00 PM
58	D.,		
59			
60			

1
2
3
4 **Page 35: [63] Deleted** **andrea** **3/8/2010 1:13:00 PM**
5 *T.W., 2005, "Ethanol Production Using Corn, Switchgrass, and Wood, Biodiesel*

6
7
8 *Production Using Soybean and Sunflower,*

9
10
11 **Page 35: [64] Formatted** **andrea** **3/8/2010 1:14:00 PM**

12 Font: Italic

13 **Page 35: [64] Formatted** **andrea** **3/8/2010 1:13:00 PM**

14 Font: Bold

15
16 **Page 35: [64] Formatted** **andrea** **3/8/2010 1:13:00 PM**

17 Font: Not Bold

18
19 **Page 35: [65] Deleted** **andrea** **3/8/2010 1:13:00 PM**

20 Y.,

21
22
23 **Page 35: [65] Deleted** **andrea** **3/8/2010 1:14:00 PM**

24 J., 2002, "Hydrolysis of lignocellulosic materials for ethanol production: a review",

25
26
27 **Page 35: [65] Deleted** **andrea** **3/8/2010 1:18:00 PM**

28 *Bioresource*

29
30
31 **Page 35: [66] Formatted** **andrea** **3/8/2010 1:14:00 PM**

32 Font: Italic

33
34 **Page 35: [66] Formatted** **andrea** **3/8/2010 1:14:00 PM**

35 Font: Italic

36
37 **Page 35: [67] Formatted** **andrea** **3/8/2010 1:14:00 PM**

38 Font: Bold

39
40 **Page 35: [67] Formatted** **andrea** **3/8/2010 1:14:00 PM**

41 Font: Not Bold

42
43 **Page 35: [68] Deleted** **andrea** **3/8/2010 1:20:00 PM**

44 P.W.,

45
46 **Page 35: [68] Deleted** **andrea** **3/8/2010 1:20:00 PM**

47 , M.K., 2003,

48
49
50 **Page 35: [68] Deleted** **andrea** **3/8/2010 1:19:00 PM**

51 "Simulation of the chemical/electrochemical reactions and heat/mass transfer for a

52
53
54 tubular SOFC in a stack", *Journal of*

55
56
57 **Page 35: [69] Formatted** **andrea** **3/8/2010 1:19:00 PM**

58 Font: Italic

1			
2			
3			
4	Page 35: [69] Formatted	andrea	3/8/2010 1:19:00 PM
5	Font: Bold		
6	Page 35: [69] Formatted	andrea	3/8/2010 1:19:00 PM
7	Font: Not Bold		
8			
9	Page 35: [70] Formatted	andrea	3/8/2010 1:19:00 PM
10	English (U.K.)		
11			
12	Page 35: [71] Deleted	andrea	3/8/2010 1:16:00 PM
13	P.,		
14			
15			
16	Page 35: [71] Deleted	andrea	3/8/2010 1:17:00 PM
17	<i>1998, "Micro-modelling of solid oxide fuel cell electrodes",</i>		
18			
19			
20	Page 35: [72] Formatted	andrea	3/8/2010 1:19:00 PM
21	Font: Italic		
22			
23	Page 35: [72] Formatted	andrea	3/8/2010 1:17:00 PM
24	Font: Italic, Italian (Italy)		
25	Page 35: [73] Formatted	andrea	3/8/2010 1:17:00 PM
26	Font: Italic, Italian (Italy)		
27			
28	Page 35: [73] Formatted	andrea	3/8/2010 1:17:00 PM
29	Font: Bold		
30	Page 35: [73] Formatted	andrea	3/8/2010 1:16:00 PM
31	Italian (Italy)		
32			
33	Page 35: [73] Formatted	andrea	3/8/2010 1:17:00 PM
34	Font: Not Bold, Italian (Italy)		
35			
36	Page 35: [73] Formatted	andrea	3/8/2010 1:17:00 PM
37	Italian (Italy)		
38	Page 35: [74] Deleted	andrea	3/8/2010 1:20:00 PM
39	P.,		
40			
41			
42	Page 35: [74] Deleted	andrea	3/8/2010 1:20:00 PM
43	C.S.,		
44			
45			
46			
47	Page 35: [74] Deleted	andrea	3/8/2010 1:20:00 PM
48	N.P.,		
49			
50			
51	Page 35: [74] Deleted	andrea	3/8/2010 1:21:00 PM
52	"Anode-supported intermediate temperature direct internal reforming solid oxide fuel		
53			
54	cell. I: model-based steady-state performance",		
55			
56			
57	Page 35: [75] Formatted	andrea	3/8/2010 1:21:00 PM
58			
59			
60			

1
2
3
4
5
6
7
8
9
10
11
12
13
14
15
16
17
18
19
20
21
22
23
24
25
26
27
28
29
30
31
32
33
34
35
36
37
38
39
40
41
42
43
44
45
46
47
48
49
50
51
52
53
54
55
56
57
58
59
60

Font: Italic

Page 35: [76] Formatted	andrea	3/8/2010 1:21:00 PM
--------------------------------	---------------	----------------------------

Font: Bold

Page 35: [76] Formatted	andrea	3/8/2010 1:21:00 PM
--------------------------------	---------------	----------------------------

Font: Not Bold

Page 35: [77] Deleted	andrea	3/11/2010 11:16:00 AM
------------------------------	---------------	------------------------------

R.,

Page 35: [77] Deleted	andrea	3/11/2010 11:16:00 AM
------------------------------	---------------	------------------------------

E.,

Page 35: [77] Deleted	andrea	3/11/2010 11:16:00 AM
------------------------------	---------------	------------------------------

E.,

Page 35: [77] Deleted	andrea	3/11/2010 11:16:00 AM
------------------------------	---------------	------------------------------

M.D.,

Page 35: [77] Deleted	andrea	3/11/2010 11:16:00 AM
------------------------------	---------------	------------------------------

M.W.,

Page 35: [77] Deleted	andrea	3/11/2010 11:16:00 AM
------------------------------	---------------	------------------------------

Page 35: [77] Deleted	andrea	3/11/2010 11:16:00 AM
------------------------------	---------------	------------------------------

P.L.,

Page 35: [77] Deleted	andrea	3/11/2010 11:16:00 AM
------------------------------	---------------	------------------------------

S.,

Page 35: [77] Deleted	andrea	3/11/2010 11:17:00 AM
------------------------------	---------------	------------------------------

, H., 2006, "Experimental and modeling study of solid oxide fuel cell operating with

syngas fuel", Journal of Power Sources,

Page 35: [78] Formatted	andrea	3/11/2010 11:17:00 AM
--------------------------------	---------------	------------------------------

Font: Not Bold

Page 35: [79] Deleted	andrea	3/11/2010 11:17:00 AM
------------------------------	---------------	------------------------------

,

Page 35: [79] Deleted	andrea	3/11/2010 11:17:00 AM
------------------------------	---------------	------------------------------

1
2
3
4
5
6
7 **Page 35: [80] Deleted** **andrea** **3/11/2010 11:17:00 AM**
8 *Design and evaluation of combined cycle system with solid oxide fuel cell and gas*
9
10 *turbine,*

11
12
13 **Page 35: [81] Formatted** **andrea** **3/11/2010 11:18:00 AM**
14 Font: Italic

15 **Page 35: [82] Formatted** **andrea** **3/11/2010 11:18:00 AM**
16 Font: Bold

17
18 **Page 35: [83] Formatted** **andrea** **3/11/2010 11:25:00 AM**
19 Font: Not Bold

20
21 **Page 35: [84] Deleted** **andrea** **3/11/2010 11:18:00 AM**
22 , Evaluation and modeling of performance of anode-supported solid oxide fuel cell,
23
24 Journal of Power Sources

25
26
27 **Page 35: [84] Deleted** **andrea** **3/11/2010 11:18:00 AM**
28 2000

29
30
31 **Page 35: [85] Deleted** **andrea** **3/11/2010 11:20:00 AM**
32 F.N.,

33
34
35 **Page 35: [85] Deleted** **andrea** **3/11/2010 11:21:00 AM**
36 F.,

37
38
39 **Page 35: [85] Deleted** **andrea** **3/11/2010 11:21:00 AM**

40
41
42
43
44 **Page 35: [85] Deleted** **andrea** **3/11/2010 11:21:00 AM**
45 2009, "On modeling multi-component diffusion inside the porous anode of solid
46
47 oxide fuel cells using Fick's model,

48
49
50
51 **Page 35: [85] Deleted** **andrea** **3/11/2010 11:21:00 AM**
52 Journal of Power Sources

53
54
55 **Page 35: [86] Formatted** **andrea** **3/11/2010 11:21:00 AM**
56 Font: Not Bold

57
58 **Page 36: [87] Deleted** **andrea** **3/11/2010 11:22:00 AM**
59
60

1
2
3 S. H.,
4
5

6 **Page 36: [87] Deleted** **andrea** **3/11/2010 11:22:00 AM**

7 K.A.,
8
9

10 **Page 36: [87] Deleted** **andrea** **3/11/2010 11:22:00 AM**

11 Z.T.
12
13

14 **Page 36: [87] Deleted** **andrea** **3/11/2010 11:22:00 AM**

15 “A complete polarization model of a solid oxide fuel cell and its sensitivity to the
16 change of cell component thickness”, Journal of Power Sources,
17
18
19

20 **Page 36: [87] Deleted** **andrea** **3/11/2010 11:22:00 AM**

21 **Page 36: [88] Formatted** **andrea** **3/11/2010 11:22:00 AM**

22 Font: Not Bold
23
24

25 **Page 36: [89] Deleted** **andrea** **3/11/2010 11:23:00 AM**

26 R.,
27
28

29 **Page 36: [89] Deleted** **andrea** **3/11/2010 11:23:00 AM**

30 E.,
31
32

33 **Page 36: [89] Deleted** **andrea** **3/11/2010 11:23:00 AM**

34 M.W.,
35
36

37 **Page 36: [89] Deleted** **andrea** **3/11/2010 11:23:00 AM**

38 P.L.,
39
40

41 **Page 36: [89] Deleted** **andrea** **3/11/2010 11:23:00 AM**

42 E.,
43
44

45 **Page 36: [89] Deleted** **andrea** **3/11/2010 11:24:00 AM**

46 M.A., 2003, “Performance comparison of Fick’s, dusty-gas and Stefan–Maxwell
47 models to predict the concentration overpotential of a SOFC anode”, Journal of
48 Power Sources,
49
50
51
52
53
54
55
56
57
58
59
60

1
2
3 **Page 36: [90] Formatted** andrea 3/11/2010 11:24:00 AM

4 Font: Not Bold

5
6 **Page 36: [91] Formatted** andrea 3/11/2010 11:24:00 AM

7 Font: Not Bold

8
9 **Page 36: [92] Formatted** andrea 3/11/2010 11:25:00 AM

10 Font: Bold

11 **Page 36: [93] Deleted** andrea 3/11/2010 11:25:00 AM

12 P.,

13
14
15 **Page 36: [93] Deleted** andrea 3/11/2010 11:26:00 AM

16 A.,

17
18
19 **Page 36: [93] Deleted** andrea 3/11/2010 11:26:00 AM

20
21
22
23 **Page 36: [93] Deleted** andrea 3/11/2010 11:26:00 AM

24 M.,

25
26
27 **Page 36: [93] Deleted** andrea 3/11/2010 11:26:00 AM

28 G., 2004, "Electrochemical model of the integrated planar solid oxide fuel cell (IP-
29 SOFC)",
30
31

32
33
34 **Page 36: [94] Formatted** andrea 3/11/2010 11:45:00 AM

35 Font: Not Bold

36
37 **Page 36: [95] Deleted** andrea 3/11/2010 11:33:00 AM

38 E.,

39
40
41 **Page 36: [95] Deleted** andrea 3/11/2010 11:33:00 AM

42 U.,

43
44
45 **Page 36: [95] Deleted** andrea 3/11/2010 11:34:00 AM

46 G., 1998, "Optimization of a 200 kW SOFC cogeneration power plant: Part I:
47 Variation of process parameters", Journal of Power Sources
48

49
50
51 **Page 36: [96] Formatted** andrea 3/11/2010 11:34:00 AM

52 Font: Not Bold

53
54 **Page 36: [97] Deleted** andrea 3/11/2010 11:34:00 AM

55 E.,
56
57
58
59
60

Page 36: [97] Deleted	andrea	3/11/2010 11:34:00 AM
J.,		
Page 36: [97] Deleted	andrea	3/11/2010 11:34:00 AM
U.,		
Page 36: [97] Deleted	andrea	3/11/2010 11:34:00 AM
1998, "Optimization of a 200 kW SOFC cogeneration power plant. Part II: variation of the flowsheet", Journal of Power Sources		
Page 36: [98] Formatted	andrea	3/11/2010 11:34:00 AM
Font: Not Bold		
Page 36: [99] Formatted	andrea	3/11/2010 11:37:00 AM
Italian (Italy)		
Page 36: [100] Formatted	andrea	3/6/2010 7:50:00 PM
Numbered + Level: 1 + Numbering Style: 1, 2, 3, ... + Start at: 1 + Alignment: Left + Aligned at: 18 pt + Tab after: 47.25 pt + Indent at: 47.25 pt		
Page 36: [101] Formatted	andrea	3/11/2010 11:37:00 AM
Font: Not Bold, Italian (Italy)		
Page 36: [101] Formatted	andrea	3/11/2010 11:37:00 AM
Italian (Italy)		
Page 36: [102] Formatted	andrea	3/11/2010 11:37:00 AM
English (U.K.)		
Page 36: [102] Formatted	andrea	3/11/2010 11:40:00 AM
Font: Bold		
Page 36: [103] Formatted	andrea	3/6/2010 7:49:00 PM
Font: 12 pt, Not Bold, Font color: Auto, English (U.K.), Do not check spelling or grammar		
Page 36: [104] Change	andrea	3/6/2010 7:48:00 PM
Formatted Bullets and Numbering		
Page 36: [105] Formatted	andrea	3/6/2010 7:49:00 PM
Font: 12 pt, Not Bold, Font color: Auto, English (U.K.), Do not check spelling or grammar		
Page 36: [105] Formatted	andrea	3/11/2010 11:39:00 AM
Font: Bold		
Page 36: [105] Formatted	andrea	3/6/2010 7:49:00 PM
Font: 12 pt, English (U.K.), Do not check spelling or grammar		
Page 36: [105] Formatted	andrea	3/6/2010 7:49:00 PM
Font: 12 pt, English (U.K.), Do not check spelling or grammar		
Page 36: [106] Deleted	andrea	3/6/2010 7:53:00 PM

1
2
3 Milewski, J., Miller, A., Sałaciński, J., 2007, "Off-design analysis of SOFC
4 hybrid system", International Journal of Hydrogen Energy, 32(6) 687-698.
5
6
7

8 V
9

10
11 **Page 36: [106] Deleted** andrea 3/11/2010 11:39:00 AM

12 J.,
13
14

15 **Page 36: [106] Deleted** andrea 3/11/2010 11:39:00 AM

16 Y.,
17
18

19 **Page 36: [106] Deleted** andrea 3/11/2010 11:39:00 AM

20 O.,
21
22

23 **Page 36: [107] Formatted** andrea 3/11/2010 11:39:00 AM

24 English (U.K.)
25

26 **Page 36: [107] Formatted** andrea 3/11/2010 11:39:00 AM

27 Font: Bold, English (U.K.)
28

29 **Page 36: [107] Formatted** andrea 3/11/2010 11:39:00 AM

30 English (U.K.)
31

32 **Page 36: [108] Deleted** andrea 3/11/2010 11:38:00 AM

33 2004, "Biogas as a fuel source for SOFC co-generators", Journal of Power Sources,
34
35

36 **Page 36: [109] Formatted** andrea 3/11/2010 11:39:00 AM

37 Font: Not Bold
38

39 **Page 36: [110] Deleted** andrea 3/11/2010 11:42:00 AM

40 Y.,
41
42

43 **Page 36: [110] Deleted** andrea 3/11/2010 11:42:00 AM

44 A.D.,
45
46

47 **Page 36: [110] Deleted** andrea 3/11/2010 11:42:00 AM
48
49

50
51 **Page 36: [110] Deleted** andrea 3/11/2010 11:42:00 AM

52 J.,
53
54

55 **Page 36: [110] Deleted** andrea 3/11/2010 11:42:00 AM

56 , G.S.
57
58
59
60

1			
2			
3			
4	Page 36: [110] Deleted	andrea	3/11/2010 11:40:00 AM
5	2005, "Fuel flexibility study of an integrated 25 kW SOFC reformer system",		
6			
7			
8	Page 36: [111] Formatted	andrea	3/11/2010 11:40:00 AM
9	English (U.K.)		
10			
11	Page 36: [111] Formatted	andrea	3/11/2010 11:40:00 AM
12	Font: Bold, Not Italic		
13			
14	Page 36: [112] Formatted	andrea	3/11/2010 11:40:00 AM
15	Font: Not Bold		
16			
17	Page 36: [113] Deleted	andrea	3/11/2010 11:41:00 AM
18	S.,		
19			
20	Page 36: [113] Deleted	andrea	3/11/2010 11:41:00 AM
21	B.J., 1994, "		
22			
23			
24	Page 36: [114] Formatted	andrea	3/11/2010 11:33:00 AM
25	Font: Bold		
26			
27	Page 36: [115] Deleted	andrea	3/11/2010 11:33:00 AM
28	"		
29			
30			
31	Page 36: [115] Deleted	andrea	3/11/2010 11:33:00 AM
32	National Aeronautics and Space Administration		
33			
34			
35	Page 36: [116] Deleted	andrea	3/11/2010 11:41:00 AM
36	R.C.,		
37			
38			
39	Page 36: [116] Deleted	andrea	3/11/2010 11:41:00 AM
40	J.M.,		
41			
42			
43	Page 36: [116] Deleted	andrea	3/11/2010 11:41:00 AM
44	, T.K.		
45			
46			
47			
48	Page 36: [116] Deleted	andrea	3/11/2010 11:41:00 AM
49	1977, "		
50			
51			
52	Page 36: [117] Formatted	andrea	3/11/2010 11:41:00 AM
53	Font: Bold		
54			
55	Page 36: [118] Deleted	andrea	3/11/2010 11:43:00 AM
56	W.,		
57			
58			
59			
60			

1
2
3 **Page 36: [118] Deleted** andrea 3/11/2010 11:43:00 AM

4 C.,

5
6
7 **Page 36: [119] Formatted** andrea 3/11/2010 11:43:00 AM

8 Font: Bold, Not Italic

9
10 **Page 36: [120] Deleted** andrea 3/11/2010 11:43:00 AM

11 Y., 2007, "Fuel ejector design and simulation model for anodic recirculation SOFC
12 system", Journal of Power Sources
13
14

15
16
17 **Page 36: [121] Formatted** andrea 3/11/2010 11:43:00 AM

18 Font: Not Bold

19 **Page 36: [122] Deleted** andrea 3/11/2010 11:43:00 AM

20 Zhu, Y., Cai, W., Li, Y., Wen, C., 2008, "Anode gas recirculation behavior of a fuel
21 ejector in hybrid solid oxide fuel cell systems: Performance evaluation in three
22 operational modes", Journal of Power Sources
23
24
25
26
27

28 **Page 36: [123] Formatted** andrea 3/7/2010 4:49:00 PM

29 Font: Not Bold

30 **Page 36: [124] Formatted** andrea 3/7/2010 4:49:00 PM

31 ASME podstawowy, Automatically adjust right indent when grid is defined, Line
32 spacing: Double, Numbered + Level: 1 + Numbering Style: 1, 2, 3, ... + Start at: 1 +
33 Alignment: Left + Aligned at: 18 pt + Tab after: 47.25 pt + Indent at: 47.25 pt, Adjust
34 sp
35
36

37 **Page 36: [125] Deleted** andrea 3/6/2010 7:50:00 PM

38 Marsano, F., Magistri, L., Massardo, A.F., 2004, "Ejector performance
39 influence on a solid oxide fuel cell anodic recirculation system", Journal of
40
41
42
43 Power Sources, 129 216-228.
44

45 **Page 36: [126] Formatted** andrea 3/7/2010 4:49:00 PM

46 Font: 12 pt, Not Bold

47 **Page 36: [126] Formatted** andrea 3/11/2010 11:44:00 AM

48 Font: 12 pt, Italian (Italy)

49 **Page 36: [127] Deleted** andrea 3/11/2010 11:44:00 AM

50 M.L.,
51
52
53
54

55 **Page 36: [127] Deleted** andrea 3/11/2010 11:44:00 AM

56 A.,
57
58
59
60

1			
2			
3	Page 36: [127] Deleted	andrea	3/11/2010 11:44:00 AM
4	L.,		
5			
6			
7			
8	Page 36: [127] Deleted	andrea	3/11/2010 12:50:00 PM
9	, A.F.,		
10			
11			
12	Page 36: [128] Formatted	andrea	3/11/2010 11:44:00 AM
13	Font: 12 pt, Italian (Italy)		
14	Page 36: [129] Deleted	andrea	3/11/2010 11:44:00 AM
15	2005, "Influence of the anodic recirculation transient behaviour on the SOFC hybrid		
16	2005, "Influence of the anodic recirculation transient behaviour on the SOFC hybrid		
17	system performance", Journal of Power Sources		
18			
19			
20			
21	Page 36: [130] Formatted	andrea	3/11/2010 11:44:00 AM
22	Font: 12 pt, Italian (Italy)		
23			
24	Page 36: [130] Formatted	andrea	3/11/2010 11:44:00 AM
25	Font: 12 pt, Not Bold, Italian (Italy)		
26			
27	Page 36: [130] Formatted	andrea	3/11/2010 11:44:00 AM
28	Font: 12 pt, Italian (Italy)		
29			
30	Page 36: [131] Formatted	andrea	3/11/2010 11:44:00 AM
31	Font: 12 pt, Italian (Italy)		
32			
33	Page 36: [132] Formatted	andrea	3/11/2010 11:44:00 AM
34	English (U.K.)		
35			
36	Page 36: [133] Formatted	andrea	3/7/2010 4:49:00 PM
37	Numbered + Level: 1 + Numbering Style: 1, 2, 3, ... + Start at: 1 + Alignment: Left +		
38	Aligned at: 18 pt + Tab after: 47.25 pt + Indent at: 47.25 pt		
39			
40	Page 36: [134] Formatted	andrea	3/7/2010 4:49:00 PM
41	Font: (Default) Times, (Asian) Times New Roman, 12 pt, English (U.K.), Do not check		
42	spelling or grammar		
43			
44	Page 36: [134] Formatted	andrea	3/7/2010 4:49:00 PM
45	Font: (Default) Times, (Asian) Times New Roman, 12 pt, English (U.K.), Do not check		
46	spelling or grammar		
47			
48	Page 36: [134] Formatted	andrea	3/7/2010 4:49:00 PM
49	Font: (Default) Times, (Asian) Times New Roman, 12 pt, English (U.K.), Do not check		
50	spelling or grammar		
51			
52	Page 36: [134] Formatted	andrea	3/11/2010 11:45:00 AM
53	Font: Bold		
54			
55	Page 36: [134] Formatted	andrea	3/7/2010 4:49:00 PM
56	Font: (Default) Times, (Asian) Times New Roman, 12 pt, English (U.K.), Do not check		
57	spelling or grammar		
58			
59	Page 36: [134] Formatted	andrea	3/7/2010 4:49:00 PM
60	Font: 12 pt		

	Page 38: [135] Deleted	andrea	3/29/2010 4:05:00 PM
1			
2			
3			
4	Figure 1 - Installation of the 5 kW Siemens Generator in Turbocare Spa		5
5			
6	Figure 2 - Basic BoP design of the SOFC generator analysed		6
7			
8	Figure 3 – Ohmic losses in the tubular cell		8
9			
10	Figure 4 - Fuel and air flows along the tubular cell		11
11			
12	Figure 5 - Cells arrangement inside a bundle		12
13			
14	Figure 6 - Ejector scheme		15
15			
16	Figure 7 - Schematic sheet describing the iteration step for determining the molar composition of the anodic exhaust		18
17			
18	Figure 8 - Detailed flow-sheet with natural gas reference case		19
19			
20	Figure 9 - Detailed flow-sheet with ethanol feeding		20
21			
22	Figure 10 - Comparison of the calculated Nernst voltage along the fuel channel (cell tube length) for both natural gas and ethanol feeding		21
23			
24	Figure 11 - Equilibrium compositions of an ethanol/water mixture in a volumetric ratio 60/40 at different temperatures		26
25			
26	Figure 12 - Schematic view of the 5 kW Generator to respect of the fuel and air feeding flows		26
27			
28	Figure 13 - Carbon boundary for the ethanol steam reforming		27
29			
30	Figure 14 - Ejector pressure increase during EtOH/H₂O mixture feeding		27
31			
32	Figure 15 - Water stoichiometry in the NG/EtOH mixture reaching the stack		28
33			
34	Figure 16 - Behaviour of stack voltage during the EtOH/H₂O feeding experiment		29
35			
36	Figure 17 - Comparison of string voltages during the EtOH/H₂O feeding experiment		29
37			
38	Figure 18 - Stack voltage and current behaviour		29
39			
40	Figure 19 - Reformer temperature drop during the ethanol experiment		30
41			
42	Figure 20 - Temperature behaviour during the ethanol experiment		30
43			
44	Figure 21 - Generator electrical AC efficiency behaviour during the EtOH experiment		31
45			
46	Figure 1 - Installation of the 5 kW Siemens Generator in Turbocare Spa		5
47			
48	Figure 2 - Basic BoP design of the SOFC generator analysed		6
49			
50	Figure 3 – Ohmic losses in the tubular cell		8
51			
52	Figure 4 - Fuel and air flows along the tubular cell		11
53			
54	Figure 5 - Cells arrangement inside a bundle		12
55			
56	Figure 6 - Ejector scheme		15
57			
58	Figure 7 - Schematic sheet describing the iteration step for determining the molar composition of the anodic exhaust		18
59			
60	Figure 8 - Detailed flow-sheet with natural gas reference case		19
	Figure 9 - Detailed flow-sheet with ethanol feeding		20

1		
2		
3		
4	Figure 10 - Comparison of the calculated Nernst voltage along the fuel channel (cell tube	
5	length) for both natural gas and ethanol feeding	24
6	Figure 11 - Equilibrium compositions of an ethanol/water mixture in a volumetric ratio	
7	60/40 at different temperatures	26
8		
9	Figure 12 - Schematic view of the 5 kW Generator to respect of the fuel and air feeding	
10	flows	26
11		
12	Figure 13 - Carbon boundary for the ethanol steam reforming	27
13	Figure 14 - Ejector pressure increase during EtOH/H₂O mixture feeding	27
14	Figure 15 - Water stoichiometry in the NG/EtOH mixture reaching the stack	28
15	Figure 16 - Behaviour of stack voltage during the EtOH/H₂O feeding experiment	28
16	Figure 17 - Comparison of string voltages during the EtOH/H₂O feeding experiment	29
17	Figure 18 - Stack voltage and current behaviour	29
18	Figure 19 - Reformer temperature drop during the ethanol experiment	29
19	Figure 20 - Temperature behaviour during the ethanol experiment	30
20	Figure 21 - After-burner and stack temperature behaviour	31
21	Figure 22 - Generator electrical AC efficiency behaviour during the EtOH experiment	31
22	Figure 1 - Installation of the 5 kW Siemens Generator in Turbocare Spa	5
23	Figure 2 - Basic BoP design of the SOFC generator analysed	6
24	Figure 3 – Ohmic losses in cell tube	8
25	Figure 4 - Fuel and air flows along the tubular cell	11
26	Figure 5 - Cells arrangement inside a bundle	12
27	Figure 6 - Ejector scheme	14
28	Figure 7 - Schematic sheet describing the iteration step for determining the molar	
29	composition of the anodic exhaust	18
30	Figure 8 - Detailed flow-sheet with natural gas reference case	18
31	Figure 9 - Detailed flow-sheet with ethanol feeding	20
32	Figure 10 - Comparison of the calculated Nernst voltage along the fuel channel (cell tube	
33	length) for both natural gas and ethanol feeding	23
34	Figure 11 - Equilibrium compositions of an ethanol/water mixture in a volumetric ratio	
35	60/40 at different temperatures	25
36	Figure 12 - Schematic view of the 5 kW Generator to respect of the fuel and air feeding	
37	flows	25
38	Figure 13 - Carbon boundary for the ethanol steam reforming	26
39	Figure 14 - Ejector pressure increase during EtOH/H₂O mixture feeding	26
40	Figure 15 - Water stoichs in the NG/EtOH mixture reaching the stack	27
41	Figure 16 - Behaviour of stack voltage during the EtOH/H₂O feeding experiment	27
42		
43		
44		
45		
46		
47		
48		
49		
50		
51		
52		
53		
54		
55		
56		
57		
58		
59		
60		

1		
2		
3	Figure 17 - Comparison of string voltage during the EtOH/H2O feeding experiment	28
4		
5	Figure 18 - Stack voltage and current behaviour	28
6		
7	Figure 19 - Reformer temperature drop during the ethanol experiment	29
8		
9	Figure 20 - Temperature behaviour during the ethanol experiment	29
10		
11	Figure 21 - After-burner and stack temperature behaviour	30
12		
13	Figure 22 - Generator electrical AC efficiency behaviour during the EtOH experiment	30
14		
15		
16		
17		
18		
19		
20		
21		
22		
23		
24		
25		
26		
27		
28		
29		
30		
31		
32		
33		
34		
35		
36		
37		
38		
39		
40		
41		
42		
43		
44		
45		
46		
47		
48		
49		
50		
51		
52		
53		
54		
55		
56		
57		
58		
59		
60		

For Peer Review

Table 1. Molar compositions of the recirculated flow entrained by the ejector and total steam fraction recirculated normalized to the primary flow entering the ejector itself

Ejector volumetric entrainment ratio 'NG feeding':				5.53
Anodic molar exhaust composition:				
H ₂ [%]	CO [%]	H ₂ O [%]	CO ₂ [%]	
16	4	52	28	
Mol(H ₂ O)/Mol(fuel_in):		2.9		
Ejector volumetric entrainment ratio 'EtOH feeding':				5.39
Anodic molar exhaust composition:				
H ₂ [%]	CO [%]	H ₂ O [%]	CO ₂ [%]	
5	13	56	26	
Mol(H ₂ O)/Mol(fuel_in):		3.0		

Tubular Cell - Model Parameters

Cathode inner diameter / mm	21.7
Mean tube diameter / mm	24
Cathode thickness / μm	2200
Electrolyte thickness / μm	40
Anode thickness / μm	100
Interconnector thickness / μm	100
Interconnector width / cm	1.3
Ni-felt thickness / cm	0.5
Tubular cell length / cm	75
Cell active area / cm^2	400
$\rho_{el,cat} / \Omega\text{m}$	$0.008114 \times \exp(500/T)$
$\rho_{el,ely} / \Omega\text{m}$	$0.00294 \times \exp(10350/T)$
$\rho_{el,an} / \Omega\text{m}$	$0.00298 \times \exp(-1392/T)$
$\rho_{el,inter} / \Omega\text{m}$	$0.1256 \times \exp(4690/T)$
$\rho_{el,felt} / \Omega\text{m}$	-
$\gamma_{an} / \text{A m}^{-2}$	7×10^8
$\gamma_{cat} / \text{A m}^{-2}$	5.5×10^8
$E_{act,an} / \text{kJ mol}^{-1}$	100
$E_{act,cat} / \text{kJ mol}^{-1}$	120
ε_{an} (anode porosity)	0.3
τ_{an} (anode tortuosity)	5
ε_{cat} (cathode porosity)	0.4
τ_{cat} (cathode tortuosity)	4
$r_{pore,an}$ (mean cathode pores radius)	3
$r_{pore,cat}$ (mean cathode pores radius)	15

Table 2 – Parameters for the cell electrochemical model



Figure 1. Installation of the 5kW Siemens Generator in Turbocare Spa.

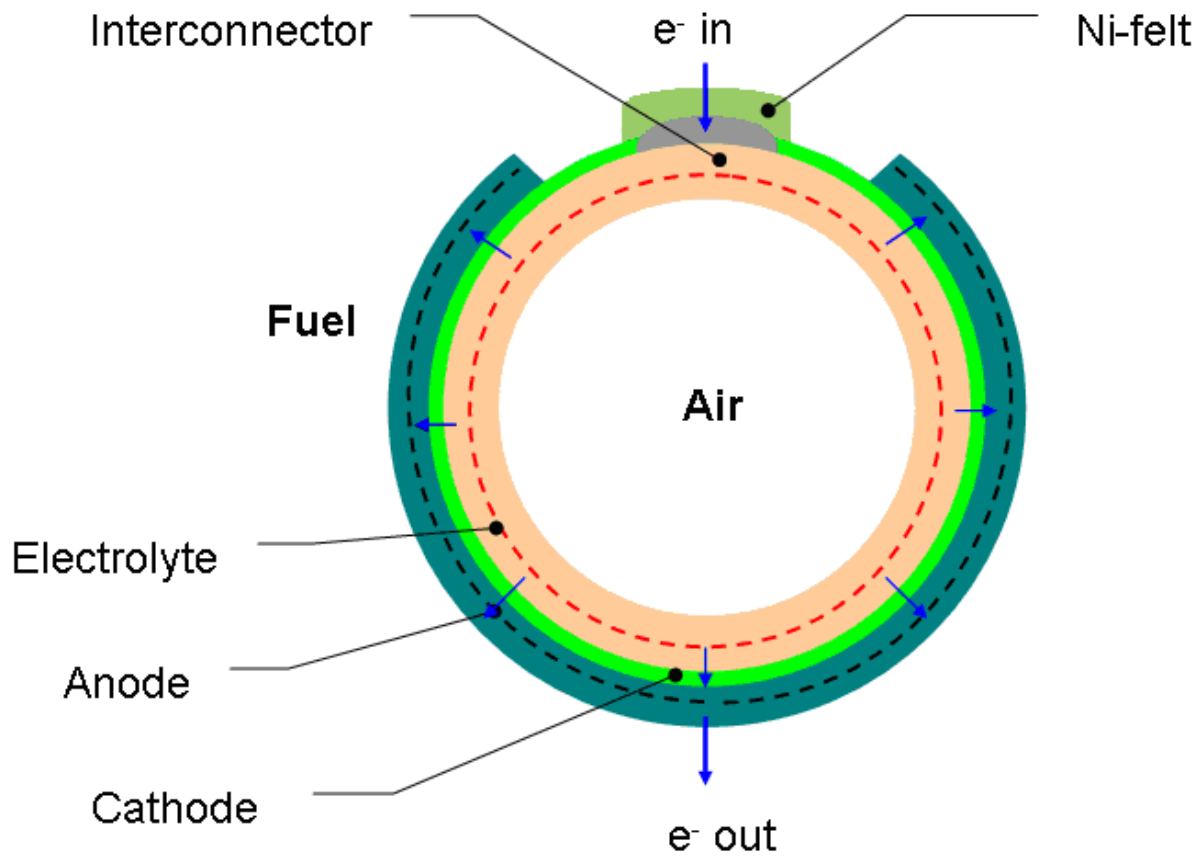


Figure 3 – Ohmic losses in the tubular cell

Review

1
2
3
4
5
6
7
8
9
10
11
12
13
14
15
16
17
18
19
20
21
22
23
24
25
26
27
28
29
30
31
32
33
34
35
36
37
38
39
40
41
42
43
44
45
46
47
48
49
50
51
52
53
54
55
56
57
58
59
60

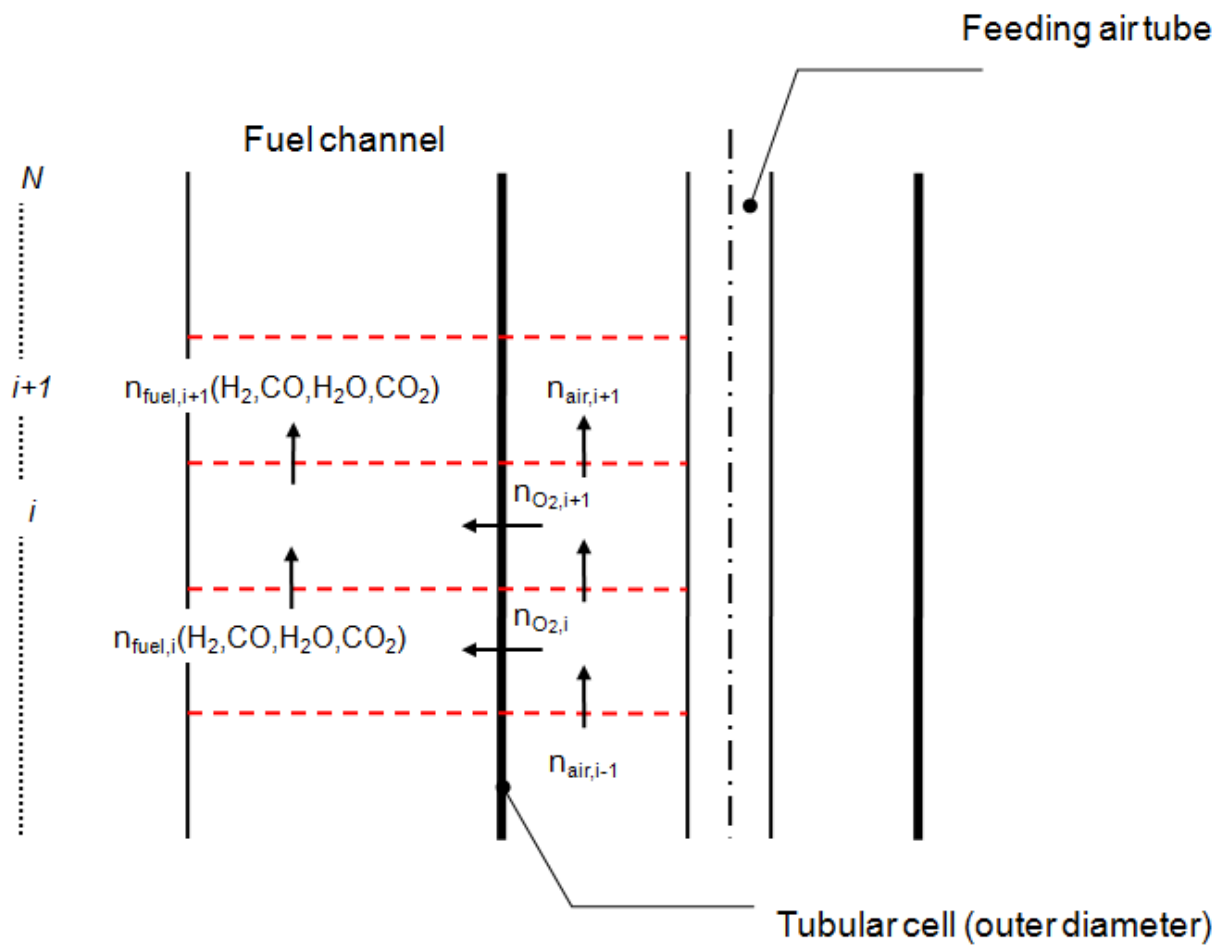


Figure 4 - Fuel and air flows along the tubular cell

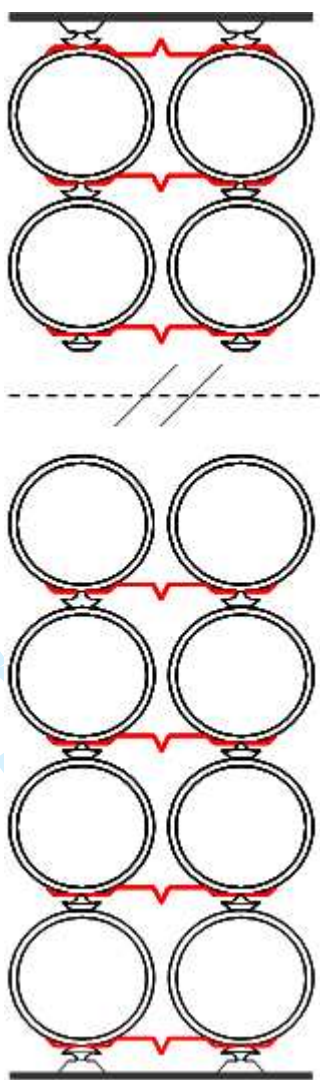


Figure 5 - Cells arrangement inside a bundle

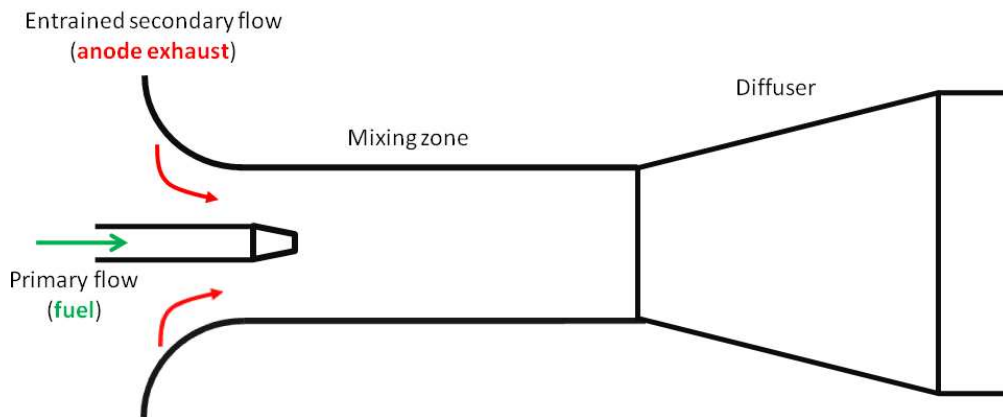


Figure 6. Ejector scheme
254x190mm (96 x 96 DPI)

Review

1
2
3
4
5
6
7
8
9
10
11
12
13
14
15
16
17
18
19
20
21
22
23
24
25
26
27
28
29
30
31
32
33
34
35
36
37
38
39
40
41
42
43
44
45
46
47
48
49
50
51
52
53
54
55
56
57
58
59
60

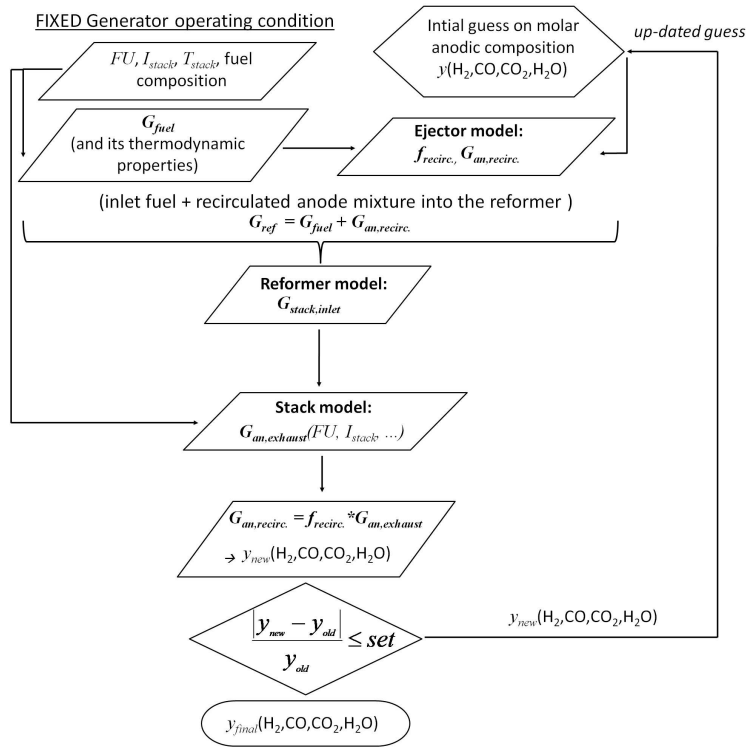


Figure 7. Schematic sheet describing the iteration step for determining the molar composition of the anodic exhaust
701x533mm (96 x 96 DPI)

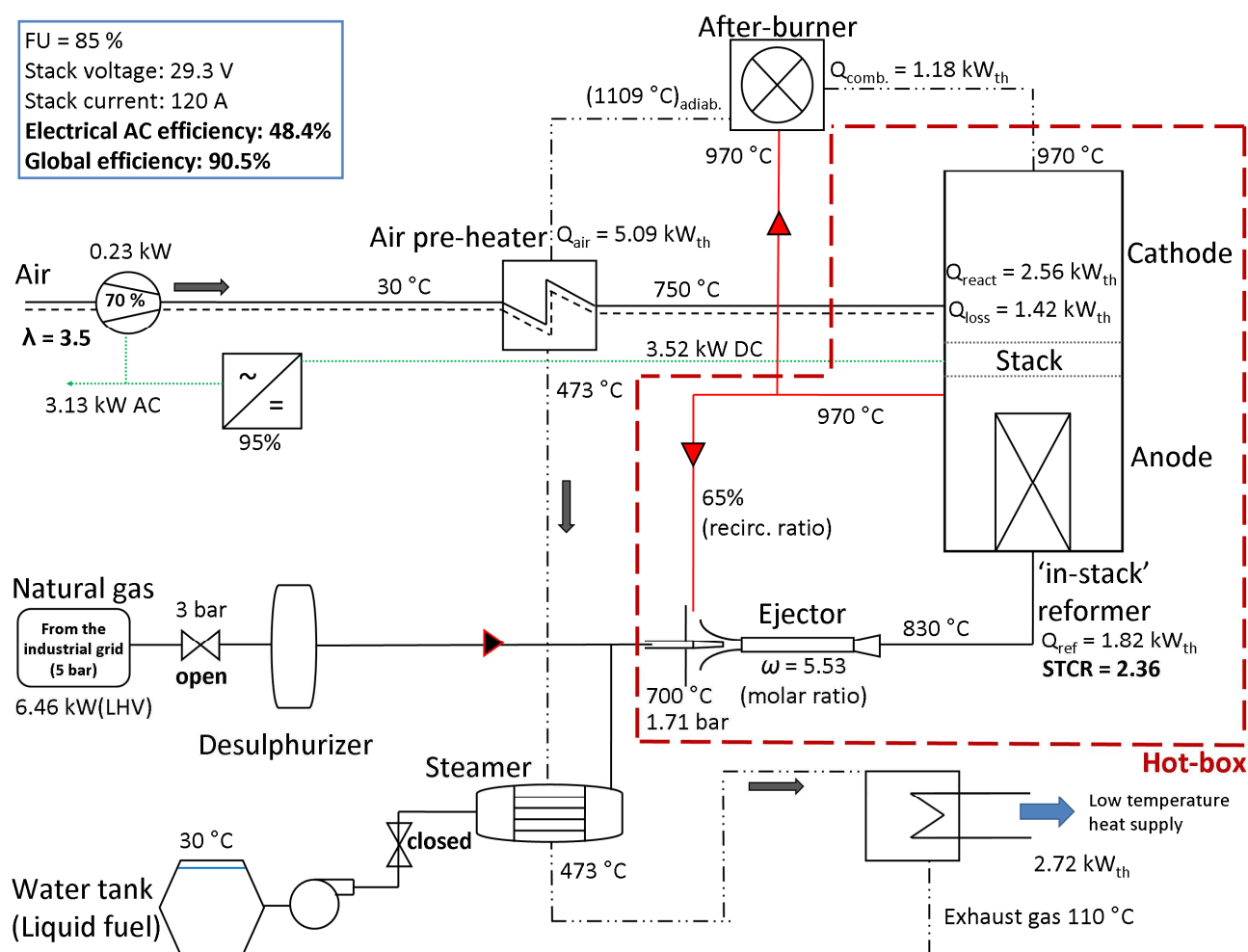


Figure 8. Detailed flow-sheet with natural gas (reference case)

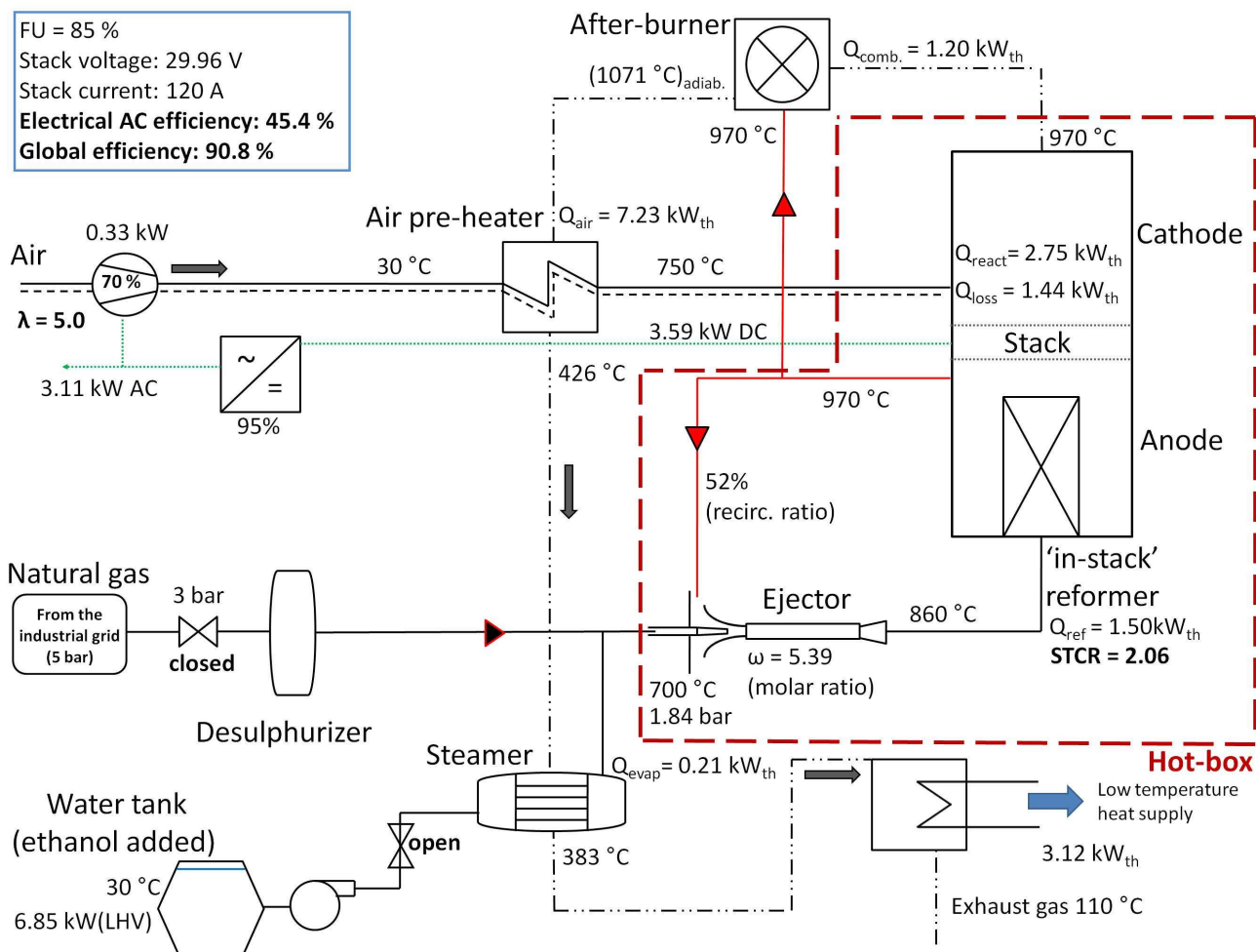


Figure 9. Detailed flow-sheet with ethanol feeding

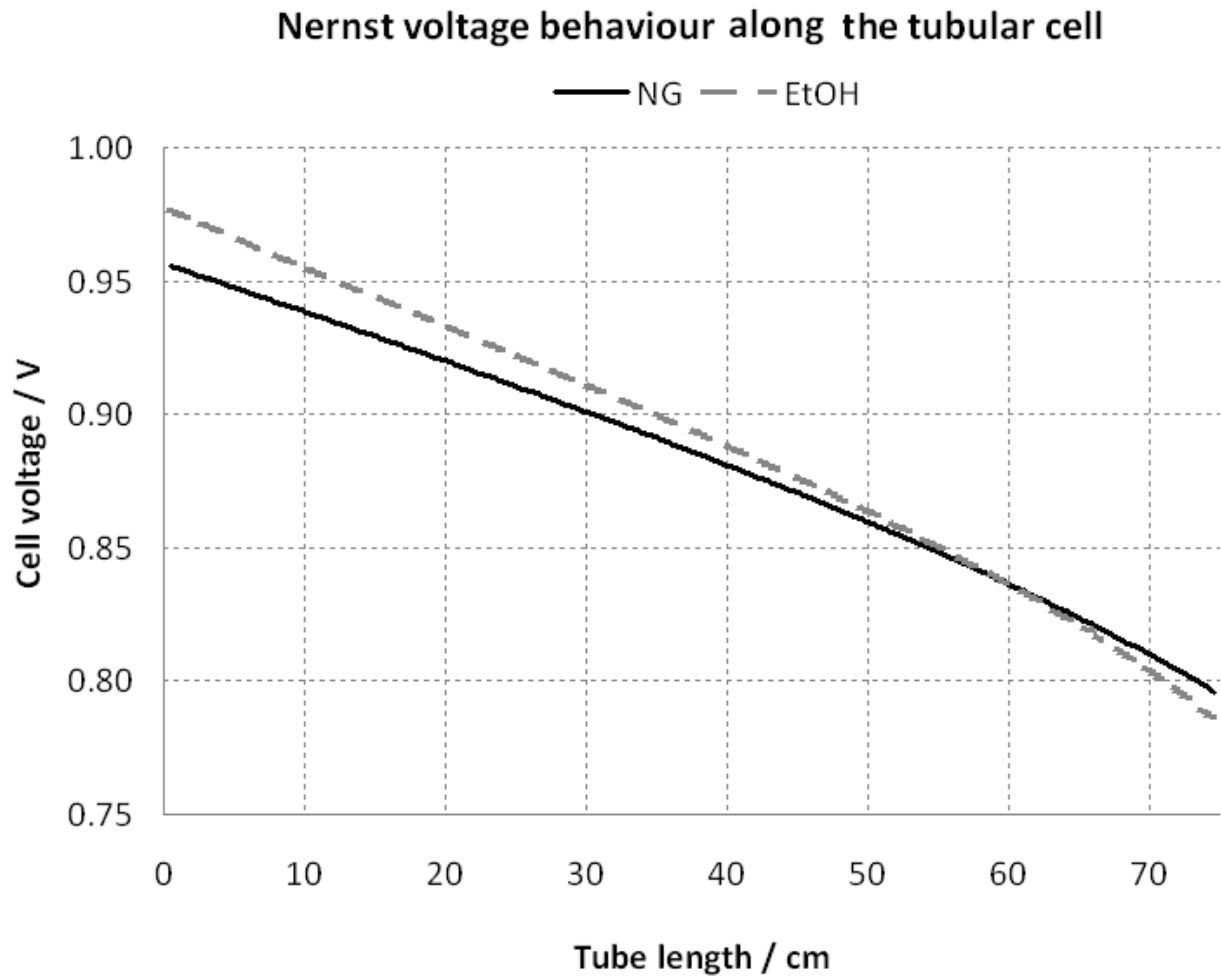


Figure 10. Comparison of the calculated Nernst voltage along the fuel channel (cell tube length) for both natural gas and ethanol feeding

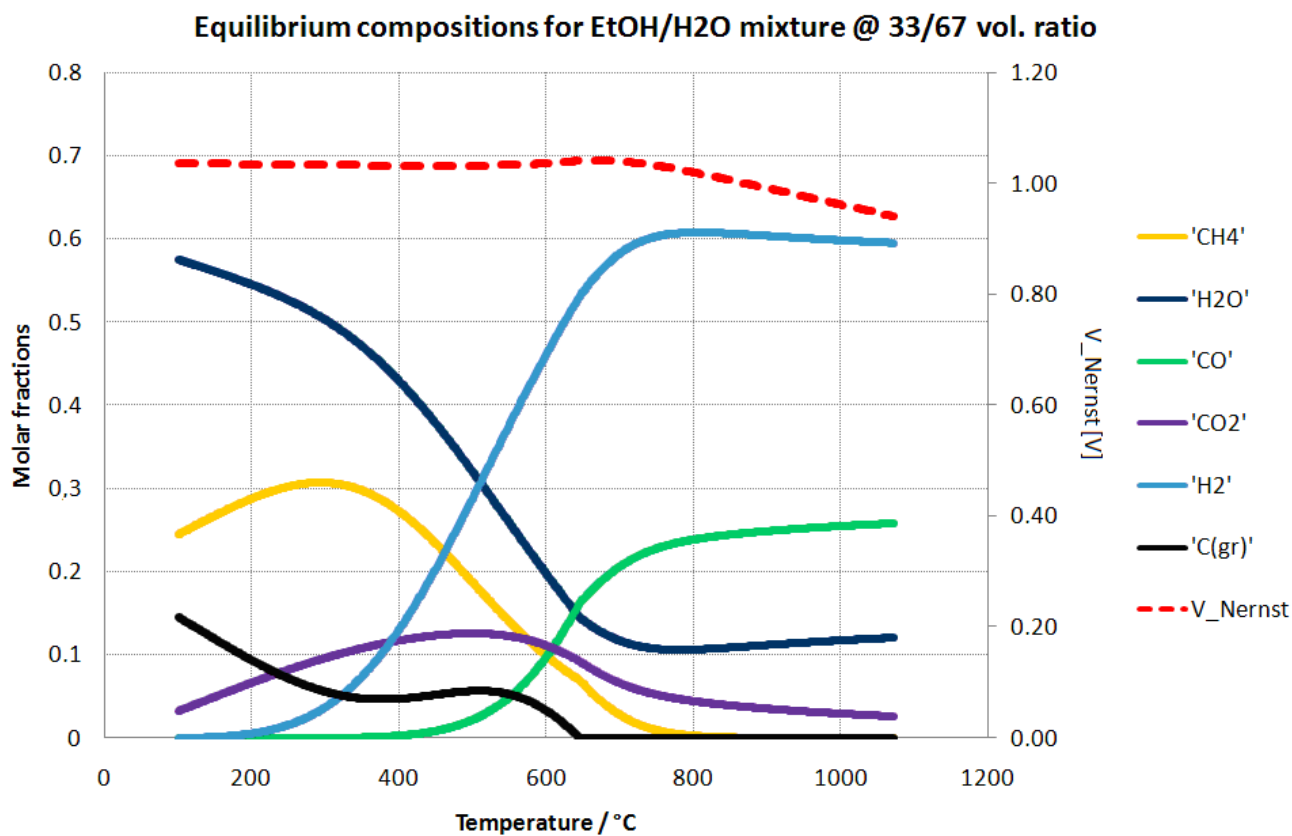


Figure 11. Equilibrium compositions of an ethanol/water mixture in a volumetric ratio 60/40 at different temperatures

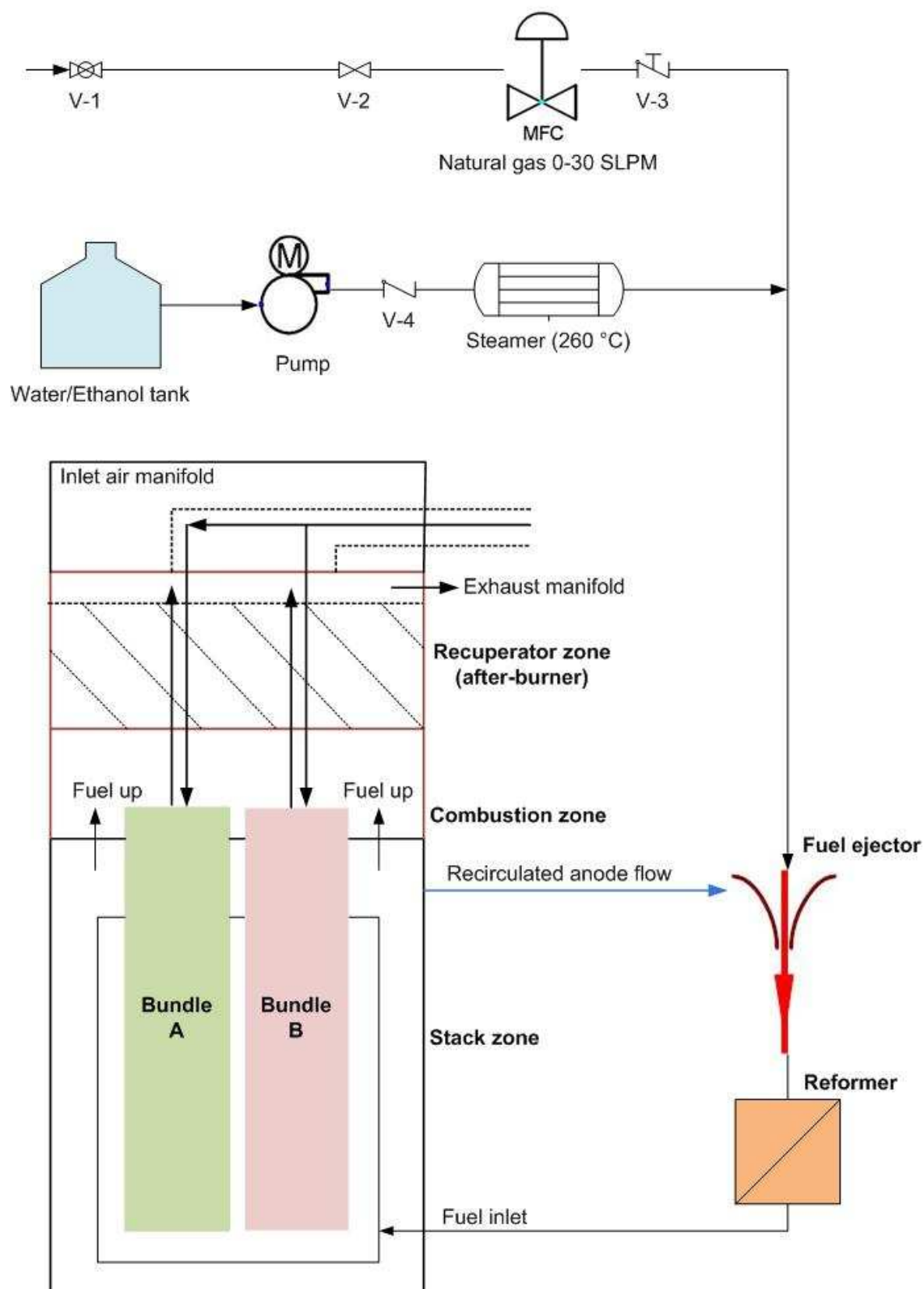
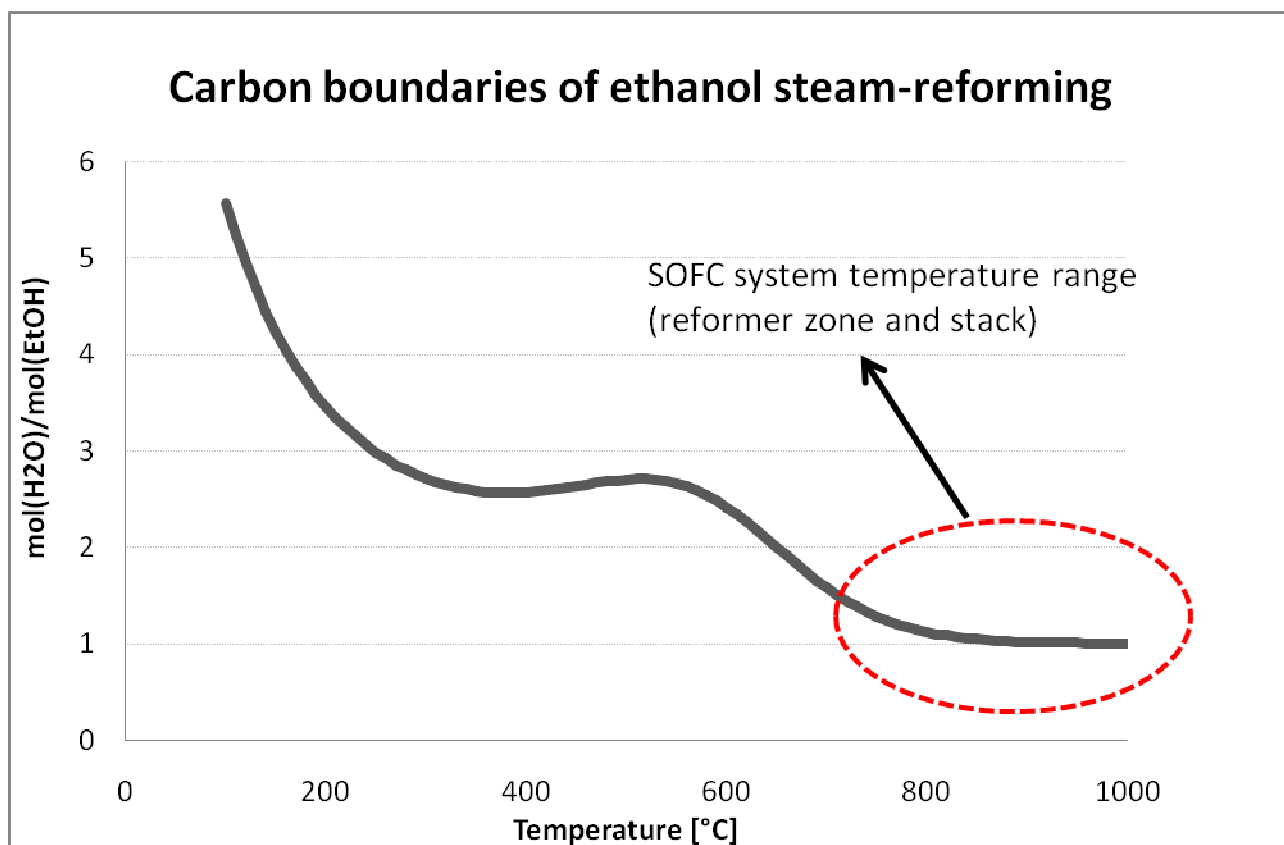


Figure 12. Schematic view of the 5 kW Generator to respect of the fuel and air feeding flows



33
34
35
36
37
38
39
40
41
42
43
44
45
46
47
48
49
50
51
52
53
54
55
56
57
58
59
60

Figure 13. Carbon boundary for the ethanol steam-reforming

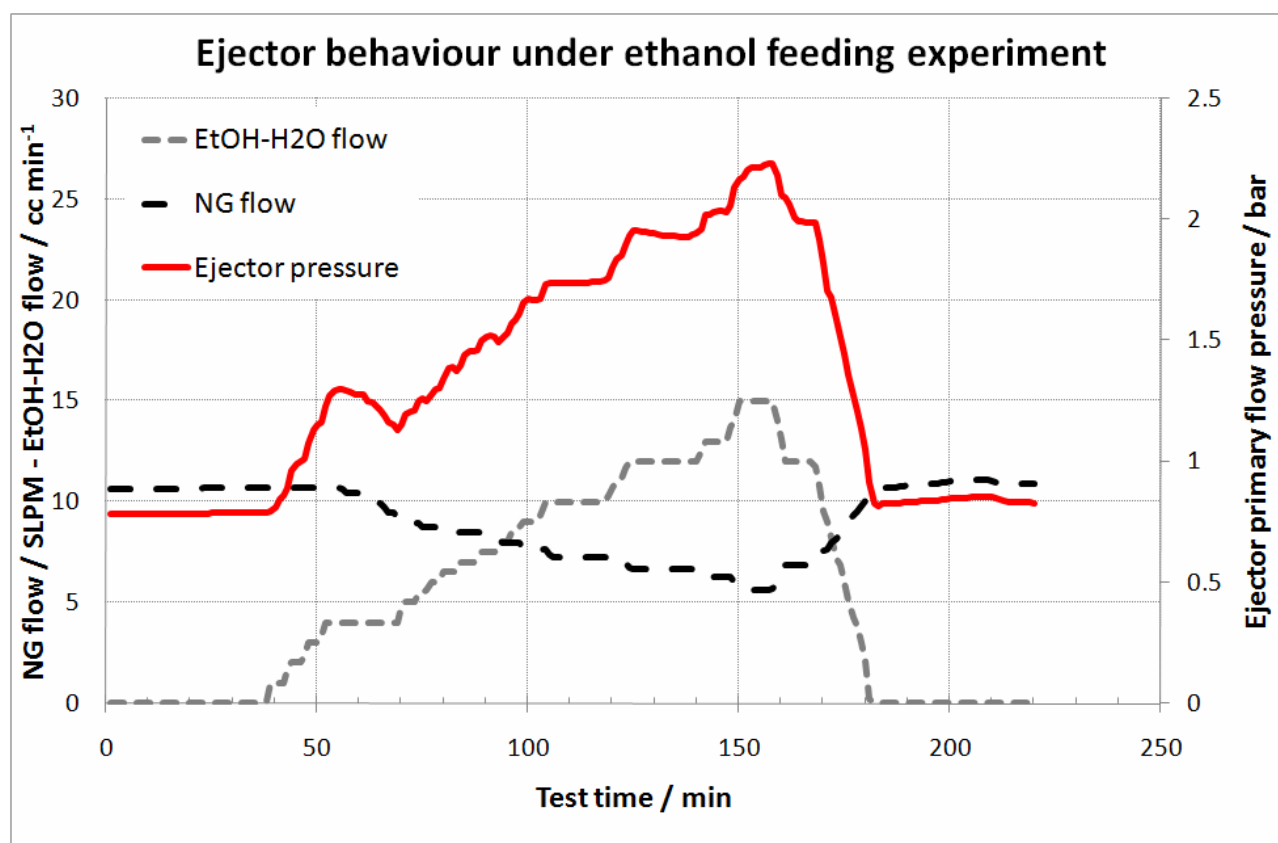


Figure 14. Ejector pressure increase during EtOH/H2O mixture feeding

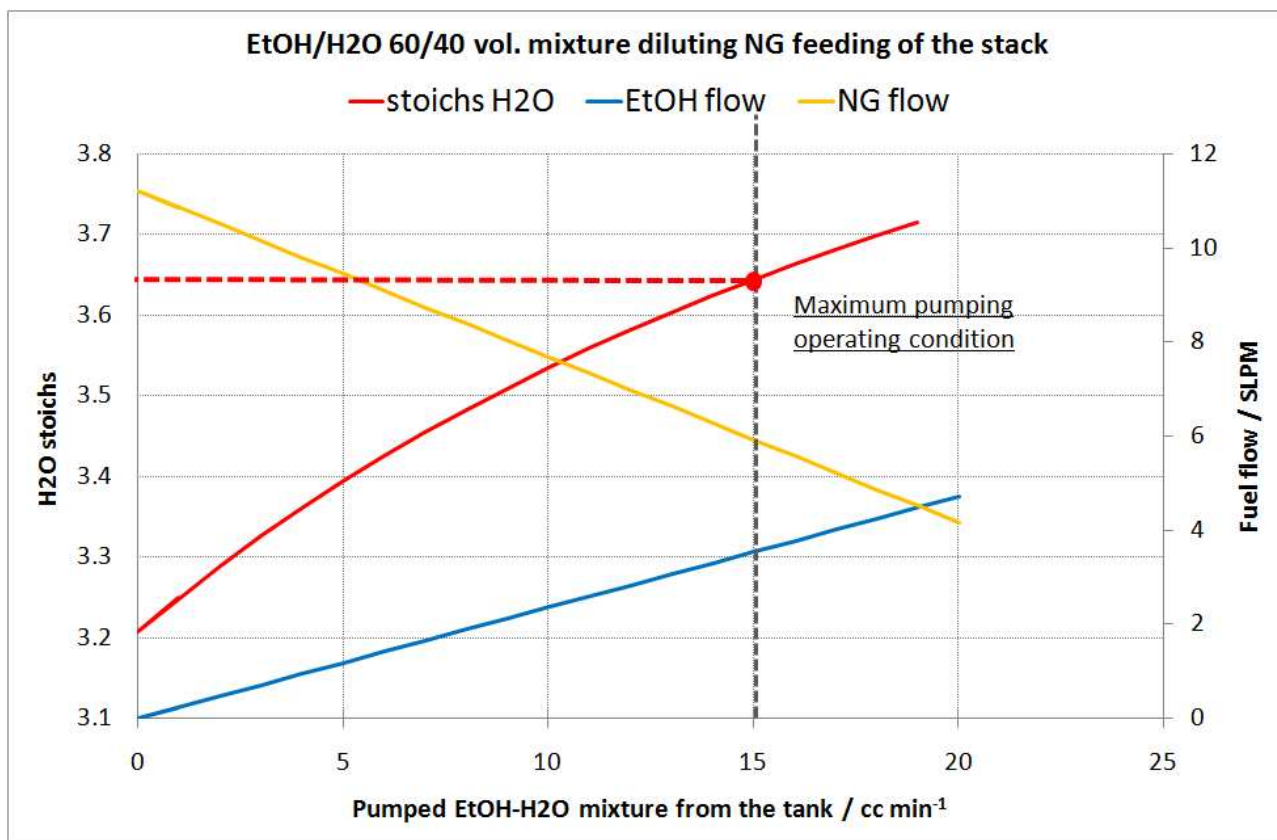


Figure 15. Water stoichiometry in the NG/EtOH mixture reaching the stack

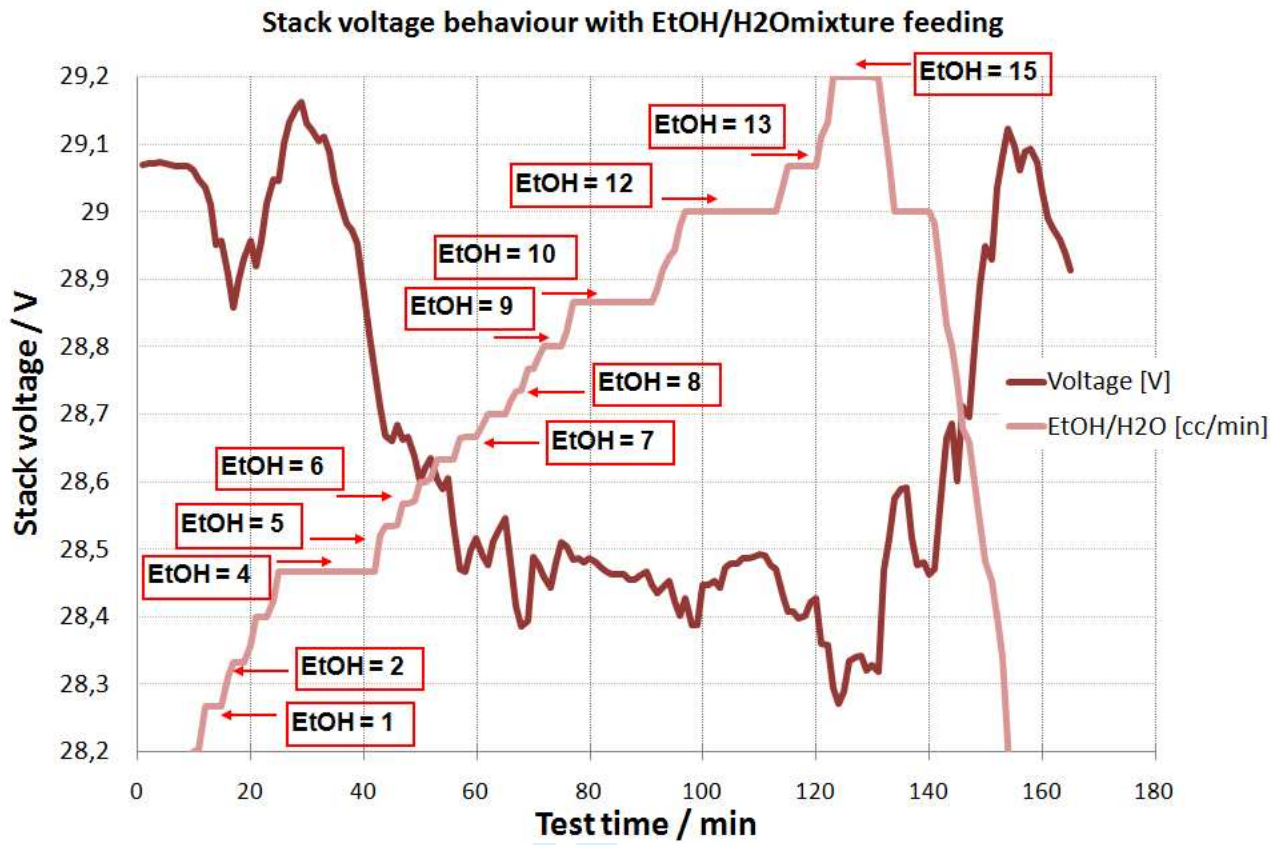


Figure 16. Behaviour of stack voltage during the EtOH/H₂O feeding experiment

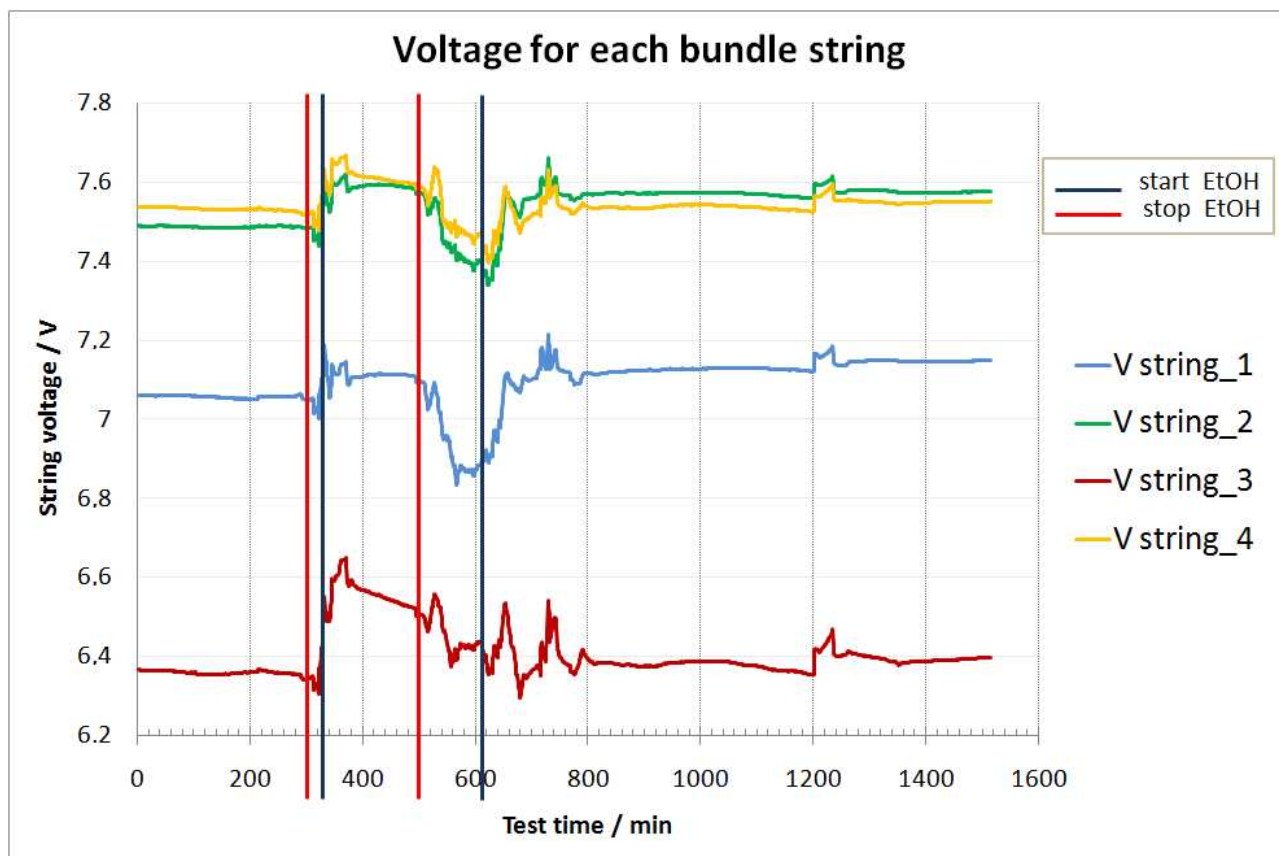


Figure 17. Comparison of string voltage during the EtOH/H₂O feeding experiment

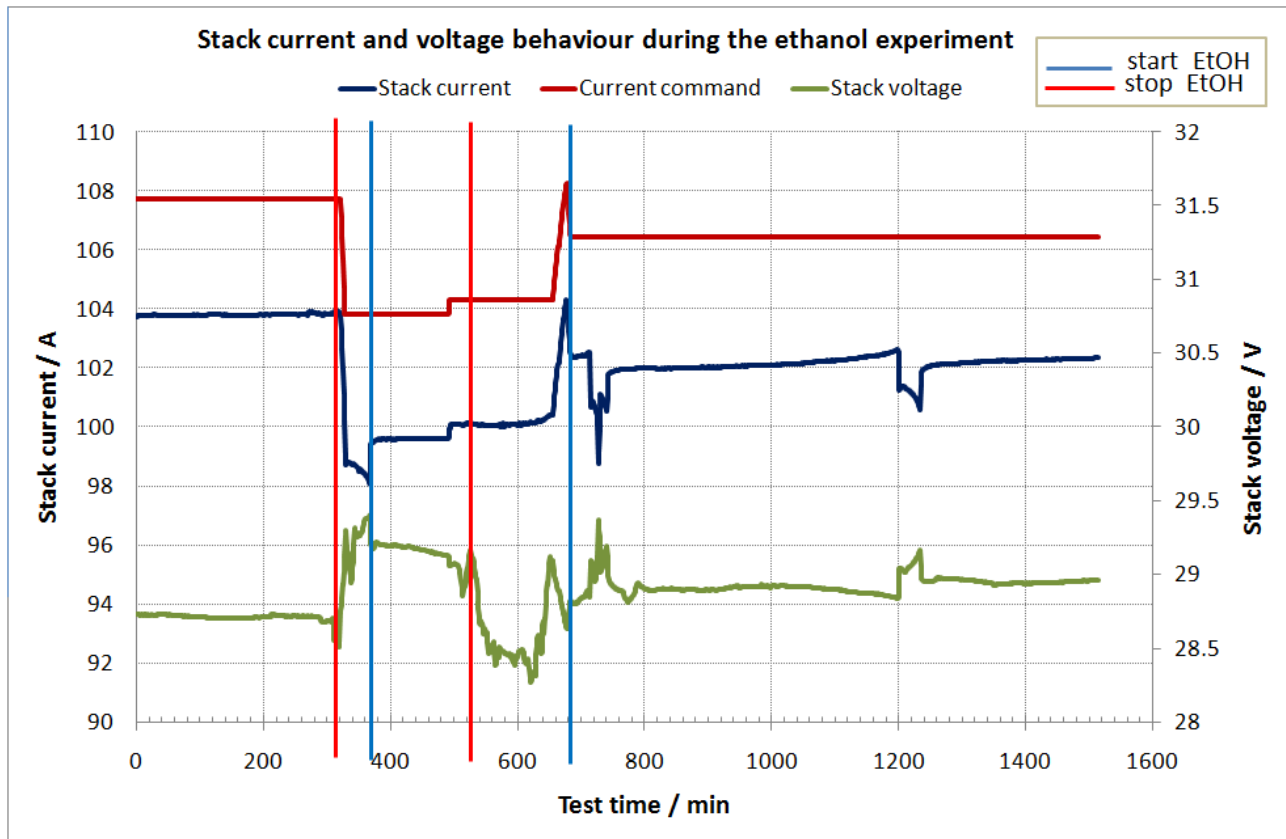


Figure 18. Stack voltage and current behaviour during the EtOH experiment

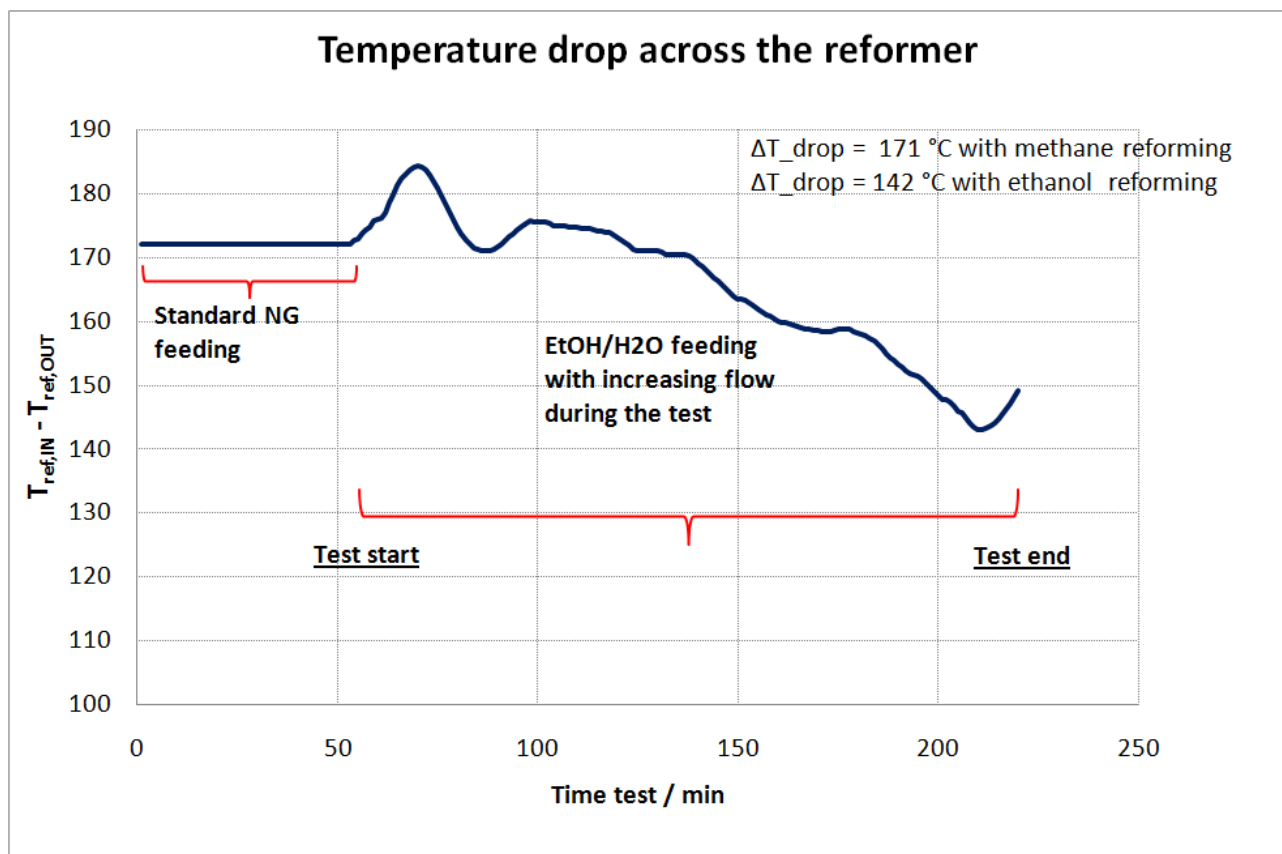


Figure 19. Reformer temperature drop during the ethanol experiment

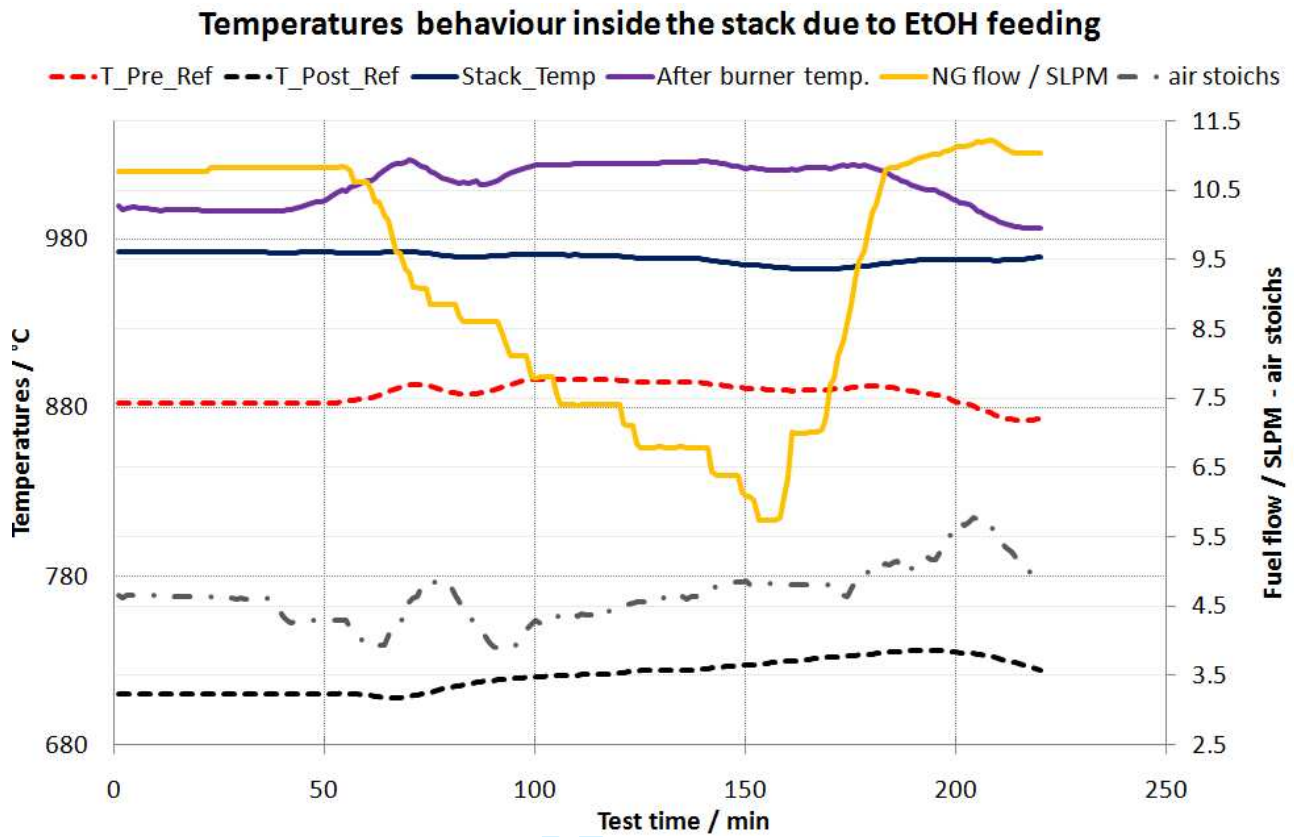


Figure 20. Generator temperatures behaviour during the ethanol experiment

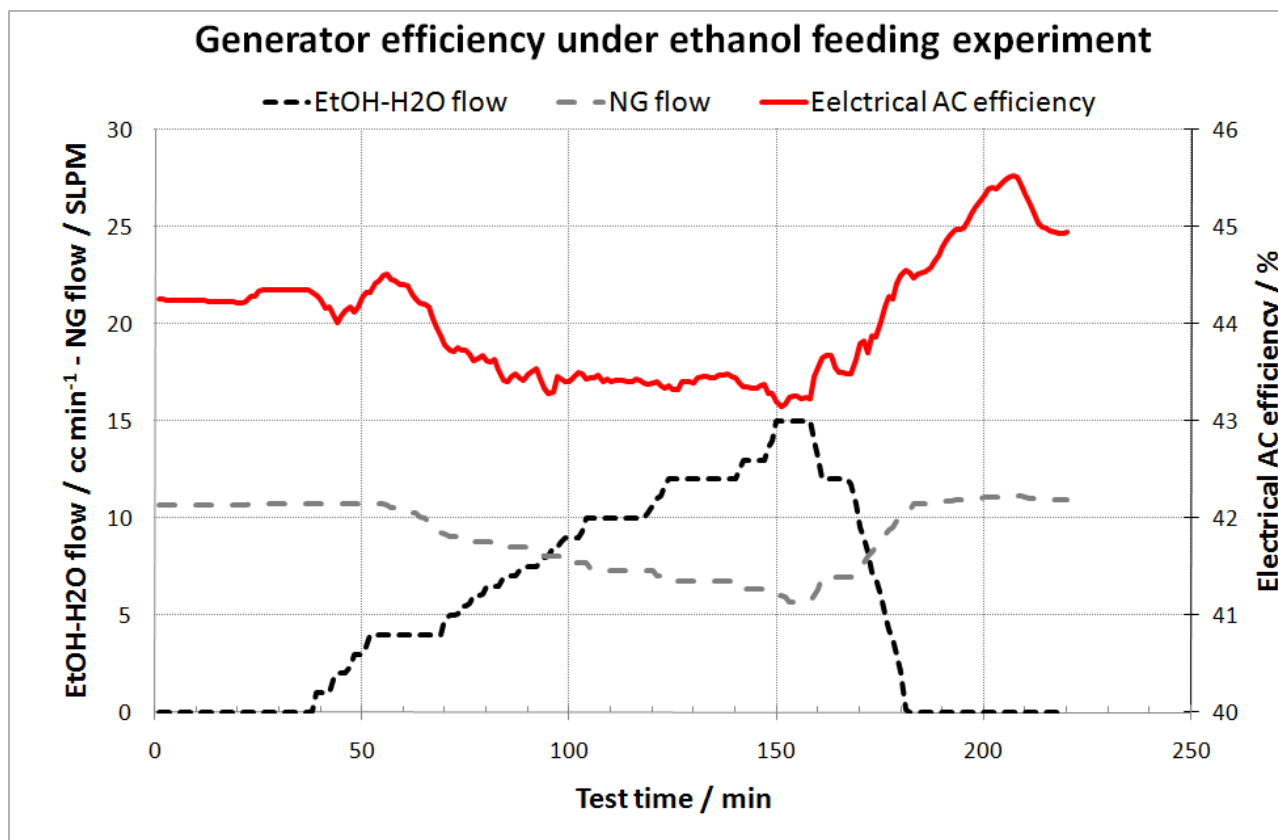


Figure 21. Generator electrical AC efficiency behaviour during the EtOH experiment